1997

Compressibility, hydraulic conductivity, and soil infiltration testing of tire shreds and field testing of a shredded tire horizontal drain

Peter Shane Zimmerman
Iowa State University

Compressibility, hydraulic conductivity, and soil infiltration testing of tire shreds and field testing of a shredded tire horizontal drain

by

Peter Shane Zimmerman

A thesis submitted to the graduate faculty

In partial fulfillment of the requirements for the degree of

MASTER OF SCIENCE

Major: Civil Engineering (Geotechnical Engineering)

Major Professors: Dr. Bruce Kjartanson and Dr. Robert Lohnes

Iowa State University

Ames, Iowa

1997

Graduate College
Iowa State University

This is to certify that the Master's thesis of

Peter Shane Zimmerman

has met the requirements of Iowa State University

Signatures have been redacted for privacy

TABLE OF CONTENTS

1 INTRODUCTION

It has been estimated that 200 to 250 million scrap tires are stockpiled annually in the United States (Edil and Bosscher 1994). These discarded tires are added to the 2 billion waste tires that have already accumulated in stockpiles and dumps (Ahmed and Lovell, 1992). The waste tire problem is one that will continue to grow until more tires are recycled or reused. The use of shredded waste tires in civil engineering projects is one way to reduce the number of tires that are stockpiled.

Many uses for shredded waste tires have been identified. Shredded tires have been used as fill in highway embankments, French drains and drainage layers for roads, leachate collection layers, and septic tank leach fields. Shredded tires have the characteristics of being lightweight, good insulators, and free draining (Humphrey, 1995). The engineering characteristics of shredded tire chips that are 6 mm to 75 mm long have been determined from many studies, however tire shreds 0.2 m to 0.4 m in length have not yet been studied. At a cost of only $1/kN ($9/ton), these large tire shreds are less expensive to produce than the smaller ones (Kersten, 1997). Larger tire shreds require less energy input than smaller chips and therefore are less expensive.

Engineering characteristics crucial for the design of subsurface drains utilizing large tire shreds are compression behavior and hydraulic conductivity of the shreds under an applied load. A related issue is the effect of soil migration into the pore spaces of the shreds. Soil migration would decrease the effective porosity of the tire shred drainage medium. Soil infiltration testing will determine if hydraulic conductivity is adversely affected by soil migration into pore space, and whether shredded tire horizontal drains will remain operational for long periods of time, or if soil migration into pore space will decrease their effectiveness. Another reason for conducting infiltration tests is to determine if a geotextile filter is needed to be placed around the shredded

tires used as a subsurface drain. A geotextile filter would make the shreds more difficult to place and more expensive to install.

Laboratory testing was undertaken to determine the hydraulic conductivity of the large tire shreds in a permeameter large enough to allow a representative volume of material to be tested. The permeameter was designed so that the tire shreds could be compressed and soil migration tests could also be conducted.

The tire shred characteristics from the laboratory tests were compared to field data collected from a 1.4 m wide by 27 m long shredded tire horizontal drain and a 2.3 m wide by 30 m long shredded tire stream crossing constructed in Fort Dodge, Iowa. These structures used the same size (0.2 m to 0.4 m) shredded tires that were tested in the lab. The purpose of the field structures was to evaluate the field performance of the shredded tires in situ, while the objective of the lab tests were to quantify the hydraulic conductivity, compressibility, and soil migration characteristics of the tire shreds with controlled boundary conditions.

The horizontal drain was installed to test specific design and performance issues. Design issues that were considered critical to construction were: 1) the cross-sectional geometry of the drain, 2) the required grade on the trench bottom, 3) the hydraulic conductivity of the shredded tires, 4) constructability, and 5) degree of compaction of backfill.

Performance issues were considered apart from design issues. The performance issues that were investigated were associated with the long-term effectiveness of the horizontal drain, and included: 1) effectiveness in lowering the water table, 2) continued water flow over time without plugging, 3) soil piping, 4) magnitude of settlement, and 5) environmental issues, such as whether leachates are generated.

The design issues of compressibility and hydraulic conductivity of the tire shreds

were tested in the laboratory and compared to field data taken from flow tests and settlement data of the horizontal drain. The required cross section of the horizontal drain was estimated using laboratory data and field observations.

The performance issues of soil piping and tire shred susceptibility to soil migration were tested in the laboratory and compared to field data and observations. Long term performance of the shredded tire horizontal drain was tested by comparing two flow tests completed eight months apart. Water table elevations were monitored over time and contour maps of the water table surface were completed in order to illustrate changes in the groundwater pattern. Settlement of the shredded tires in the horizontal drain was measured and compared to lab compressibility results.

Laboratory and field testing results were studied and compared in order to recommend guidelines for the design and construction of horizontal drains. These guidelines will outline the information needed for an effective horizontal drain placed in the most efficient and safe manner possible.

2 TIRE SHRED CHARACTERISTICS

Tire shreds from Fort Dodge, Iowa, and Perry, Iowa were tested. The size distribution of the Fort Dodge, Iowa tire shreds can be seen in Figures 1 and 2. A total of 454 Fort Dodge and 75 Perry shreds were measured to characterize the size distribution. Length was measured as the longest shred dimension. Width was measured perpendicular to length at the widest point of the shred. Figure 1 gives the distribution of lengths of the shreds and Figure 2 shows the width distribution. The lengths of most of the shreds were between 0.2 and 0.4 m, whereas the widths were between 0.1 m and 0.2 m. The minimum and maximum lengths ranged from less than 0.1 m to 0.9 m respectively. 2.235 kN of Fort Dodge tire shreds were used while 2.668 kN of Perry shreds were tested.

The Fort Dodge shreds were produced using a Shred-Pax AZ-80 shredder. The shredder operated with high torque and low rpm. Whole tires were added to the shredder to produce a large size tire shred.

The specific gravity of the tire shreds was measured using the standard test method for specific gravity and absorption of coarse aggregate (ASTM C 127-88). The results of the specific gravity tests ranged between 1.09 and 1.27. The section of the tire from which the shred was produced affected the results. For instance, shreds from the tread of the tire had much higher specific gravity than shreds from the sidewall, which had no wire reinforcement. The large sizes of tire shreds made it difficult to test a homogenous, representative sample during each test. Some collections of shreds contained more shreds from the tread, which resulted in higher specific gravities, than others.

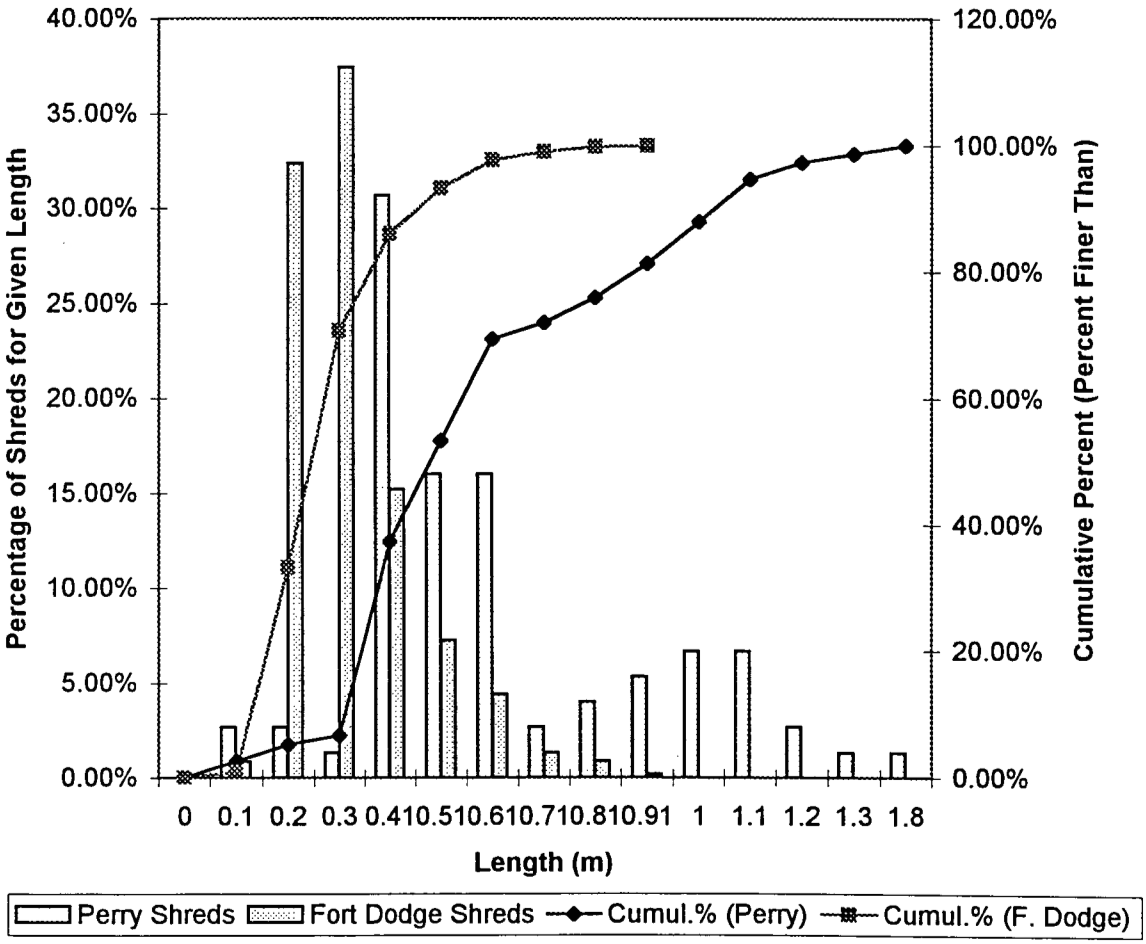

Figure 1. Lengths of the Fort Dodge and Perry tire shreds

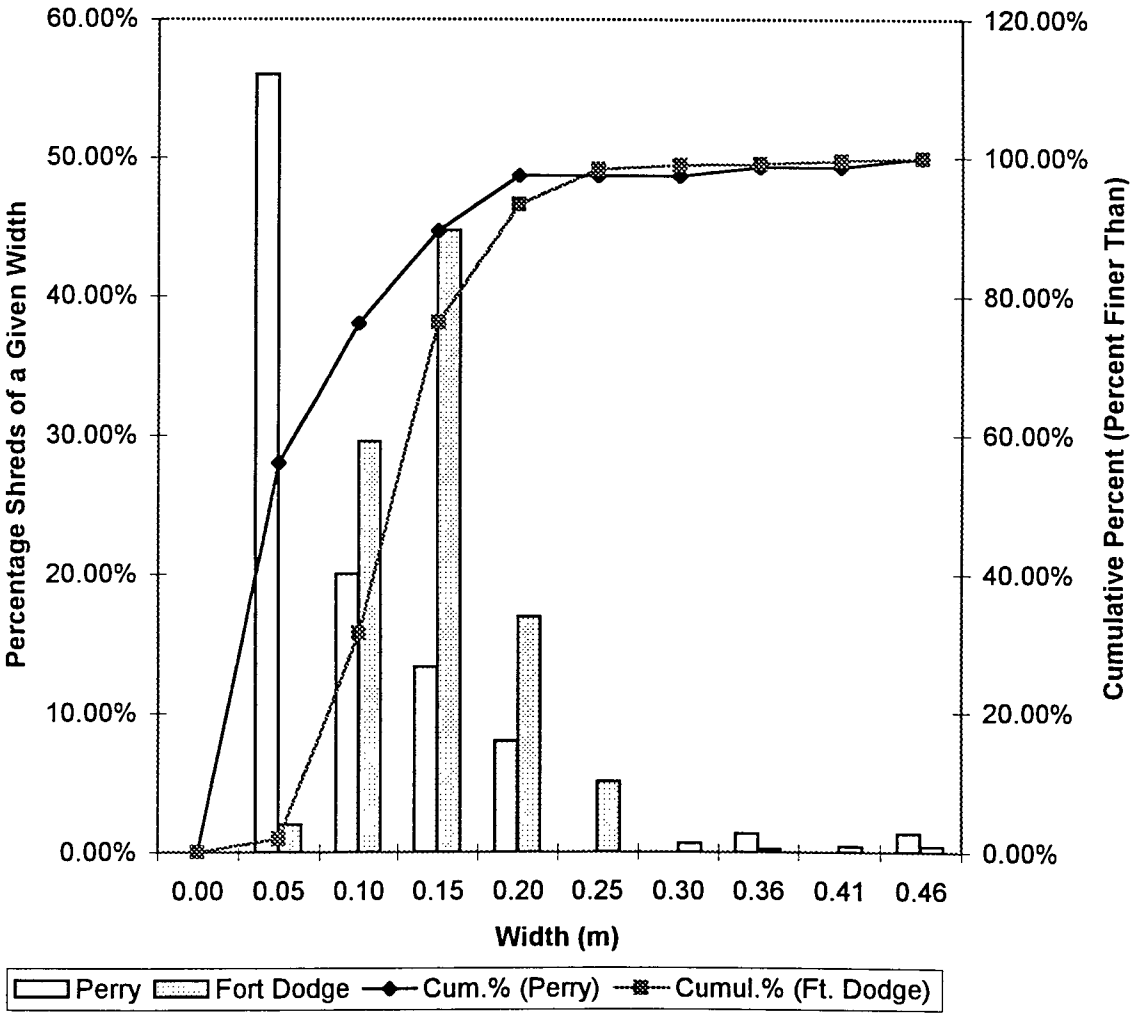

Figure 2. Widths of Fort Dodge and Perry tire shreds.

3 LABORATORY TESTS

3.1 Equipment

The permeameter equipment consisted of a steel reaction frame, a hydraulic ram, a Lexan plastic permeameter cell with steel reinforcement, a pump, a reservoir, a flow gage, and various pipes and fittings. Figure 3 shows the equipment arrangement used in permeability and compressibility testing. Figure 4 shows a top view of the permeameter cell and steel reaction frame.

3.1.1 Permeameter Dimensions and Material

The dimensions of the permeameter cell used here were 0.91 m x 0.91 m in cross section with a height of 1.22 m. The design of the permeameter was partially based on equipment used by Shackelford and Javad (1991) for large-scale laboratory permeability testing of a compacted clay soil.

The permeameter cell was constructed using 9.5 mm thick Lexan plastic sheets for the sides and base. This allowed observation of the tire shred layer during testing. The top was left open. A 25.4 mm diameter hole was drilled in the bottom to allow water to circulate through the cell. Standpipes were installed through holes drilled the side of the permeameter wall in the positions shown in Figure 3. The permeameter cell was reinforced on the outside with a steel frame.

3.1.1.1 Shred Size to Permeameter Width Ratio

Edil and Bosscher (1994) used a cell with an inside diameter of 0.28 m to test the permeability of tire chips with a length of 50 to 76 mm. The diameter of their cell was 3.7 times the largest chip size and about 4.5 times the average chip size. Humphrey et al. (1992) used a permeameter with inside diameter of 0.295 m to measure the permeability of chips with maximum length 76 mm. His permeameter had a diameter 3.9 times the largest chip size and about 4.5 times the average chip size.

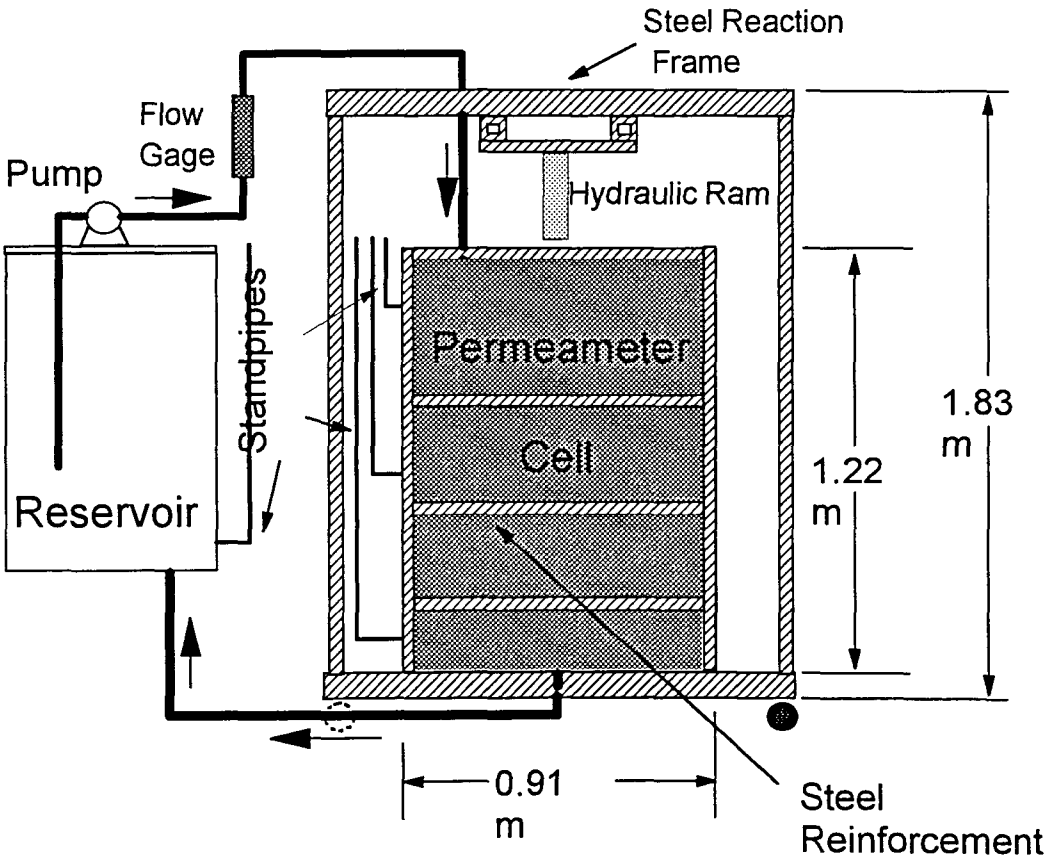

Figure 3. Testing apparatus

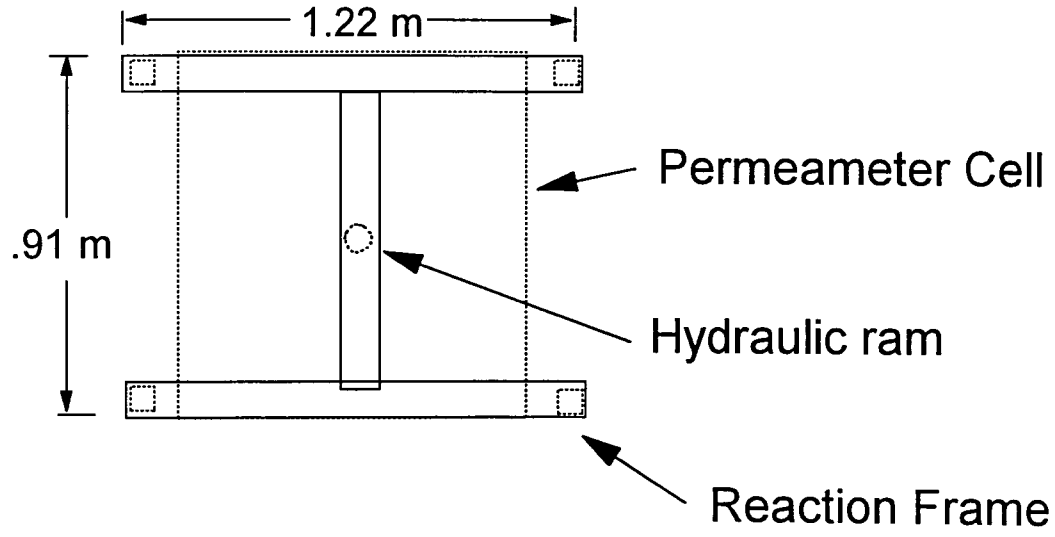

Figure 4. Top view of permeameter cell and reaction frame

The permeameter that was used in our tests was the same width as the largest shred length and about 2.25 times the length of the average shred size. If a width equal to 4.5 times the average tire shred length would have been used, the permeameter required would have been 1.8 m in width. This size of permeameter was not practical. Therefore, a smaller permeameter width to shred size ratio was chosen. It is believed that the smaller ratio did not impact the results of the testing.

3.1.2 Reaction Frame

A steel reaction frame provided a mount for the hydraulic ram and support for the permeameter base. The shredded tires were compressed by using the hydraulic ram attached to the reaction frame.

3.1.3 Hydraulic Ram

An Enerpac ram with a stroke of 0.25 m was used for compression. Extensions for the ram were employed that extended its stroke past the length needed for 50% compression of the tire shreds, which was on the order of 0.5 m.

3.1.4 Compression Cap

A compression cap, which was constructed of structural tubing, was used to uniformly compress the shredded tires. Gaps were left between the tubes to form a grid pattern, which was able to compress the entire tire shred layer uniformly. The cap weighed 388 N. The compression cap was ideal for soil infiltration testing because it left much of the top of the tire shred layer exposed.

3.1.5 Floor Grate and Collar

A steel grate with 25.4 mm sized openings was set on 50 mm spacers inside the permeameter above its base. The grate provided support for the shredded tires while allowing free drainage. During initial testing, the space underneath the grate was kept unobstructed and water was allowed to circulate freely at the bottom of the

permeameter. There were, however, two problems with this design. First, it was evident from both observation through the Lexan walls and from the standpipes that the preferred flow path for the water was along the sides of the permeameter. The tire shreds along the sides of the permeameter were less of a barrier to flow than the entangled tire shreds in the center. The standpipes indicated virtually no head loss along the sides of the permeameter even though it was observed that water was flowing rapidly along the sides. The second problem with having the space below the grate open was that during the soil infiltration tests it was expected that very little soil would settle on the bottom and instead would be carried in the water or would clog the pipes. Installing a 0.30 m square collar around the drainage hole in the permeameter cell base solved these problems. The collar had a height equal to the spacers that held the walkway grate off of the cell base, and it obstructed flow along the permeameter base, thus minimizing preferred flow down the sides of the cell and through the drain. During the soil infiltration tests, the bottom of the permeameter acted like a large silt trap. The soil filtered down onto the bottom, but was not carried past the collar.

3.1.6 Reservoir

The reservoir used in the setup (See Figure 3) was a plastic drum. A standpipe was attached near the bottom of the drum to monitor the water level in the reservoir. The pump, sitting on a board placed across the top of the reservoir, drew water up from the reservoir, through a flow meter, and into the permeameter cell. A 25.4 mm pipe connected the permeameter cell at the bottom of the reservoir.

3.2 Correction For Head Loss In Empty Permeameter

Originally, the hydraulic conductivity tests were to be run as constant head tests with losses in head to be measured across the tire shred sample using the standpipes.

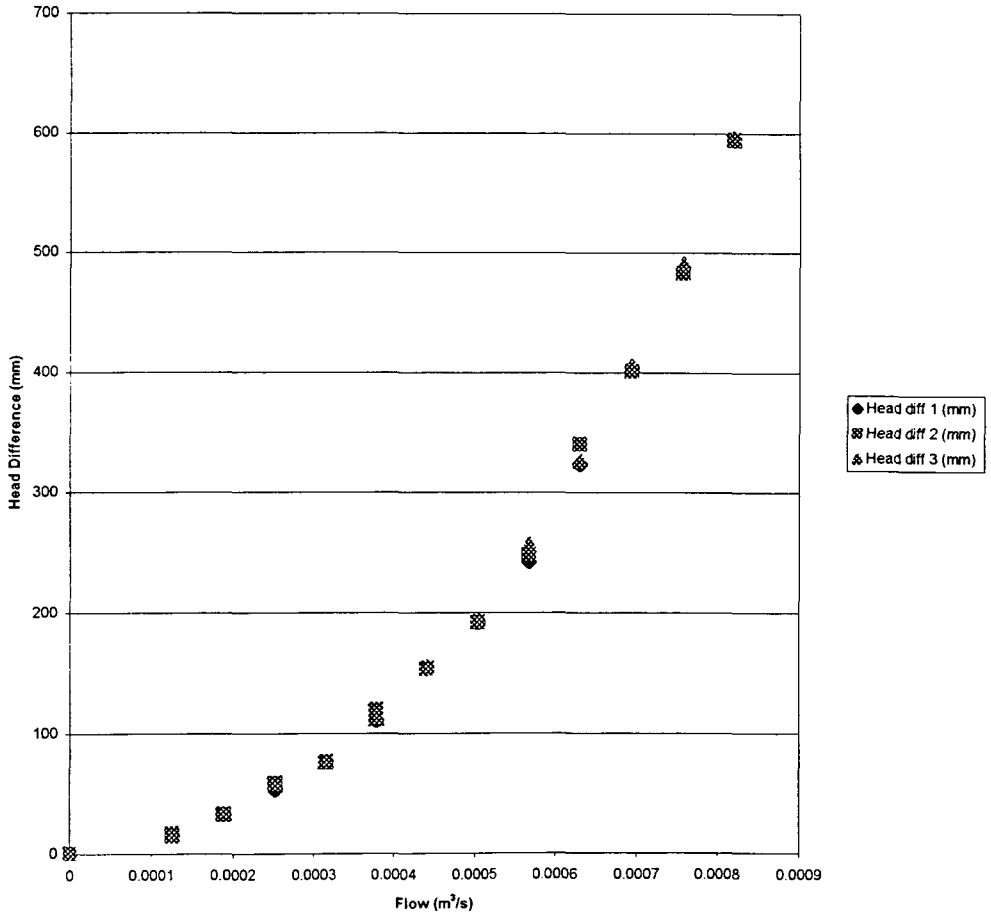

Figure 5. Head difference between permeameter and reservoir during tests with no tire shreds.

It turned out to be impossible to measure head losses along the side of the cell because of significant sidewall preferential flow problems. It was decided to continue to run the tests as constant head tests, but to measure the total head loss between the reservoir and the water level above the tire shreds rather than using the standpipes. The amount of head loss in the 25.4 mm pipe, however, forced the use a correction factor. This factor took into account head loss in the empty permeameter.

Head loss occurred between the reservoir and the permeameter cell when the cell did not contain shredded tires. In a system with no frictional head loss, the water level in the reservoir would always be the same as the water level in the permeameter cell. In our system, however, the water level in the permeameter cell was higher than the water level in the reservoir when the pump circulated water through the empty system.

3.2.1 Empty Permeameter Tests

Tests were carried out with an empty permeameter cell to quantify the head loss that occurred at various flow rates through the permeameter system itself. Two tests were performed before shredded tire testing, and one after all other testing was completed. The results of these tests can be seen in Figure 5. The difference in water levels was higher at higher flow rates and ranged from 15.24 mm at a flow of 0.000126 m^3/s (2 gallons/minute (gpm))to 595 mm at 0.00082 m^3/s (13 gpm). For the most part, results for all three tests were very close. Some flow rates, however, did have slightly different results for the three empty permeameter tests.

3.2.2 Correction Factor

The frictional head loss had to be considered when analyzing the data obtained from shredded tire hydraulic conductivity testing. For each flow rate used in testing, a correction factor was applied that was equivalent to the head loss that occurred at that

Table 1. Correction factors for each flow rate and how they were chosen.

Flow (m3/s)	Correction Factor (mm)	How Correction Factor Was Chosen
0.000126	15.2	2 tests with same measurement
0.000189	33.0	3 tests with same measurement
0.000252	58.4	2 tests with same measurement
0.000315	76.2	3 tests with same measurement
0.000378	113.8	Average of three measurements
0.000441	153.7	2 tests with same measurement
0.000505	191.8	2 tests with same measurement
0.000568	248.9	Average of three measurements
0.000631	330.2	Average of three measurements
0.000694	403.4	Average of three measurements
0.000757	486.4	Average of three measurements
0.000820	594.4	2 tests with same measurement

flow rate through the empty permeameter. The corrected test data, therefore, represented only head loss that occurred only due to seepage force losses through the shredded tires.

One correction factor was determined for each flow rate. If all three empty permeameter tests showed the same head difference, then that head difference was used as the correction factor. If two out of three head difference measurements agreed, then the measurement that was duplicated in the two tests was used as the correction factor. If none of the three measurements were the same, then the three measurements were averaged to arrive at a correction factor for that flow rate. Table 1 lists the correction factors and explains how each of them was chosen.

3.3 Compressibility And Hydraulic Conductivity Test Procedures

3.3.1 Compression Testing Procedure

Compression tests were carried out on dry tire shreds placed in the permeameter cell. Tire shreds were added to the permeameter cell one by one. Shreds that were placed on the sides of the cell were placed so that they fit closely to the side. Shreds were added to the corners of the cell that fit as tightly as possible into the corner. Tire shreds were placed in the center of the cell in a more random manner. The reason for adding shreds in this manner was to reduce the amount of preferential flow along the permeameter sides during hydraulic conductivity testing.

The initial thickness of the tire shred layer was measured. The compression cap was placed on top of the tire shreds and the thickness of the shreds was again measured.

The pressure gage on the ram was used to control the test. As the pressure increased on the gage, the ram extension was measured at constant pressure intervals.

3.3.2 Hydraulic Conductivity Testing Procedure

The goal of this phase of testing was to measure the hydraulic conductivity when water was circulated under a constant flow rate through the permeameter cell that contained shredded tires. The same procedure was used for all tests so that the data could be used for the comparison with all other test results.

3.3.2.1 Darcy Equation

Darcy's equation (equation1) was used to calculate hydraulic conductivity. Variables are defined as follows. Q = flow rate (m^3/s), K = hydraulic conductivity (m/s), i = hydraulic gradient (equation 2), Δh = head loss (m), L = length over which head loss occurs (m), A = the cross sectional area of the permeameter cell (m^2).

$$Q = KiA \quad (1)$$

$$i = \Delta h/L \quad (2)$$

The Darcy equation has the limitation that it is applicable for calculations with laminar flow conditions only. While some of the permeameter test measurements were taken while laminar flow occurred, some of the measurements were taken with turbulent flow. Because the Darcy equation provided results that were within the same order of magnitude as the laminar flow measurements for even the most turbulent measurements, it was used to calculate hydraulic conductivity in these tests.

3.3.2.2 Testing Preparation

After the tire shreds were placed in the permeameter cell, the compression cap was lowered onto them. The shreds were then compressed to the desired strain. Water was added to the permeameter until the water level was brought up to the top of the tires. The pump was started and water was circulated through the system at a constant flow rate. A gate valve controlled the amount of flow entering the permeameter and flow (Q) was determined by reading a flow meter downstream from the gate valve.

3.3.2.3 Measuring Head Loss

Flow through the permeameter was from the top to the bottom of the tire shred layer. After a constant flow (Q) was established through the testing apparatus, a period of ten minutes was required for the heads in the permeameter and the reservoir to come to equilibrium. Thus, ten minutes after a constant flow was established, the water levels in the reservoir and the permeameter cell were measured to the nearest 1.3 mm (0.05 inch). The difference in elevation between the reservoir and the permeameter cell, after the correction factor had been applied was used for the Δh value in the Darcy equation (see equation 3).

$$h_{t\,(permeameter)} - h_{t\,(reservoir)} - \text{correction factor} = \Delta h \quad (3)$$

3.3.2.4 Changing Flow Rates

After measurements were taken, the flow rate was changed. Water was either added or drained from the system in order to keep the water level near the top of the shredded tires.

3.3.2.5 Changing Tire Shred Layer Thickness

The thickness of the tire shred layer was determined from the hydraulic ram extension (equation 4). The head loss through the tires divided by the thickness of the shredded tire layer represented the hydraulic gradient (equation 2).

L = initial tire shred layer thickness - ram extension (4)

3.4 Soil Infiltration Testing

The goal of these tests was to evaluate the effect of soil infiltration on the hydraulic conductivity of the tire shreds. Hydraulic conductivity values determined for tire shreds containing soil from infiltration were compared with test results of clean tire shreds. Tests were conducted with glacial till from Ames, Iowa and loess from western Iowa. Grain size distributions for the two soils can be seen in Figure 6. Field experience has shown that loess has a high susceptibility to erosion.

Two separate tests were completed for each soil type. The two types of tests differed only in the method of allowing soil to infiltrate into the tire shreds. The first test allowed the soil to migrate into the tire shreds with a constant flow of water over a period of days. In the second test, soil was forced into the tire shred layer by adding soil to the shreds while washing it in with water. The first test demonstrated how much soil would migrate into the tire shreds under conditions simulating severe field conditions. The second test was designed to force a large amount of soil into the tire shreds without

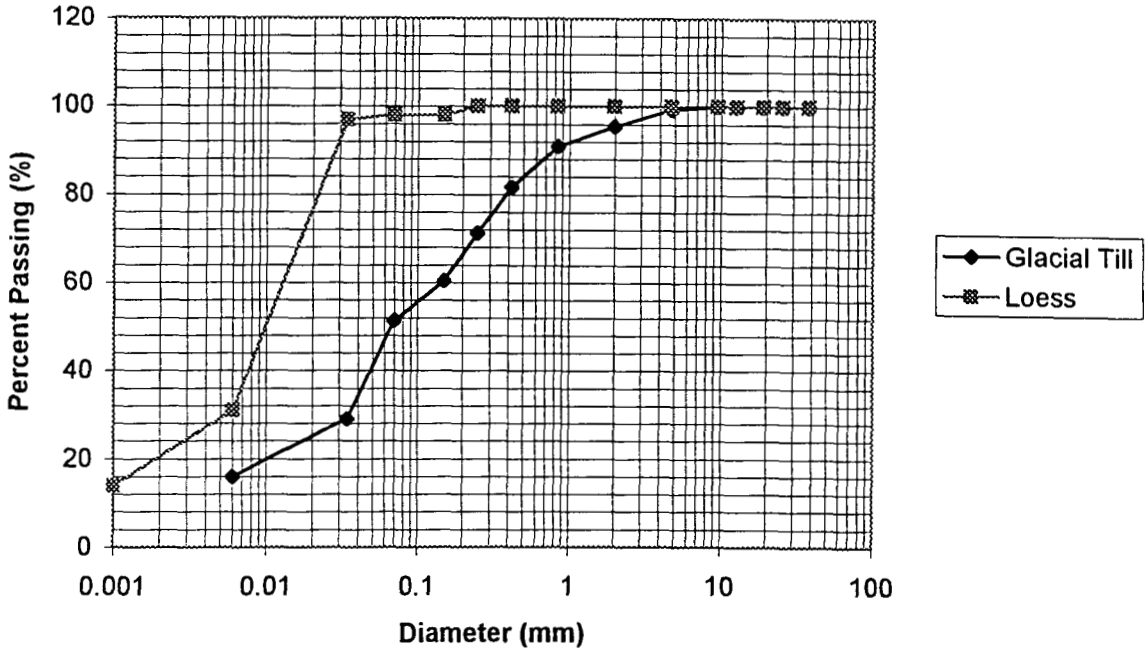

Figure 6. Particle size analysis for glacial till and loess. (Glacial till data from Ng, 1997. Loess data from Fung, 1946.)

regard to potential field conditions.

3.4.1 Soil infiltration Testing - Test Phase I

3.4.1.1 Testing Preparation

The first step in the infiltration test was to fill the permeameter cell with the same clean tire shreds used in hydraulic conductivity testing. The tire shreds were placed in the same manner as for permeability testing. The tire shreds were then compressed to 40% vertical strain and held at this strain.

A layer of soil of known weight and moisture content was then placed in the permeameter cell directly on top of the shredded tire layer. The soil was not compacted and had an initial thickness of approximately 0.254 m. Any soil clods were broken up before being placed in the cell. The test arrangement can be seen in Figure 7. The testing configuration allowed gravity to assist the migration of the soil particles into the shredded tire layer. This was an attempt to simulate the worst case soil migration scenario.

3.4.1.2 Constant Flow

A constant flow of 2.52×10^{-4} m^3/s (4 gpm) was maintained through the permeameter for a total of 50 hours for the glacial till test and 75 hours for the test with loess. The loess test time was changed to a more severe test because it was expected that the loess would more easily infiltrate the tire shreds, and more time was allowed for this to happen. During this circulation time, a head of 0.07 to 0.10 m of water was always evident above the soil layer. The water that circulated through the soil and into the tire shreds carried soil particles with it. The soil particles were either deposited in the pore spaces of the tire shreds or were carried through the shredded tires and deposited on the base of the permeameter.

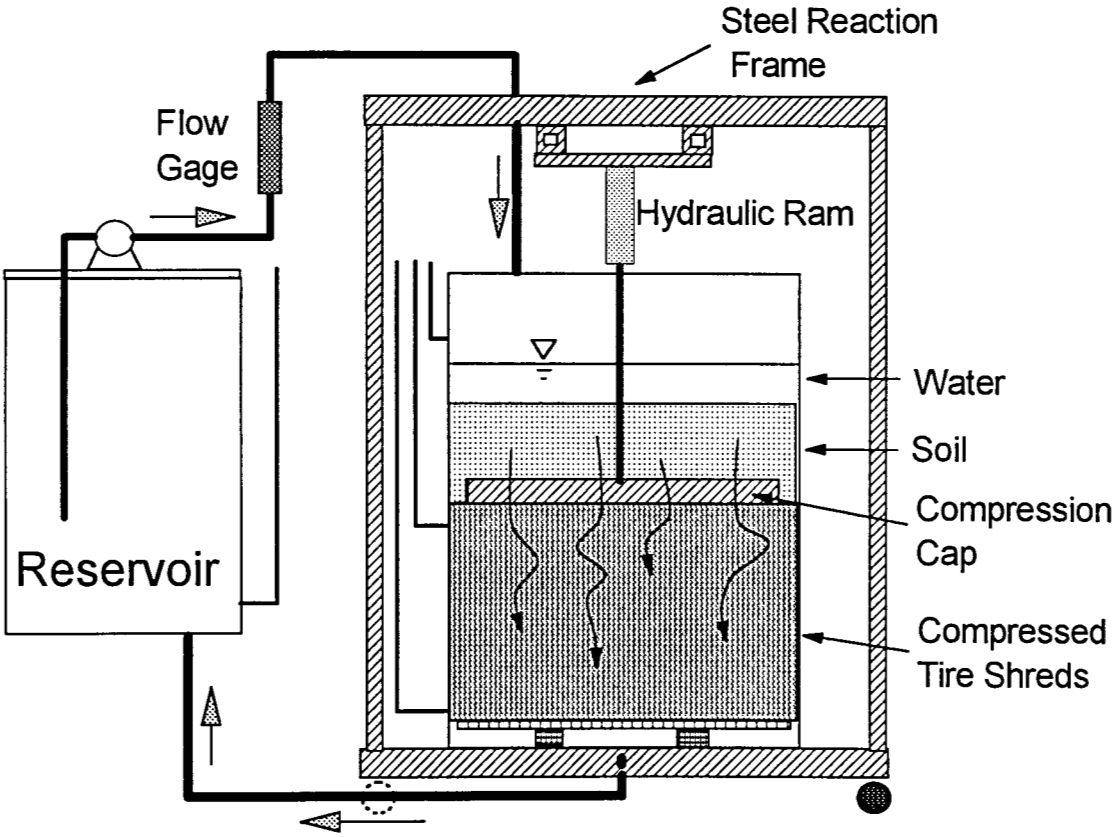

Figure 7. Soil infiltration test setup

3.4.1.3 Soil Piping

Occasionally, soil would locally pipe into the tire shreds. The resulting cavity in the soil layer created a direct route for water to travel into the tire shreds. Water would then flow through these channels instead of infiltrating through the soil. In order to promote soil infiltration instead of channel flow, the soil cavities were filled in. This usually caused other areas to pipe, thereby forcing higher quantities of soil to migrate into the tire shreds than would have occurred without filling the cavities.

3.4.1.4 Removal of Remaining Soil Layer

After steady state flow circulation was completed, all soil that had not infiltrated into the tire shreds was removed with a small trowel. The tire shreds and the compression grate were left undisturbed. All soil that was removed was allowed to air dry for several days, and then the dry weight was determined.

3.4.1.5 Hydraulic Conductivity

With the tire shreds compressed to 40% strain, hydraulic conductivity tests were carried out on the tire shreds at this strain using the same test procedure that was used for the clean tire shreds.

3.4.2 Soil Infiltration Testing - Phase II

3.4.2.1 Soil Addition

After completion of the phase I soil infiltration tests, more soil was added to the system. The compression grate was removed, which allowed the tire shreds to rebound between 0.1 and 0.15 m. Soil was then washed into the shreds by placing small amounts of soil on top of the tire shreds and washing them into the pore space using water. This method of soil addition was different than in phase I because the soil was forced into the tire shreds rather than letting it migrate into them under steady state flow. The object of this was to force as much soil into the tire shreds as possible. The soil

was washed into the tire shreds as uniformly as possible. Using this method of forced soil infiltration, a much larger amount of soil was allowed to enter the tire shreds than would have been possible using the techniques of phase I testing.

3.4.2.2 Compression Resumed

The load on the compression cap was reapplied and the tire shreds were re-compressed to 40% strain. At this point in the test, the permeameter cell contained a mass of tire shreds with soil within some of its pore space. Permeability tests were conducted using the same procedure that was used for the clean shreds.

3.4.2.3 Removal of Tire Shreds

When testing was completed on the tire shreds, they were removed from the permeameter cell. The soil that had accumulated on the bottom of the permeameter was removed and weighed. Moisture contents for the soil were determined. The same tire shreds were used for both the glacial till and loess experiments. The shreds were washed between experiments.

3.4.3 Observations Made Of The Soil Infiltration Testing

3.4.3.1 Observations Through Permeameter Sides

The contents of the permeameter could be seen through the clear Lexan plastic sidewalls. This made it possible to observe the tire shreds and soil during testing. Therefore, qualitative observations augmented the quantitative data acquired during testing. Any soil piping and soil migration along the sides of the permeameter was seen through the clear sides. Other observations included the relative amount of pore space that was clogged with soil, the sizes of pores that became filled, and the times at which most soil migration occurred.

3.4.3.2 Observation During Tire Shred Removal

After the soil infiltration and hydraulic conductivity tests were completed the tire shreds were removed. The amount of soil trapped within the pore space was observed as the shreds were removed. The distribution of soil through the thickness of the tire shred layer was noted. For instance, if more soil was trapped at the top of the tire shred layer than in the middle of bottom, that distribution was noted.

3.5 Results

3.5.1 Compression Testing

3.5.1.1 Specific Gravity and Void Ratio

The objective of the confined, one-dimensional compression testing was to develop relationships between strain, void ratio, and applied vertical stress. In order to calculate void ratio, it was necessary to know the specific gravity of the shreds. Humphrey (Humphrey et al. 1992 and Manion and Humphrey 1992) listed the apparent specific gravity of many different types of tire chips. The values ranged from 1.10 to 1.27. Void ratios for the Fort Dodge and Perry shreds were calculated using a specific gravity of 1.15, which is an average of the measured values quoted previously.

3.5.1.2 Number of Tests

Three compression tests were performed on the tire shreds from Fort Dodge with the same material used for each test. One compression test was also performed on tire shreds from Perry. The initial void ratio of the Fort Dodge tire shreds varied from 2.73 to 2.89. The Perry tire shreds had an initial void ratio of 3.19.

3.5.1.3 Height to Permeameter Width Ratio of Tire Shred Sample

When placed in the permeameter, the tire shred sample was nearly as thick as it was wide. Humphrey (1995) recommended that the ratio of height to diameter for a

sample of tire shreds should be less than one because higher ratios are influenced more by side friction that would lead to less compression and therefore lower strain measurements. Humphrey applied this criterion to compression tests performed in circular compression cells. The equipment used here had a square compression chamber, and the ratios were calculated using the width of the cell, which represented its smallest cross section. Also, the tire shreds had little contact with the corners of the cell. For these reasons, it was determined that the sample width to height could exceed 1 by a small amount and still produce satisfactory results. Before compression, the Fort Dodge tire shreds had a sample thickness to width ratio ranging from 1.01 to 1.05. The ratio of the Perry tire shreds was 1.13

3.5.1.4 Comparison of Results

The results of the compression testing, plotted as vertical strain versus applied vertical stress, can be seen in Figure 8. The vertical stress was calculated by dividing the force applied by the hydraulic ram by the cross sectional area of the permeameter cell. All of the tests showed similar trends in their results. The Perry tire shreds showed results nearly identical to those exhibited by the Fort Dodge shreds.

3.5.1.5 Strain as a Function of Vertical Stress

Figure 8 shows that the tire shreds underwent very large strain during the initial stages of loading. A large percentage of the initial strains are probably due to bending of the tire shreds to take up void space. The curve flattens as strain increases. This strain hardening is typical of any particulate system in confined compression.

3.5.1.6 Void Ratio as a Function of Vertical Stress

The results of the compression testing are plotted as void ratio as a function of vertical stress in Figure 9. It was assumed that individual tire shreds were incompressible. The effects of individual tire shred compression would be very small

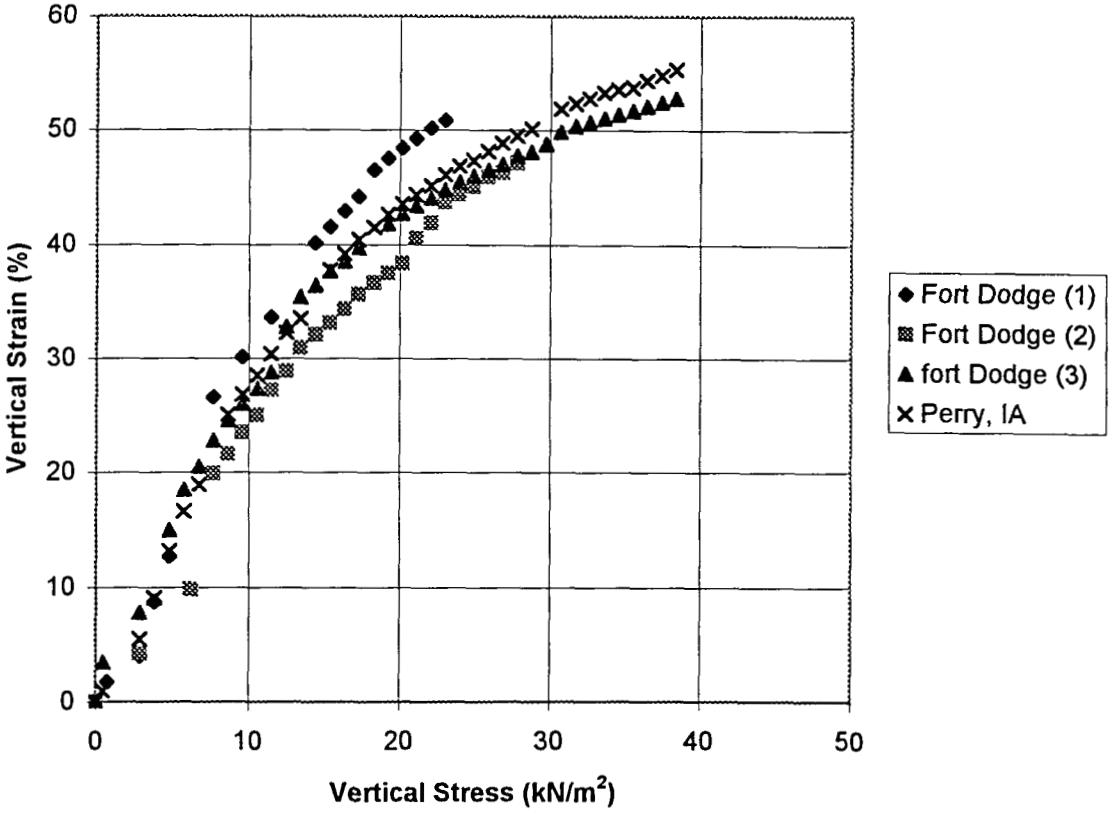

Figure 8. Strain as a function of vertical stress.

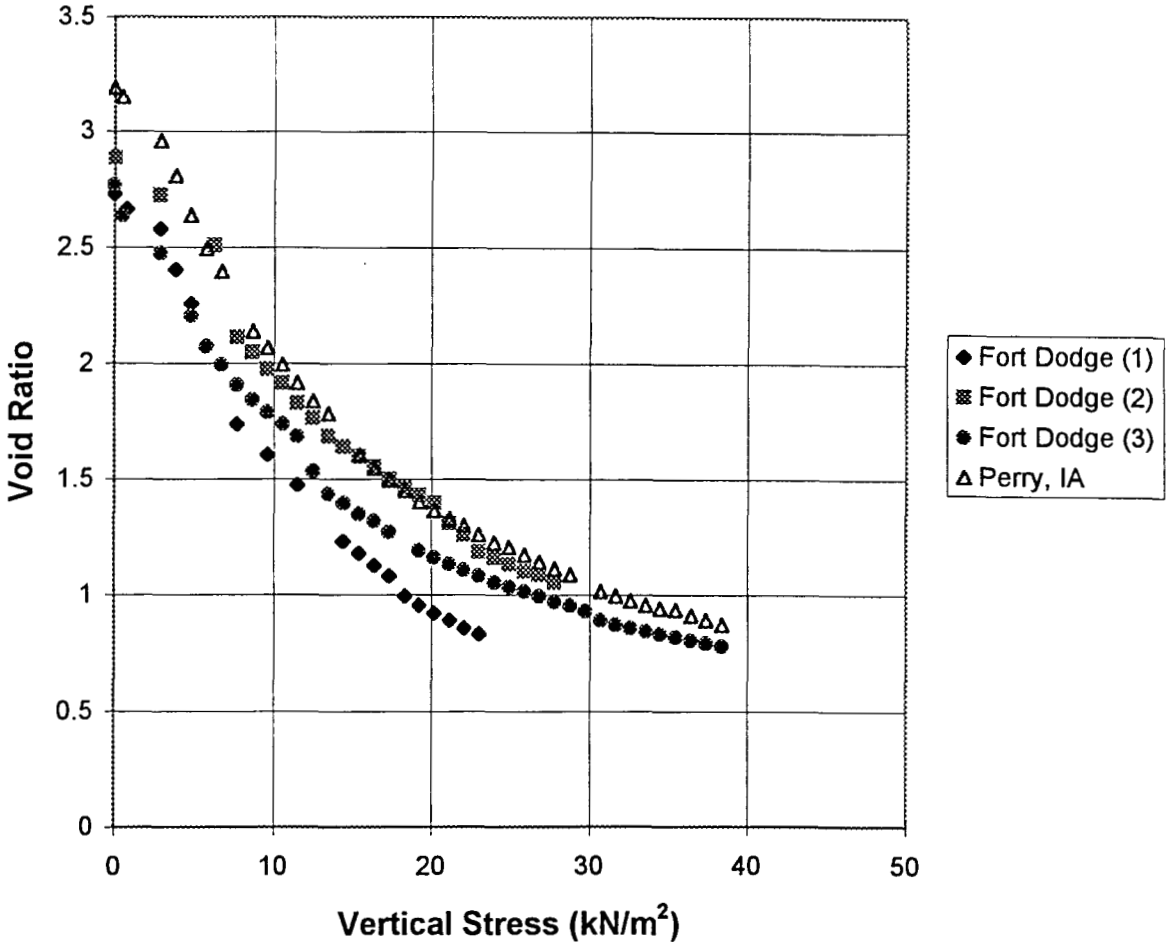

Figure 9. Void Ratio of tire shreds as a function of vertical stress. (Assuming a specific gravity of 1.15)

compared to the compression due to loss of void space.

The void ratios for either uncompressed or compressed tire shreds were much higher in these experiments than those that would be expected in sand or gravel, which typically have void ratios of 0.25 to 0.54 (Fetter 1994).

3.5.2 Hydraulic Conductivity Testing

3.5.2.1 Perry Shreds

The hydraulic conductivity of the tire shreds was expected to be very high because of the high void ratios and large interconnected pore spaces. The results of testing on the Perry shreds can be seen in Figure 10. Figure 10 shows data points from testing as well as logarithmic best fit lines calculated by the spreadsheet program.

Logarithmic trendlines were used as best-fit lines because they provided the best visual fit of data. The trendlines are not used to represent exact values of the shredded tire hydraulic conductivity. Nearly every test showed results with some scatter of the data points. The best-fit lines show an average trend of the data points, but the actual hydraulic conductivity of the shredded tires might actually lie somewhere within the data scatter. The trendlines are not meant to represent a degree of accuracy that may not actually exist. For a complete analysis of the potential errors involved with hydraulic conductivity, please see Appendix A.

3.5.2.2 Fort Dodge Shreds

The hydraulic conductivity of the Fort Dodge shreds showed results similar to the Perry shreds (see Figures 11 and 12). Figure 11 shows the hydraulic conductivity calculated from the results of tests at various vertical strains. Figure 12 shows logarithmic trendlines calculated by the spreadsheet program using the data points from each of the Fort Dodge shred hydraulic conductivity tests.

3.5.2.3 Effects of Strain on Hydraulic Conductivity

In both the Perry and Fort Dodge tests, tire shreds that underwent increased vertical strain tended to have lower hydraulic conductivity than tire shreds at lower strains. For instance, the Fort Dodge shreds at 0% vertical strain showed a higher hydraulic conductivity than those at 53% vertical strain. Compression of the tire shreds caused a decrease in void ratio, which resulted in fewer and smaller pore spaces. Decreased pore size caused more head loss due to friction when water was circulated through the tire shreds. Increased head loss translated to lower hydraulic conductivity.

For the lower strains (0% to 32% vertical strain), the hydraulic conductivity showed a dependence on flow rate and gradient. This characteristic indicated that non-laminar flow was occurring at that strain (Edil and Bosscher, 1994). The tire shreds under the higher vertical strains of 40% to 53% showed very little dependence on flow rate, indicating that flow was laminar.

The hydraulic conductivity of the tire shreds was noticeably different between vertical strains of 0% and vertical strains of 50%. However, there was virtually no difference in hydraulic conductivity measured between tire shreds at 30%, 40%, and 50% vertical strain.

3.5.2.4 Field Application

Depending on the field application of a tire shred horizontal drain, either very high or very low amounts of water could pass through the drain. If the horizontal drain had no open inlet and the only water that entered the drain was from the surrounding soil, very low flows would typically be expected. For instance, if a 30 meter horizontal drain was placed in glacial till with a hydraulic conductivity of 0.0003 cm/s (Tsai, 1991),

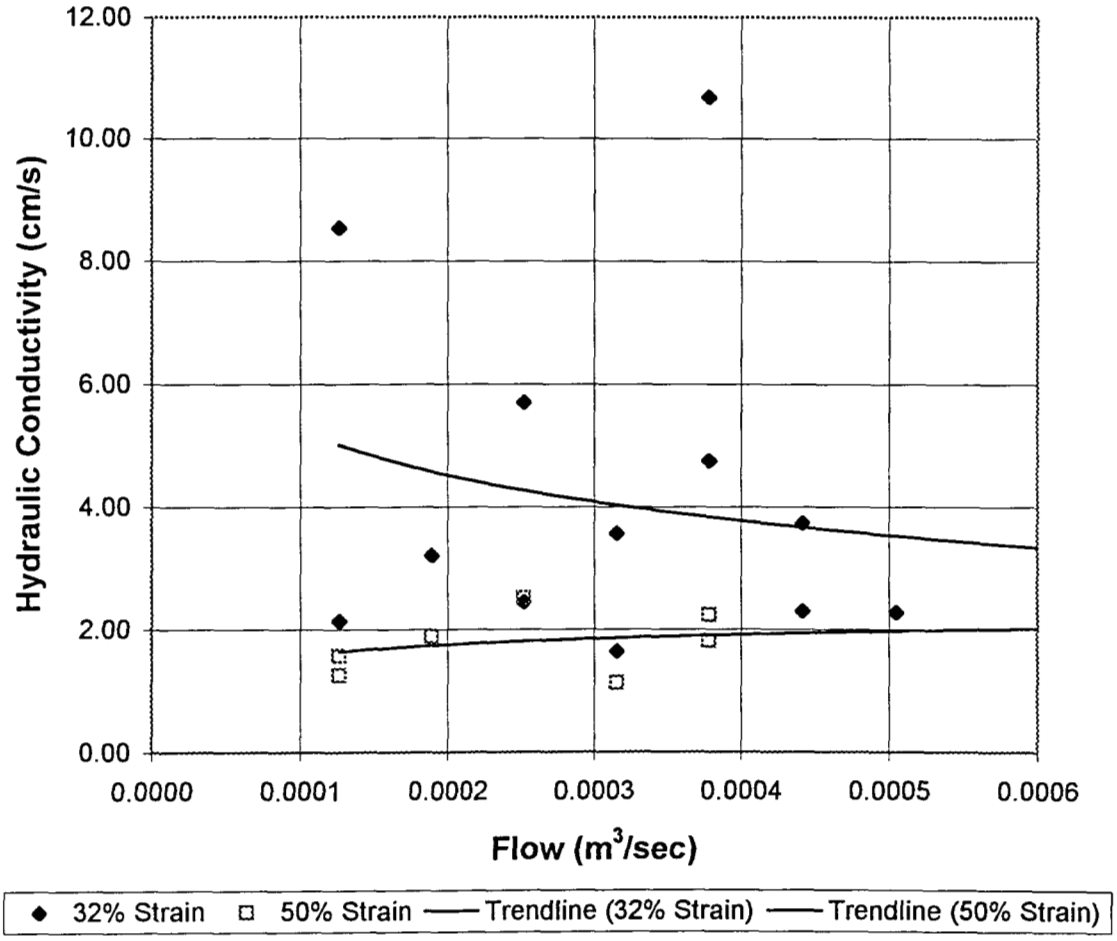

Figure 10. Hydraulic conductivity of Perry tire shreds. Data points and logarithmic best-fit trendlines are presented.

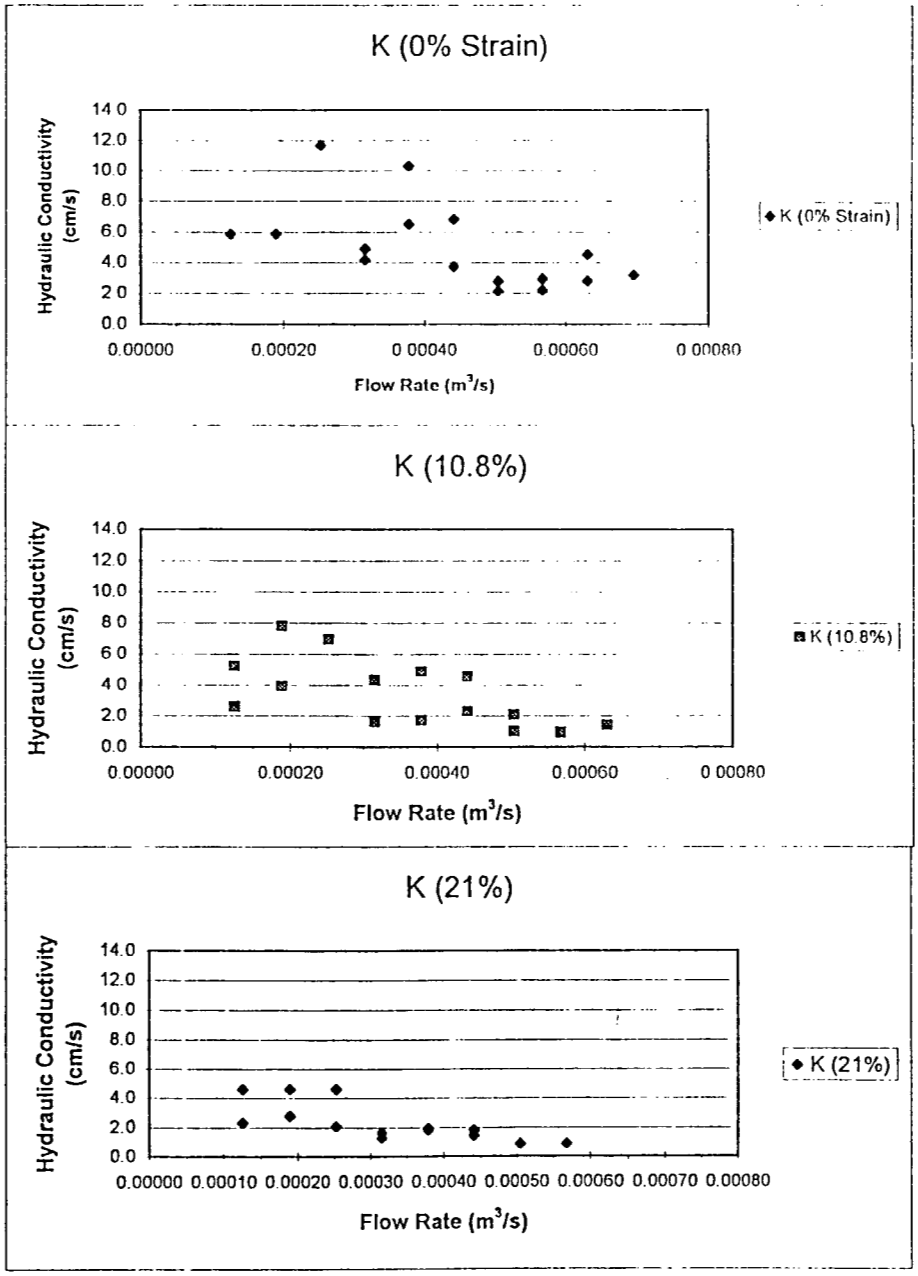

Figure 11. Hydraulic conductivity data points for Fort Dodge tire shreds at various vertical strains

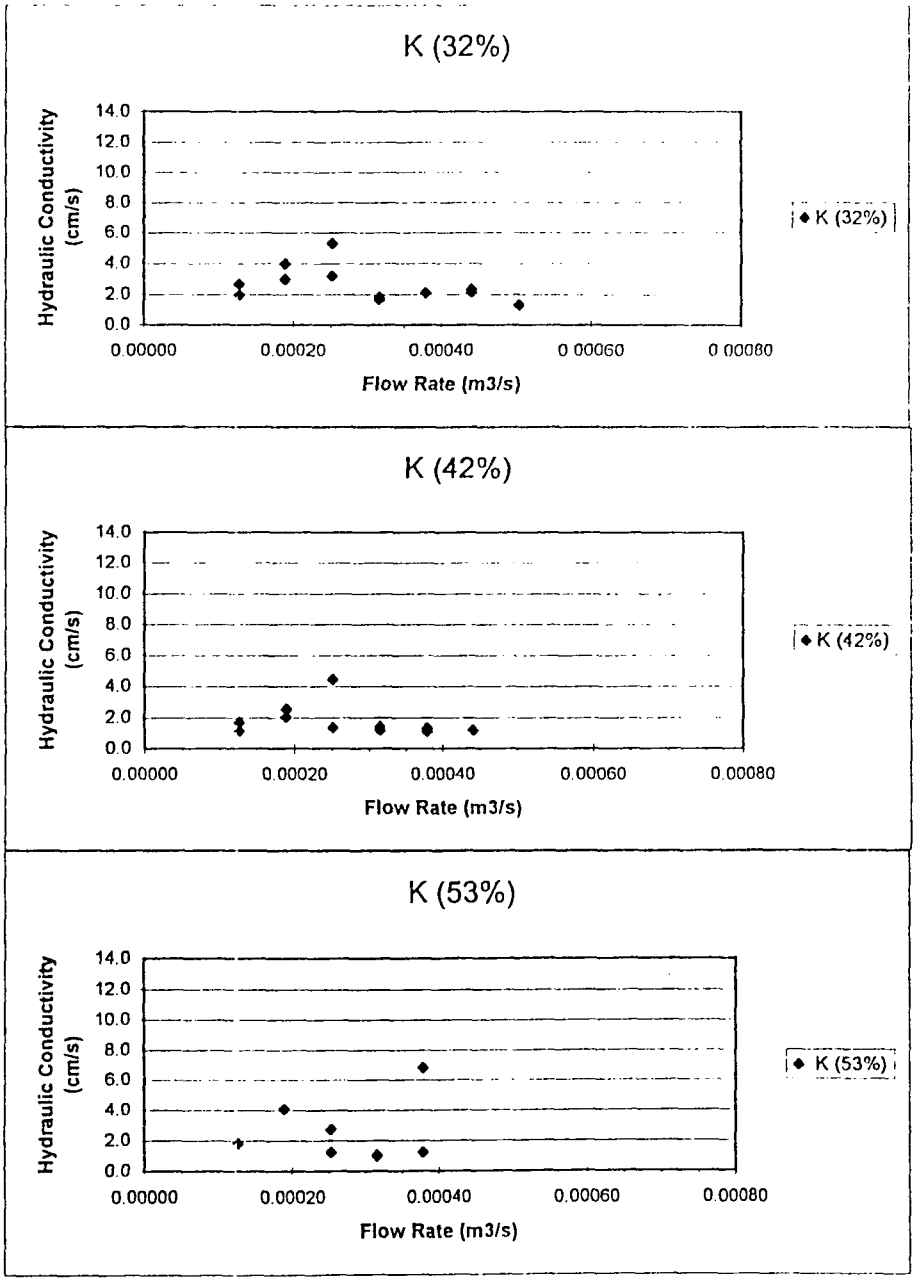

Figure 11 (Continued).

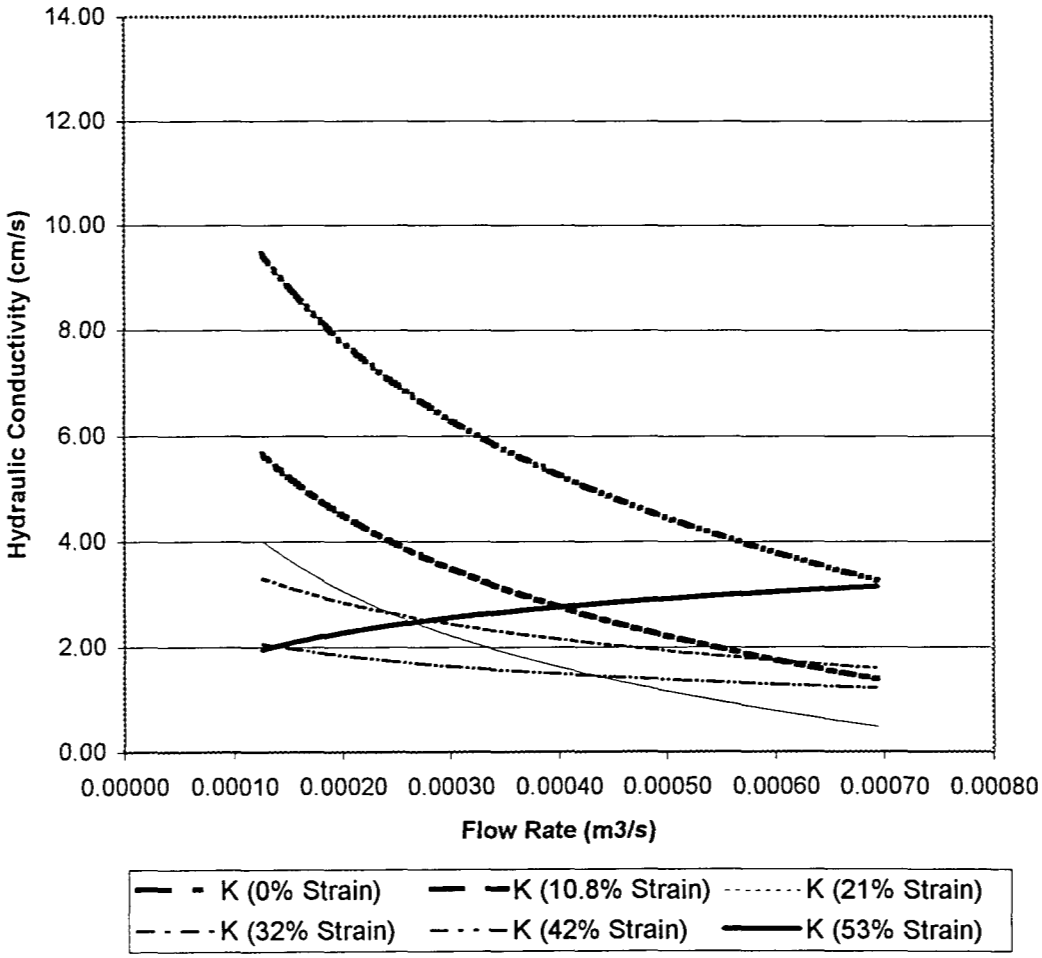

Figure 12. Logarithmic trendlines for Fort Dodge tire shred hydraulic conductivity data.

with the groundwater table 1 m above the bottom of the drain, a flow rate of about 0.000003 m^3/s (0.04 gpm) would be expected to exit the drain. At this low flow rate, laminar flow would be expected regardless of the tire shred vertical strain.

If, however, the tire shred horizontal drain was designed to serve as a culvert, with both an open inlet and an outlet, much larger flow rates could be expected. Depending on the size of the catchment area, flows greater than the 0.0008 m^3/s (13 gpm) used during hydraulic conductivity testing could be expected. In these cases, non-laminar flow could occur.

3.5.3 Soil Infiltration Testing

Figure 13 shows the results of the soil infiltration experiments using glacial till. Figure 14 shows the results for those involving loess. The weight of the soil within the tire void spaces for each of the groups of tests is indicated. The addition of these weights of soil to the shredded tires did not significantly reduce their hydraulic conductivity.

3.5.3.1 Differences Between Lab And Field Conditions

3.5.3.1.1 Gradients. There are several types of applications where a shredded tire horizontal drain would have standing water above it. For instance, drains placed in low areas might have ponded water on the backfill after wet periods. Also, the backfill could have a lower surface elevation than the surrounding ground surface due to surface settlement when the shredded tires settled. The resulting depression above the horizontal drain could allow water to pond.

The two phases of soil addition during the soil infiltration testing were designed to simulate extreme conditions of soil migration. Such extreme conditions would rarely occur in the field. A much thinner layer of soil was placed above the tire shreds

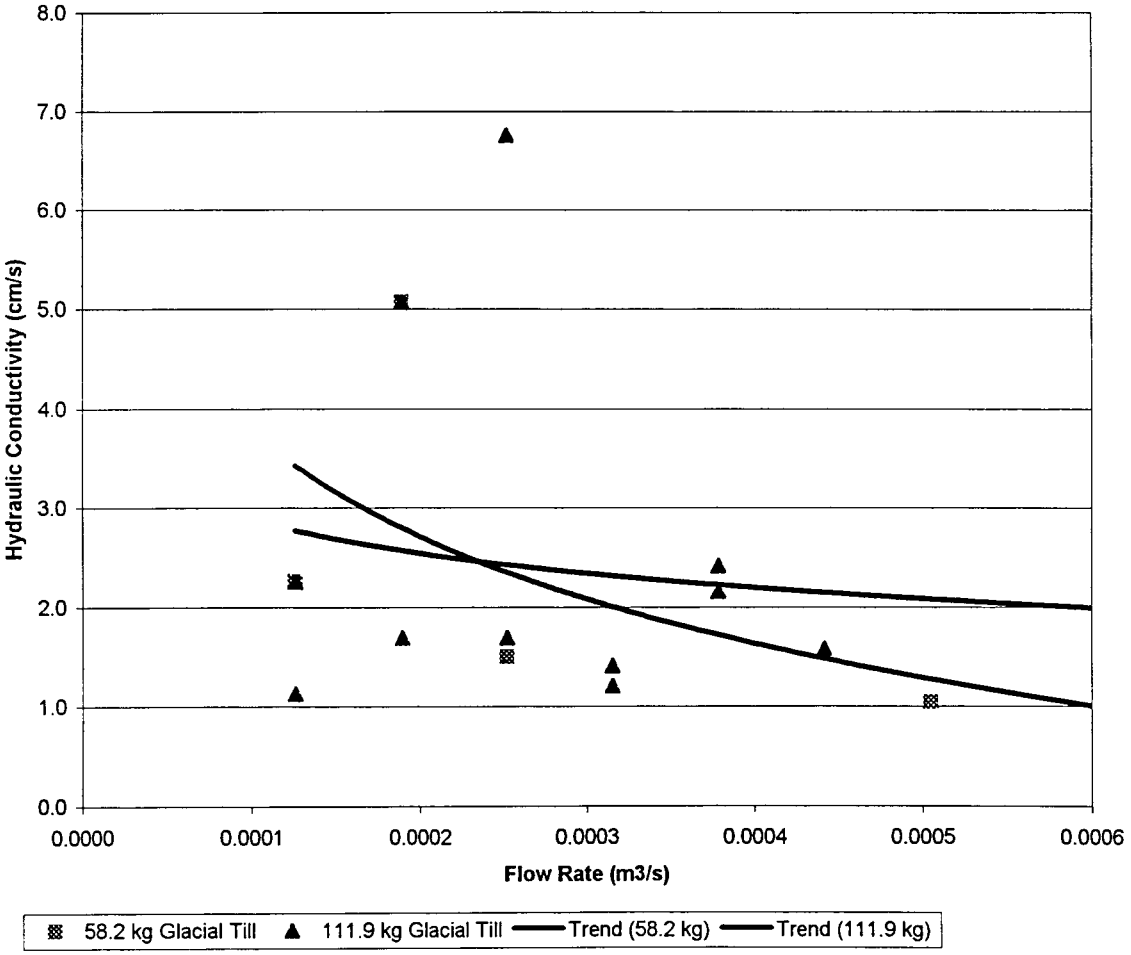

Figure 13. Hydraulic conductivity of tire shreds at 40% vertical strain with glacial till soil infiltration

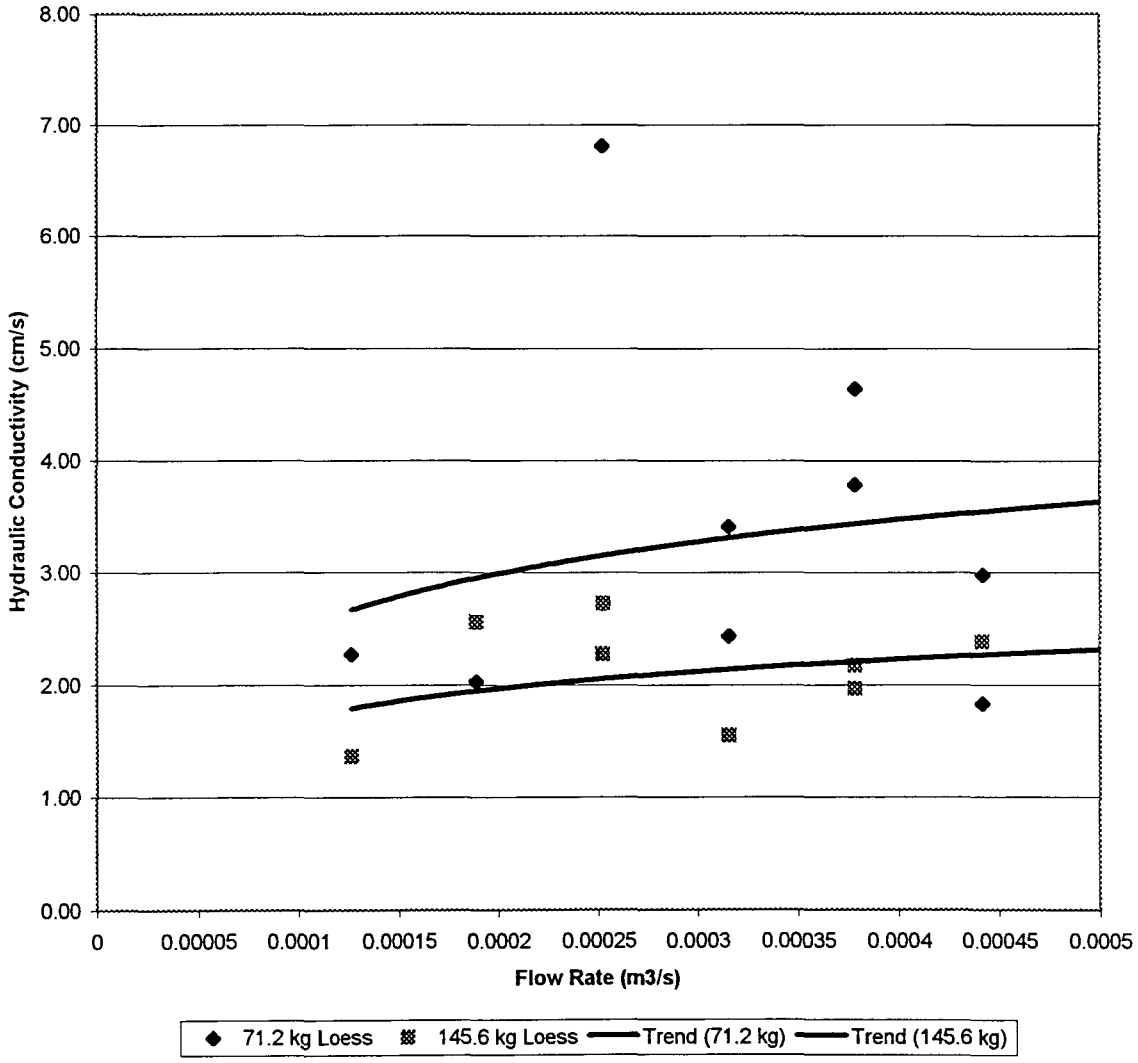

Figure 14. Hydraulic conductivity of tire shreds at 40% vertical strain with loess soil infiltration.

than would be placed in the field. This led to much higher gradients through the soil during the lab testing than would normally be found in the field. In the lab tests, a 0.25 m thick layer of soil was placed above the tire shreds with 0.1 m of water above the soil. Assuming that the bottom of the soil layer was free draining (pressure head equal to zero) the gradient through the soil was 1.4. A horizontal drain placed in the field would probably have at least 0.6 m of backfill placed above the shredded tires. If 0.1 m of water was standing above a 0.6 m layer of free draining soil, the gradient through the soil would be only 1.16. Lower gradients would result in less chance of soil piping occurring.

3.5.3.1.2 Soil Piping. Soil piping tends to occur where cracks and joints concentrate flow within a soil mass (Townsend et al., 1987). If the hydraulic gradient becomes high enough, piping erosion commences. In the soil infiltration experiments soil piping occurred frequently along the side of the permeameter or in the center where the ram extension entered the soil layer. The sides of the permeameter probably acted as a vertical soil crack, concentrating the flow along the permeameter sides. A horizontal drain could have vertical cracks due to desiccation and backfill settlement. The laboratory tests served to simulate the worst-case field scenario. Because of lower gradients piping is much less likely to occur in the field.

3.5.3.1.3 Amount of Flow. The lab test was designed to circulate a large amount of water through the soil layer in a relatively short period of time. It was possible to estimate the amount of time that would be required for an equal amount of water to pass through the same area of a field drain. A modified Darcy equation (equation 6) was used to arrive at an estimate. Q = total volume of flow (m^3), t = time (s).

$$Q/t = KiA \qquad (6)$$

It was assumed that the only flow through the soil layer and into the tire shreds

was vertical as the result of standing water above the soil. The soil layer was assumed to be a uniform thickness of 0.6 m with 0.1 m of standing water. This would result in a gradient of 1.16. The hydraulic conductivity of the soil layer was assumed to equal that of weathered glacial till (0.000003 m/s) (Tsai, 1991). The area of flow was taken to be equal to the cross-sectional area of the lab permeameter (0.8 m^2). The total volume of flow during laboratory testing was 45.4 m^3 for the glacial till lab infiltration test and 63.5 m^3 for the loess test.

3.5.3.1.4 Time Simulated by Test. It would take 189 days for 45.4 m^3 of water to flow through a 0.8 m^2 area of the field drain using the stated assumptions. Using the same assumptions, it would take 264 days for 63.5 m^3 of water to flow through a 0.8 m^2 area of the field drain. Taking the calculation one step further, we might assume that the field drain would have standing water above it for a maximum of 30 days per year. In this case, the lab test would have simulated a period of 6.3 years for the glacial till test and 8.8 years for the loess test.

3.5.3.2 Observations Made During Testing

3.5.3.2.1 Soil Migration. During the initial phase of testing, it was observed that much of the soil migration occurred very early in the test, soon after flow was started. Towards the end of the test, no soil was observed migrating into the tire shred void spaces. From what could be seen through the clear sides of the permeameter, large pores tended to fill quickly with soil. Piping occurred above some of the large pores, which accelerated the infiltration process. Once the large pores were clogged, smaller pores were forced to carry the water flow. Assuming continuity of flow, the smaller pores then had a higher velocity of flow (see equation 7). The lower velocities of the larger pores was not enough to carry the migrating soil, so the soil settled in the pore space. The higher velocities of the smaller pores carried the migrating soil through the pores.

$$V_1A_1 = V_2A_2 \qquad (7)$$

This is not to say that no small pores were plugged. The smaller pores in some ways were more prone to plugging because of their smaller diameter and sinuosity. However, small pores that were forced to carry a large amount of flow because of clogging of an adjacent large pore, had high velocities and did not become clogged. Figure 15 illustrates a large pore becoming clogged while a connecting small pore remains open. In the 'before' illustration, water flows through both the large and small diameter pores. In the 'after' illustration, the same amount of flow occurs, but the entire flow is concentrated in the small pore. The same flow is required to move through a smaller area, thereby increasing the velocity of flow (equation 7). The increased velocity in the smaller pore would then prevent clogging. Examples of this behavior were observed during testing.

3.5.3.3 Soil Infiltration

3.5.3.3.1 Amount of Soil Deposited. Table 2 shows the weights of soil trapped in the shred voids versus those deposited on the bottom of the permeameter. Because the tires were not removed between the two phases of soil addition, data on how much soil was deposited on the bottom during the first tests is not available.

3.5.3.3.2 Void Ratio of Tire Shreds. Table 3 shows the void ratios of the shredded tires before and after soil infiltration testing. Void ratios were reduced as soil infiltrated the pore spaces of the tire shreds. Table 3 also shows the percentage of void space that was lost due to soil infiltration.

3.5.3.3.3 Removal of Shreds. The amount of soil that had infiltrated into the tire shreds was observed as the shreds were removed. When the glacial till tests were completed, most of the infiltrated soil was found in the top half of the shredded tire layer. The coarser fractions of the glacial till were caught in void spaces and had not migrated

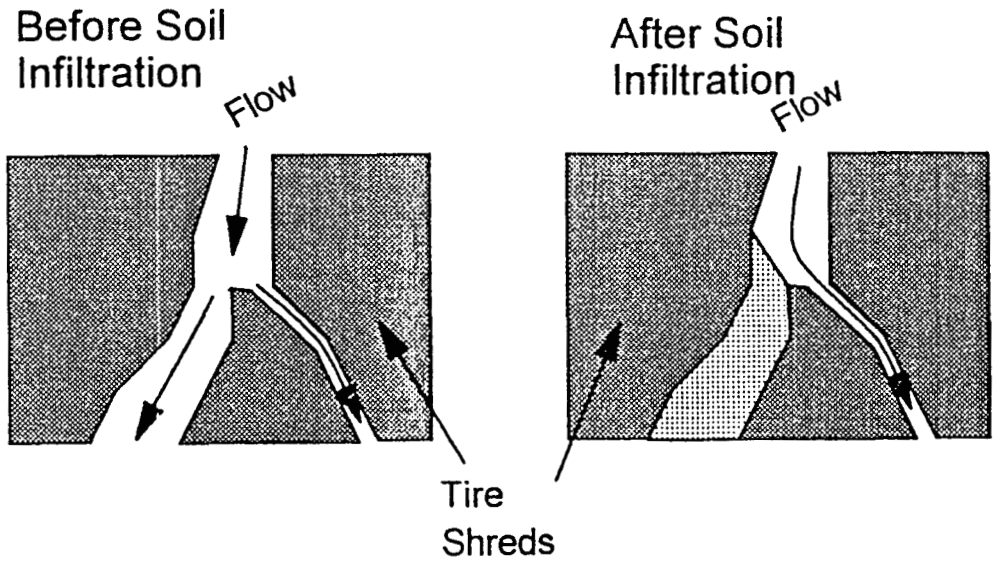

Figure 15. An illustration of two pore spaces before soil infiltration (left) and after soil infiltration (right). After soil infiltration, the smaller pore space must conduct the same amount of water that the two pores originally carried. The velocity of the smaller pore is increased, and it does not become clogged.

to the bottom of the permeameter. The bottom half of the tires had a thin layer of silt and clay covering the shreds.

The results of the loess testing differed slightly from the glacial till tests. When the tires were removed after testing, the majority of the loess was observed to be trapped within the pore space in the top half of the tire shred mass. However, the loess was more uniformly distributed through the remaining mass of tire shreds than was the glacial till. Table 2 shows that more than eight times as much loess than glacial till was deposited on the floor of the permeameter.

3.5.3.4 Hydraulic Conductivity

The addition of glacial till into the tire shreds had a negligible effect on the tire shred hydraulic conductivity. The hydraulic conductivity of the tire shreds after the first phase of infiltration testing was nearly identical to the hydraulic conductivity after the second phase. The results of glacial till infiltration on the hydraulic conductivity of the tire shreds can be seen in figure 13.

The loess experiments (figure 14) had only slightly different results than the glacial till tests. Loess infiltration had little effect on the hydraulic conductivity of the tire shreds. The addition of loess during the second phase of infiltration testing lowered the

Table 2. Results of Soil Infiltration

Test	**Soil Trapped in Shred Void Spaces (kN)**	**Soil Deposited On Permeameter Bottom (kN)**
Glacial Till		
1st Phase Soil Infiltration	0.571	Not Available
2nd Phase Soil Addition	1.080	0.023
Loess		
1st Phase Soil Infiltration	0.698	Not Available
2nd Phase Soil Addition	1.230	0.196

Table 3. Void ratio reductions during soil infiltration testing.

Test	Void Ratio Before Test	Void Ratio After Test	Total Percentage of Void Space Lost
Glacial Till			
1st Phase Soil Infiltration	1.16	0.94	19
2nd Phase Soil Addition	0.94	0.78	33
Loess			
1st Phase Soil Infiltration	1.16	0.90	22
2nd Phase Soil Addition	0.90	0.69	41

hydraulic conductivity from 3 cm/s to 2 cm/s. More soil was deposited on the bottom of the permeameter, probably because of the higher fines content of the loess. The water moving through the tire shreds carried the smaller particles more easily. If the tire shreds had been part of a horizontal drain, the loess either would have settled on the bottom of the drain or would have been carried through the drain outlet. Soil infiltration over an extended period of time could cause clogging of the drain starting from the bottom up. It is not clear from these tests how much soil it would take to decrease the hydraulic conductivity, what period of time would be required, or even if a drain would be likely to become clogged after a long period of time.

Table 3 shows the void ratios of the shredded tires before and after soil infiltration testing. The volume of soil that had migrated into the shredded tires was calculated using a specific gravity of 2.65 for the soil particles. Void ratios were reduced as soil infiltrated the pore spaces of the tire shreds. Table 3 also shows the percentage of void space that was lost due to soil infiltration.

The addition of soil to the tire shreds had little effect on their hydraulic conductivity because the tire shreds had a very high void ratio with many large

interconnected pore spaces. Even when many of the large pore spaces were observed to be filled with soil, many smaller pores remained open and connected. The flow merely bypassed the blocked pores and moved through the smaller ones. The hydraulic conductivity tests that were done used flow rates of 0.0001 m^3/s (2 gpm) to 0.0005 m^3/s (8 gpm). Only a small number of interconnected pores were required to conduct the water flow. Flow was controlled by these open pores rather than by the blocked pores. At least for low flow rates, such as those used in these tests, hydraulic conductivity would not be much affected by soil addition until no large interconnected pores remained.

3.6 Discussion Of Lab Testing

A large-scale permeameter was developed for testing the compressibility and hydraulic conductivity of large size tire shreds. The effect of soil migration into the tire shreds on hydraulic conductivity was also studied.

3.6.1 Hydraulic Conductivity

The tire shreds were compressed to vertical strains of 50% at vertical stresses of 20 to 30 kN/m^2. This represents a depth of backfill (γ_t = 17.5 kN/m^3) of 1.1 m to 1.7 m.

The hydraulic conductivity, determined for the tire shreds at a number of vertical strains, was dependent on the hydraulic gradient at lower strains, but was fairly constant when tested at strains of 40% or greater. The results obtained from testing are lower than some other researchers have reported. Chen, Lawrence, and Humphrey (1997) documented much higher values for hydraulic conductivity using smaller tire shred sizes with much lower void ratios. Table 4 shows tire shred characteristics from a number of sources.

A possible explanation for the lower hydraulic conductivities of the Fort Dodge and Perry tire shreds than other published results was that the design of this

Table 4. Summary of Tire Shred Characteristics

Tire Shred or Media Type	Vertical Strain (%)	Density (kN/m^3)	Void Ratio	Hydraulic Conductivity (cm/s)	Reference
Fort Dodge	0 32 53	3.00 4.46 6.35	2.77 1.53 0.78	9.0 3.2 1.8	
Perry, IA	0 32 50	3.22 4.75 6.45	3.19 1.78 1.09	N/A 5.0 1.8	
7.6 cm chip 7.6 cm chip	N/A N/A	5.90 7.88	1.11 0.58	15.4 4.8	Humphrey et al. (1992, 1993)
Pine State	0 17	6.58 7.85	0.86 0.55	16.3 5.6	Chen et al. (1997)
3.8 cm chip	N/A	N/A	N/A	2.6	Hall (1990) as reported by Humphrey (1993)

permeameter differed from the design used by other investigators. The collar that was used to slow down sidewall leakage in the Fort Dodge and Perry testing led to lower hydraulic conductivity values than would have been measured without the collar. It is possible that flow along the permeameter sides produced higher hydraulic conductivities for the smaller tire chips used in other studies. Regardless of how the results differed from other published studies, these hydraulic conductivities were all very high. Values for hydraulic conductivity of the shredded tires from all studies were much higher than sands and gravels, which range from 1 to 10^{-3} cm/sec (Fetter, 1994).

3.6.2 Soil Infiltration

The results of the soil infiltration tests indicate that soil migration into the shredded tire void spaces does not measurably decrease hydraulic conductivity. The

hydraulic conductivity of the tire shreds was between 1.5 and 3 cm/s with or without soil infiltration. The results of the glacial till and loess infiltration tests indicate that a geotextile filter might not be necessary for subsurface drains placed in glacial till. During glacial till testing, soil mainly migrated into the top half of the shredded tire layer, very little soil was deposited on the bottom of the permeameter, and hydraulic conductivity was not much affected by the added soil. During loess infiltration testing, over 1.42 kN of loess migrated into the tire shreds without affecting the hydraulic conductivity. Of that 1.42 kN, 1.23 kN of the loess was trapped in the pore space of the tire shreds.

The infiltration tests represented extreme conditions. Field subsurface drains are not likely to be exposed to these situations. The results of these tests indicate that the shredded tires could be effectively used as a horizontal drain with little potential future clogging.

The data collected from these laboratory tests indicate that large shredded tires are an effective medium for subsurface drains. The tire shreds have high hydraulic conductivity even when compressed to strains on the order of 50%, and they are not significantly affected by soil migration into their pores.

4 FIELD RESEARCH

4.1 Site Location

The shredded tire field structures were constructed on the property of Dodger Enterprises, Fort Dodge, Iowa. The field structures were placed at NE ¼, NE ¼, Sec. 21, T. 89 N, R. 28 W. The location is shown on the USGS topographic map reproduced in Figure 16. The contour interval of the map is 10 feet.

The structures were built in an industrial area in the southern portion of Fort Dodge, IA. The structures are situated in an area bordered to the east by buildings and to the west by a gravel quarry. The buildings are currently used for a tire collection and recycling operation. The gravel quarry sometimes is used as a source of sand and gravel.

4.2 Site Geology

4.2.1 Site Stratigraphy

The geology of the field site was thoroughly characterized before installation of the field structures. Topographic maps, USDA Soil Surveys, and USDA aerial photographs of the area were studied in detail in order to gain a preliminary understanding of the geology and topography of the area. Two hand augured boreholes were completed to depths of 2 m and a drill rig was used to auger ten 4.6 m deep holes and one 7.6 m deep hole. Piezometers were installed in each of the thirteen boreholes. Figure 17 shows the site layout and borehole locations. When the subsurface investigation was completed, a detailed study of the site stratigraphy was carried out.

4.2.2 Soil Characteristics

. The thirteen boreholes were used for stratigraphic characterization. Soil textures and colors were logged as the boreholes were augured. Boring logs are located in Appendix B. Samples were collected for laboratory tests, including: grain size

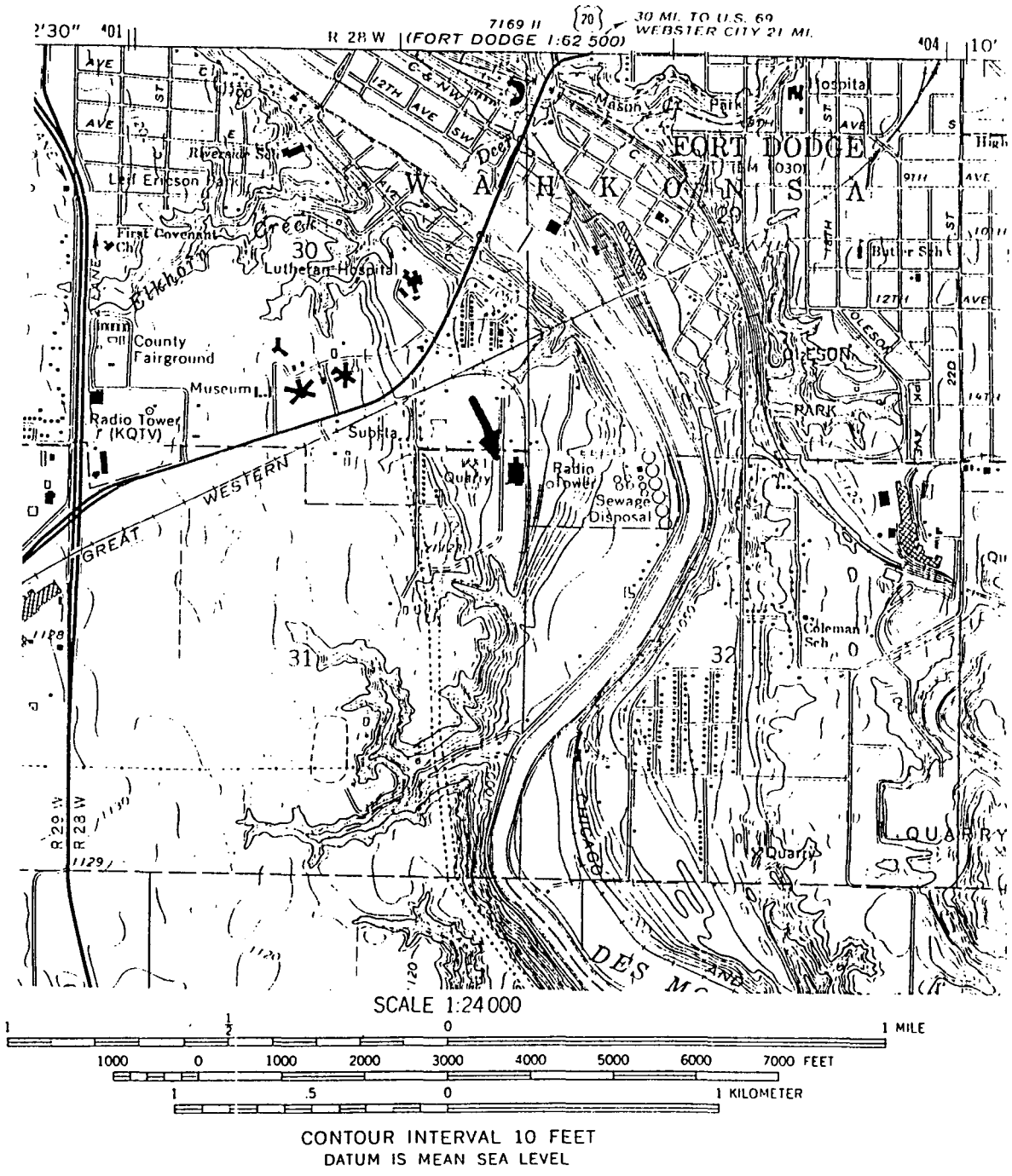

Figure 16. Location of field site on USGS Fort Dodge South topographic map.

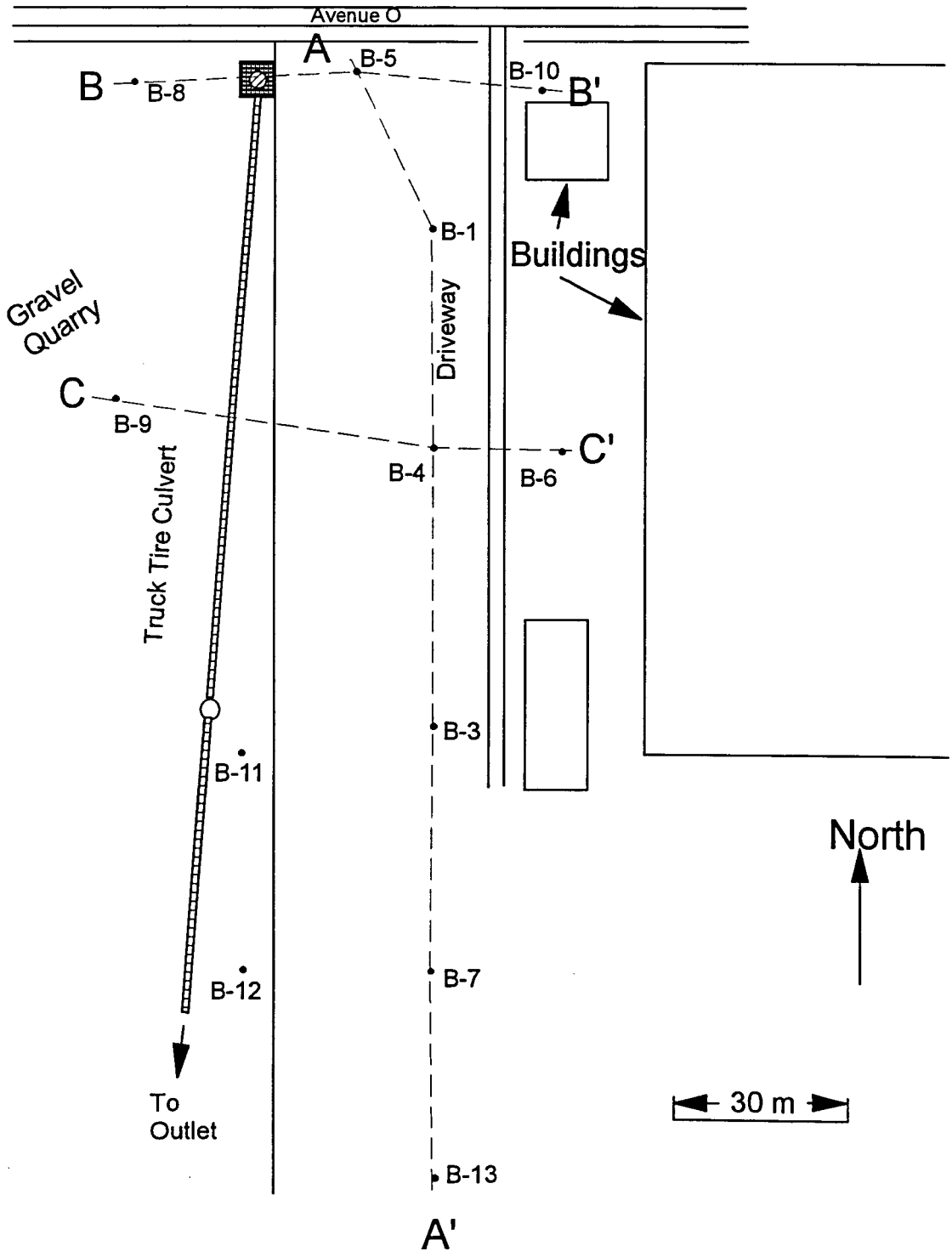

Figure 17. Site layout and location of boreholes.

distribution, and Atterberg limits. This data was used to classify the soils according to the USCS classification. The data is in Appendix B. Soils found on site were mainly sands and glacial till.

According to the USDA Soil Survey of Webster County, Iowa, the soil series present at the site are the Talcott and the Wadena. These series consist of loams and clay loams overlying sands and gravels. The Soil Survey states that both of these soil series formed in loamy alluvium that is underlain by sands and gravels. Both soils form on benches, and the Wadena series commonly occurs on benches or terraces along the Des Moines River.

4.2.3 Geologic Interpretation

The field site is located on a terrace of the Des Moines River (see figure 16). Fluvial deposits of sand and silty sand overlie glacial till and a layer of topsoil overlies the sand. During trench excavation for the drain structures, crossbedding was evident in the sand layers.

Figure 18 shows a north-south cross section of the field site that was drawn from the information obtained using borehole logging and sampling. Figure 19 shows two east-west cross sections of the field site. All of the cross sections show USCS classification of the soils.

4.3 Tire And Shredded Tire Structures

4.3.1 Truck Tire Culvert

Three scrap tire test structures were constructed on the property of Dodger Enterprises. The first structure that was constructed was a whole truck tire culvert, similar to a truck tire culvert that was already in place on the property. This structure was constructed by placing whole truck tires side by side in a trench so that the inner open space of the tires formed a conduit.

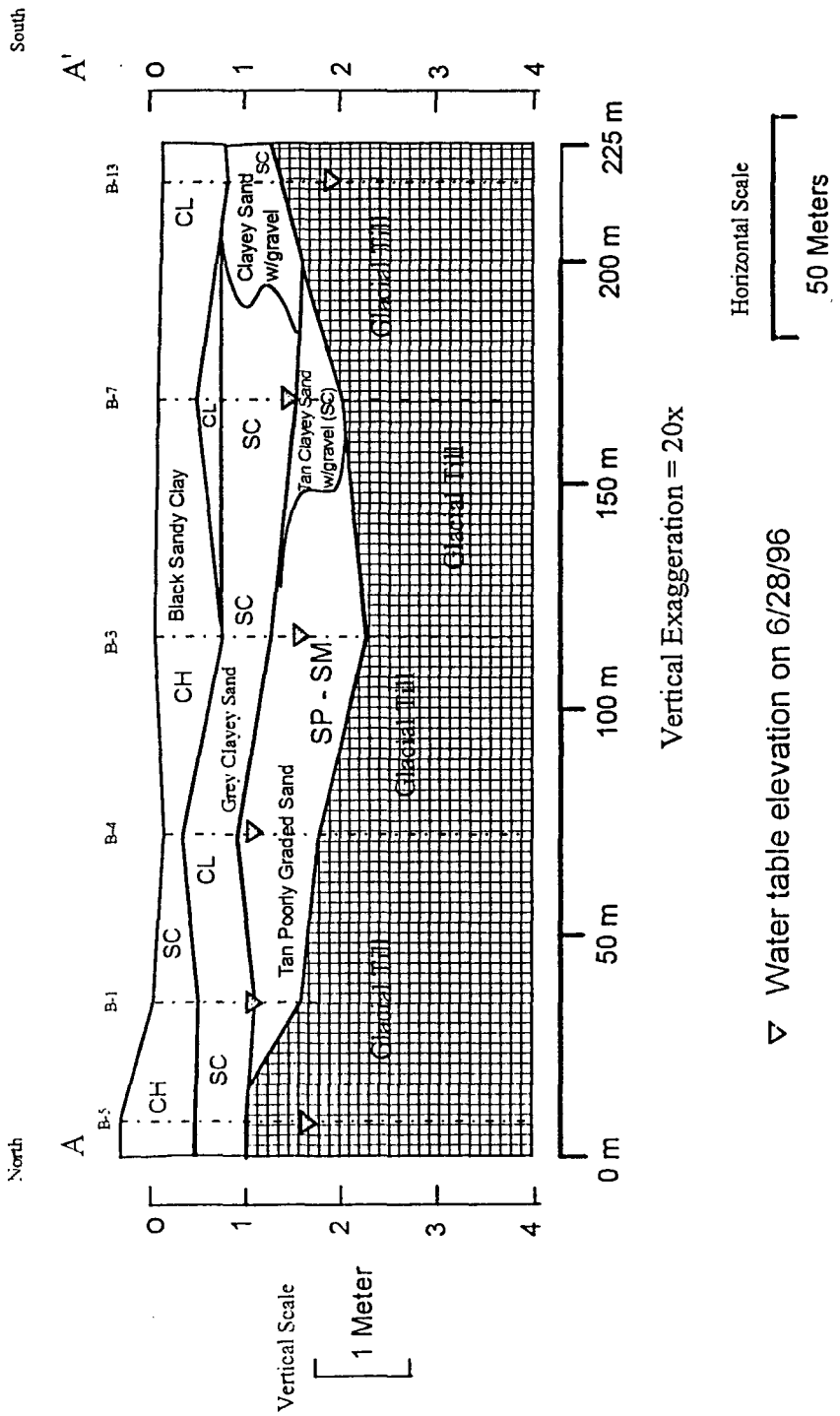

Figure 18. North-south stratigraphic cross section of field site

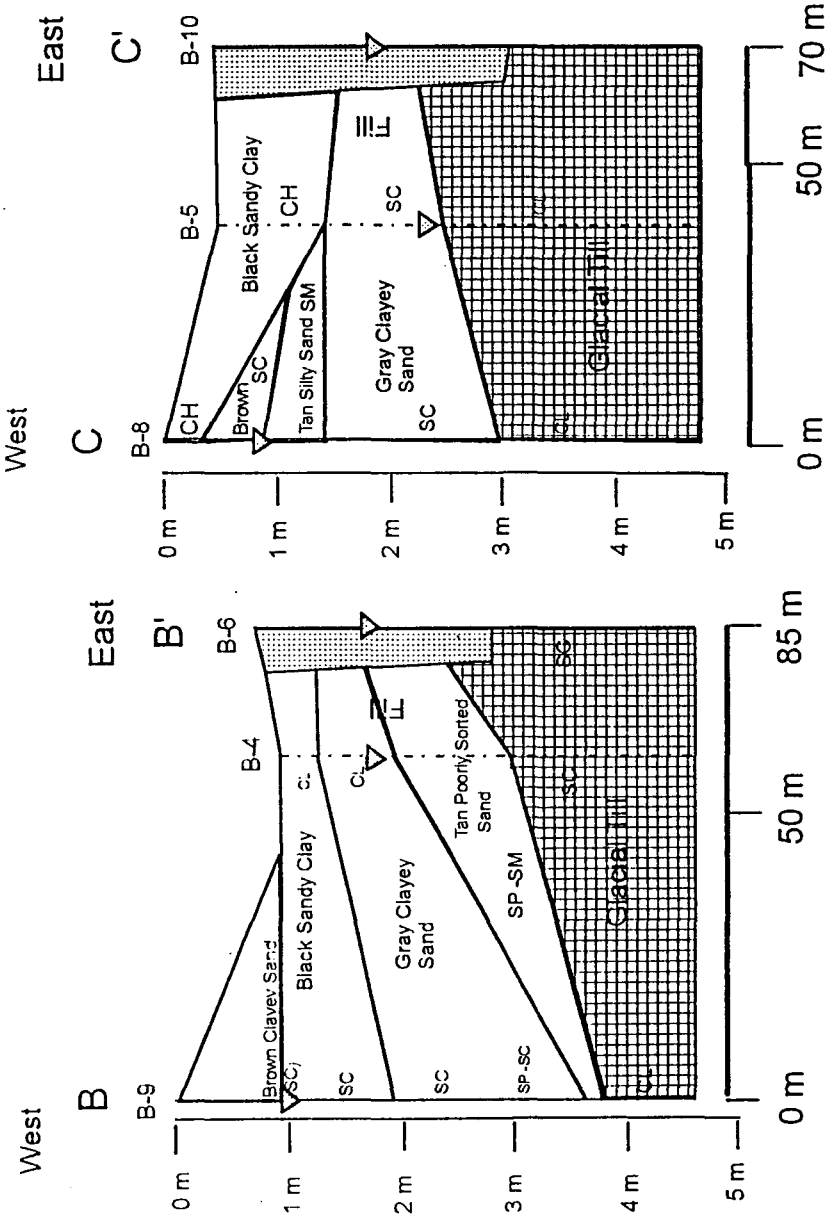

Figure 19. East-west cross sections of field site.

4.3.2 Shredded Tire Stream Crossing

The next structure constructed was the stream crossing. This was a 2.4 meter wide trench filled with shredded tires and backfilled with soil over the shredded tires. The stream crossing was designed to allow vehicles to cross a stream or ravine. The shredded tires conducted water while still allowing vehicles to pass over the crossing.

4.3.2.1 Flow Test Inlet.

An open trench with gently graded side slopes was left between the truck tire culvert and the stream crossing so that water levels could be measured and water could be added to the system for flow testing.

4.3.3 Shredded Tire Horizontal Drain

The last structure built was a horizontal drain, which was similar to the stream crossing, except that its width was only 1.37 m. Figure 20 shows a longitudinal cross section of the horizontal drain.

These structures were built in series to allow water to flow through the truck tire culvert then into the stream crossing and finally out of the horizontal drain. The truck tire culvert inlet was connected to the inlet for the existing truck tire culvert and the horizontal drain outlet was connected back into the existing truck tire culvert further down grade (see figure 21). This arrangement allowed the structures to conduct water from the inlet and back into the existing truck tire culvert, which eventually led to an outlet. Figure 21 shows the plan view of the tire and shredded tire experimental field structures after construction was complete.

4.3.3.1 Leads

Three leads, one connecting to each of the three structures, were constructed by excavating a trench, with a 3% grade that conducted water into the tire structures, and backfilling with shredded tires. The leads were designed to increase effective drainage

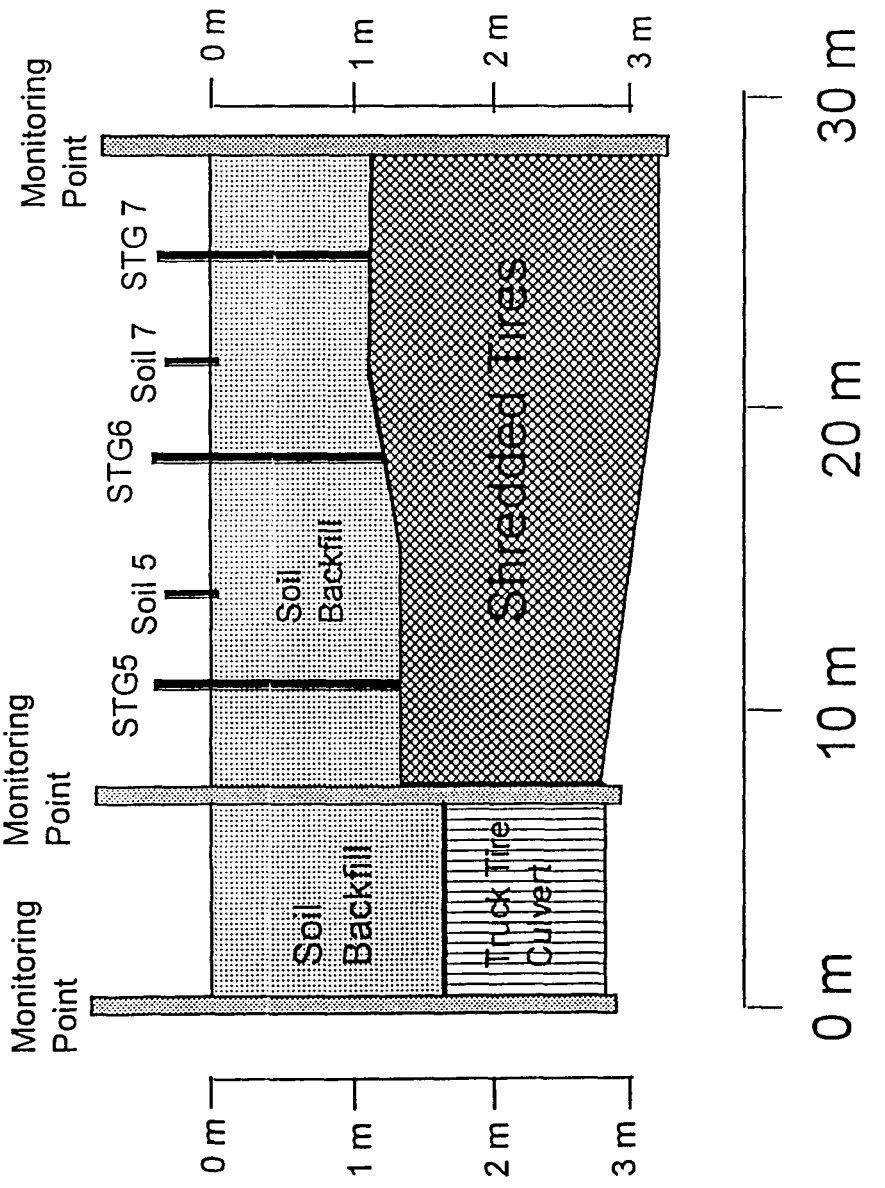

Figure 20. Longitudinal cross section of shredded tire horizontal drain

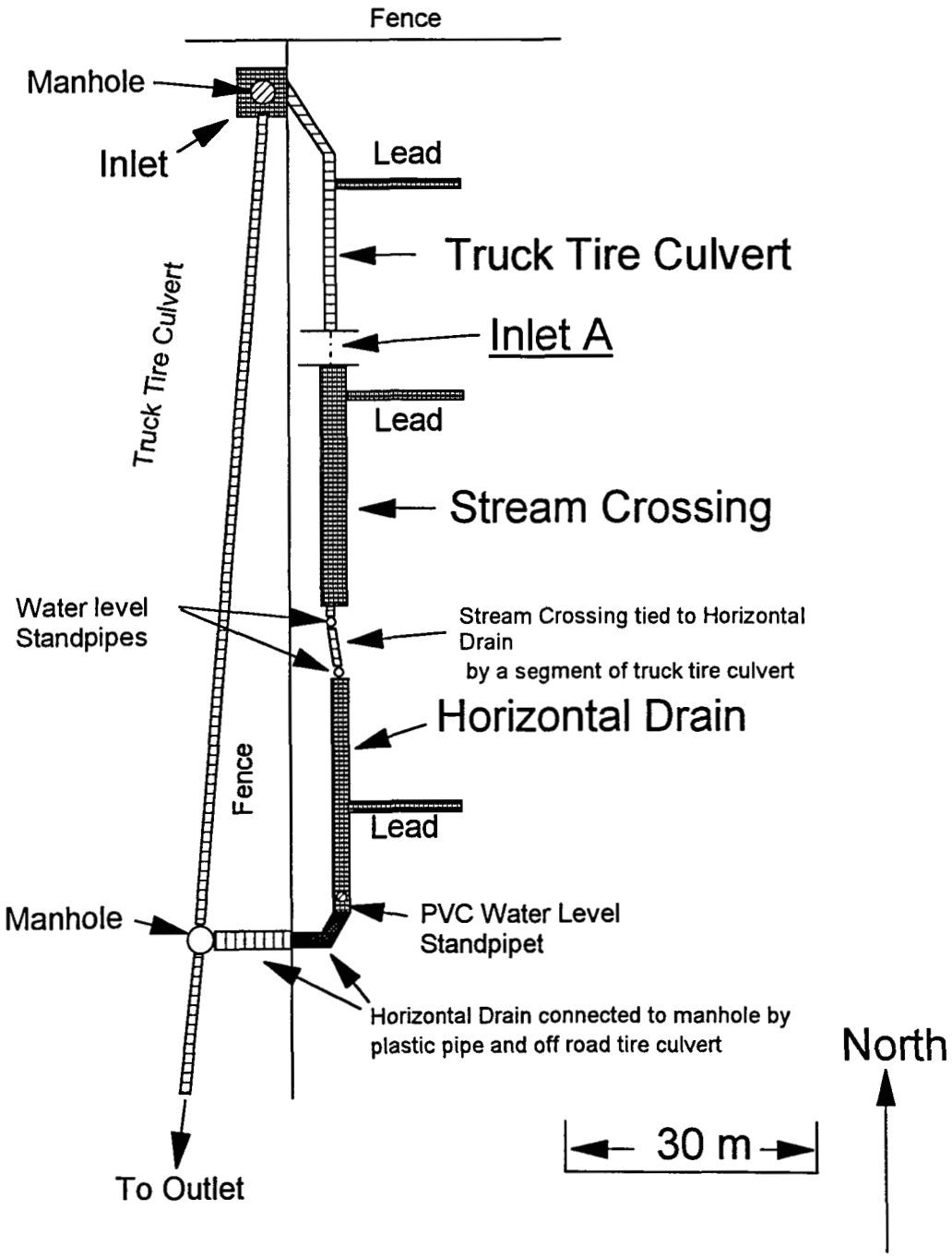

Figure 21. Plan view of the tire structure location

area of the structures, thereby controlling the water table elevations by conducting groundwater into the shredded tire drainage structures.

4.3.3.2 Water level Standpipes

The stream crossing was connected to the horizontal drain with a section of truck tire culvert. Two large diameter wells were installed, one at the end of the stream crossing and one at the beginning of the horizontal drain. These 0.20 m diameter perforated sections of PVC pipes served as water level standpipes. A 0.10 m diameter slotted PVC pipe was installed to measure water at the end of the horizontal drain. With the water level standpipes in place, the shredded tire drainage structures were covered with soil, but water levels could still be measured.

4.3.3.3 Settlement Plate Installation

To measure the compression of the tire shreds and the soil backfill, settlement plates were installed during construction. The settlement plates were plywood squares attached to the end of a vertical pipe. The plywood plates were placed on the tire shred layer and within the backfill. The vertical pipe was inside a larger diameter pipe that acted as a sleeve. The sleeve was in contact with the soil, allowing the inside pipe to move freely (see Figure 22). As the plate settled, the top of the pipe was surveyed to record elevation changes. Settlement gages were placed directly on the shredded tires before the excavator bucket had compressed the shreds. Soil gages were placed within the top 0.15 m of backfill after some compaction of the soil with the excavator bucket.

4.3.4 Horizontal Drain Design Issues

The horizontal drain was installed to test specific design and performance issues. Design issues that were considered critical to construction were: 1) the cross-sectional geometry of the drain, 2) the required grade on the trench bottom, 3) the hydraulic conductivity of the shredded tires, 4) constructability, and 5) degree of compaction of

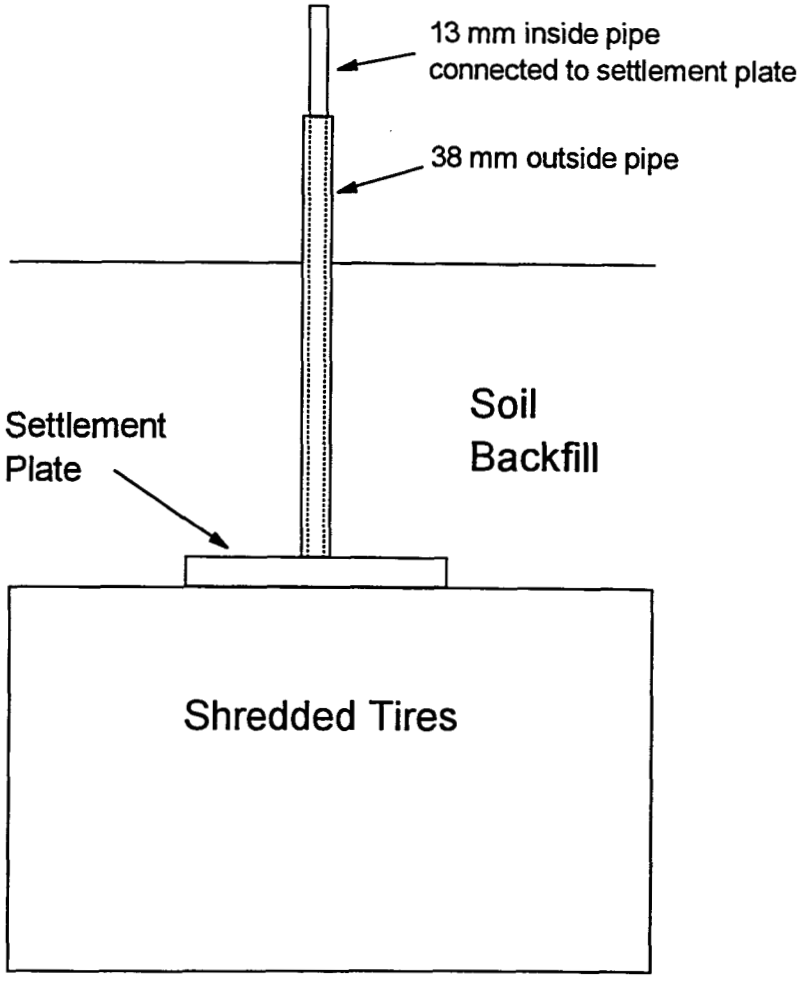

Figure 22. Diagram showing settlement plate

backfill.

4.3.4.1 Cross-Sectional Geometry

The cross sectional area of the horizontal drain was an important consideration for several reasons. If a drain were not made wide enough, it could be more prone to becoming plugged with soil, or it might not allow enough water to pass through. A drain that was too wide would add unnecessary expense to the construction. The drain that was constructed in Fort Dodge was made the minimum possible width using appropriate construction equipment, i.e., the same width as that of the bucket on the excavator, 1.37 m. By making the horizontal drain the same width as the excavator bucket, ease of construction was increased.

The laboratory soil infiltration testing indicated that as long as some interconnected pores remained open, soil migration did not affect the hydraulic conductivity of the tire shreds. During soil infiltration testing, soil tended to get caught in the pore space close to soil source. All shredded tire horizontal drains need to be wide enough so that soil entering the drain from the side does not affect the performance of the drain. A minimum width of 0.9 m would allow enough pore space that soil infiltration would not be a problem.

4.3.4.2 Grade

A horizontal drain requires a slope along its length so that it can effectively drain water. Steeper grades would conduct water more quickly than a gentler slope. Because the shredded tire drain was designed to connect back into the existing truck tire culvert, the choice of grade was rather limited. The horizontal drain grade was designed to be equal to the grade of the existing truck tire culvert, which was 1%.

Agricultural tile drains are installed with grades ranging from 0.1% to 0.5% for long sections and up to 1% for short distances (Roe and Ayres, 1954). These drains are

designed to transport water at a velocity high enough that sediment is not left in the drain, but not with so high of a velocity that churning at the joints results in undermining of the tile.

A shredded tire horizontal drain would not have the concentrated volume of water flow of a tile drain, and it would not be subject to undermining, as there are no joints in the drain. Therefore, slightly different gradient criteria must be applied to a shredded tire horizontal drain.

4.3.4.3 Constructability

The construction of the horizontal drain was planned to be as simple as possible. A trench was excavated to the correct depth using the excavator and a level. As the trench was excavated, a front-end loader loosely placed the shredded tires. The tire shreds were placed in the trench as soon as possible in order to prevent the sides from caving. Generally, 7.5 m segments of trench were completed and filled with shredded tires. This method of construction was fast and relatively safe, as a person was not required to enter the trench at any time.

4.3.4.4 Backfill Placement

Because shredded tire horizontal drains were designed to be easy and inexpensive to install, little quality control was used during soil backfill placement. Backfill was placed and then compressed by the excavator bucket and tracks.

4.3.5 Horizontal Drain Performance Issues

Performance issues were considered apart from design issues. The performance issues that were investigated were associated with the long-term effectiveness of the horizontal drain, and included: 1) effectiveness in lowering the water table, 2) continued water flow over time without plugging, 3) soil piping, 4) magnitude of settlement , and 5) environmental issues, such as whether leachates are generated.

This last issue is considered in a literature review outline in Appendix C.

4.4 Observations

4.4.1 Groundwater

Water table levels were monitored in piezometers, which were installed in each borehole, using a Solinst water level indicator. The water table at the field site was generally 1 to 2 m from the ground surface due to a perched aquifer above the glacial till. The depth to the groundwater surface was quite variable depending on precipitation. Figure 23 shows a groundwater contour map of the field site before construction of the experimental field structures. The direction of groundwater flow varied over the site area.

Before the Iowa State University (ISU) experimental structures were constructed, groundwater in the northern half of the site tended to flow to the southeast, towards the Des Moines River. In the southern half of the site, the truck tire culvert that was in place before the ISU structures influenced the groundwater by acting as a subsurface drain. Groundwater flowed toward the truck tire culvert where it was collected and conducted to the culvert outlet. The groundwater in the northern half of the site was not influenced by the truck tire culvert because the groundwater table was located below the elevation of the culvert. In the southern half of the site, the culvert influenced the direction of groundwater flow because it was located below the water table.

Immediately after construction was completed, the water table levels and subsurface drainage patterns around the drainage structures began to change. Figure 24 shows contours of the groundwater levels on 9/12/96, which is twelve days after the horizontal drain was completed. It is evident from this illustration that the groundwater contours are quite different than those shown in Figure 23, which indicates the water

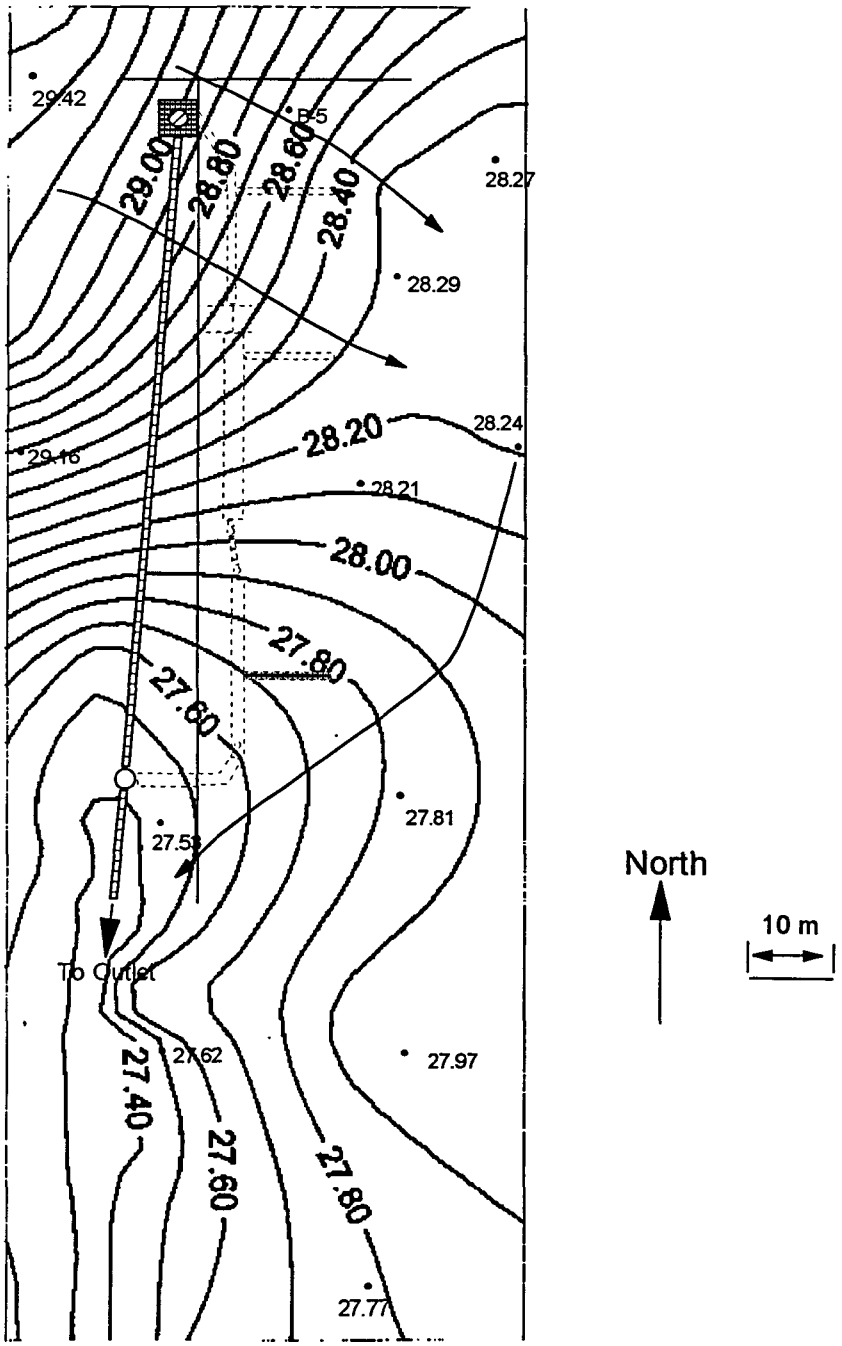

Figure 23. Water table contour map from data taken before installation of field test Structures (7/15/96). Future location of structures is shown in dashed lines and existing truck tire culvert is shown with solid lines. Contour interval is 0.1 m. Contours generated using SURFER.

table elevations before construction. Figure 24 shows that the groundwater levels around the horizontal drain and stream crossing were lowered by at least 0.4 m. The largest decreases in the water table elevation were measured in the groundwater standpipes located downstream of the stream crossing and upstream of the horizontal drain. The 0.4 m drop in water table elevation corresponded to the difference in elevation of the water table before the drainage structures were completed and the elevation of the bottom of the completed structures. After completion of the ISU experimental drainage structures, the groundwater around the ISU truck tire culvert began to flow south toward the horizontal drain instead of southwest toward the Des Moines River.

Figure 25 shows the groundwater levels at the site ten months after construction was completed. On this date, groundwater flow was towards the horizontal drain in the entire area around the structures. Groundwater in the northern half of the site, that formerly flowed southeast, now flowed southwest into the drainage structures. 4.4.2

Precipitation

Figure 26 shows precipitation data and groundwater elevation data for piezometer B-3. The groundwater elevation at B-3 was influenced by its proximity to the horizontal drain, but it rose and fell depending on the amount of precipitation. The groundwater elevation tended to show some delay before raising after rain events, rising between one and two days after a heavy rain. The groundwater usually reached a peak three days after rain.

4.4.3 Settlement

It was evident from the lab testing that large settlements of the tire shreds would occur. However, it was unclear how much settlement would occur because of initial compression of the tire shreds due to backfill placement, and how much would

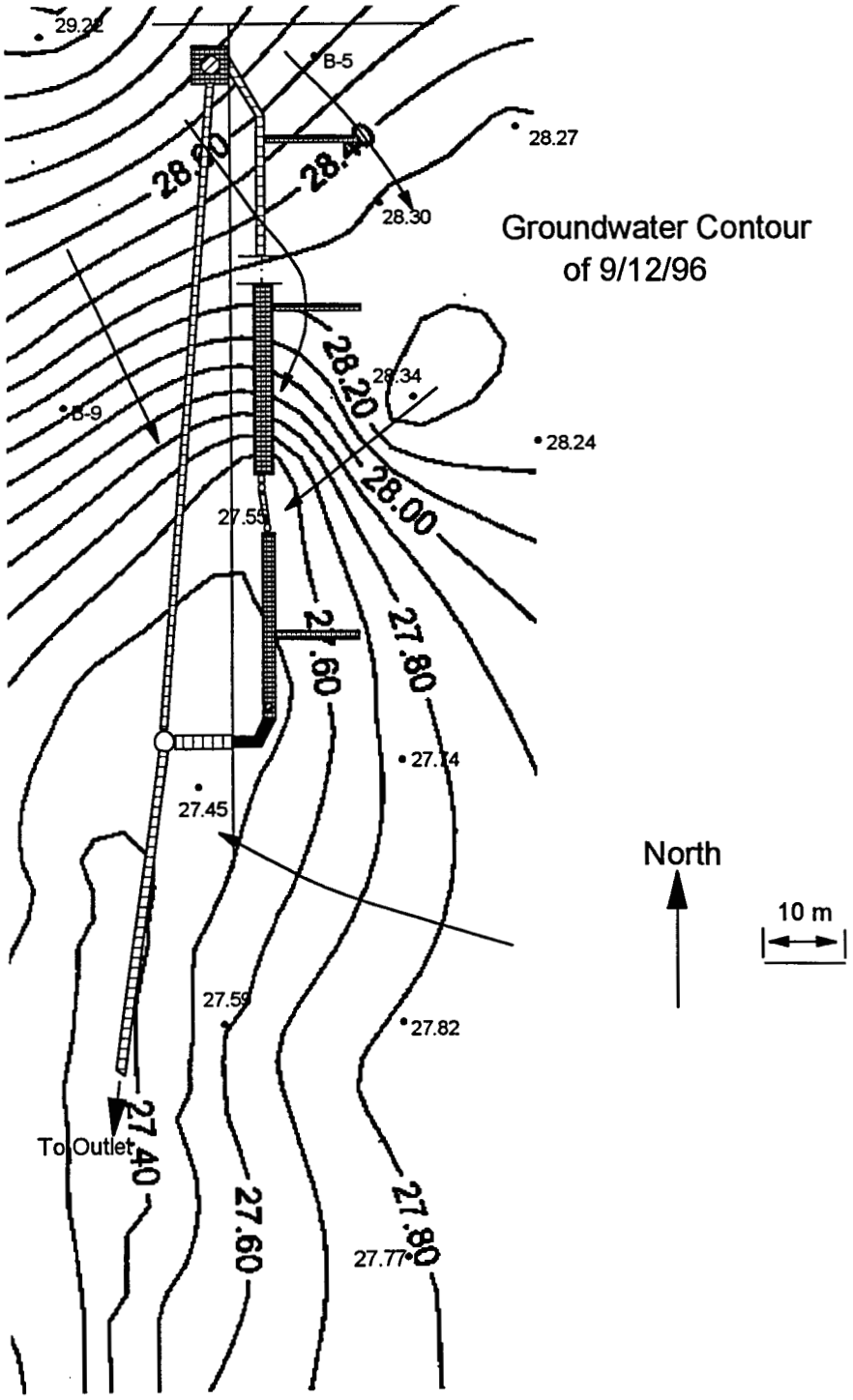

Figure 24. Water table contour map of 9/12/96, twelve days after completion of the horizontal drain. Contours generated using SURFER.

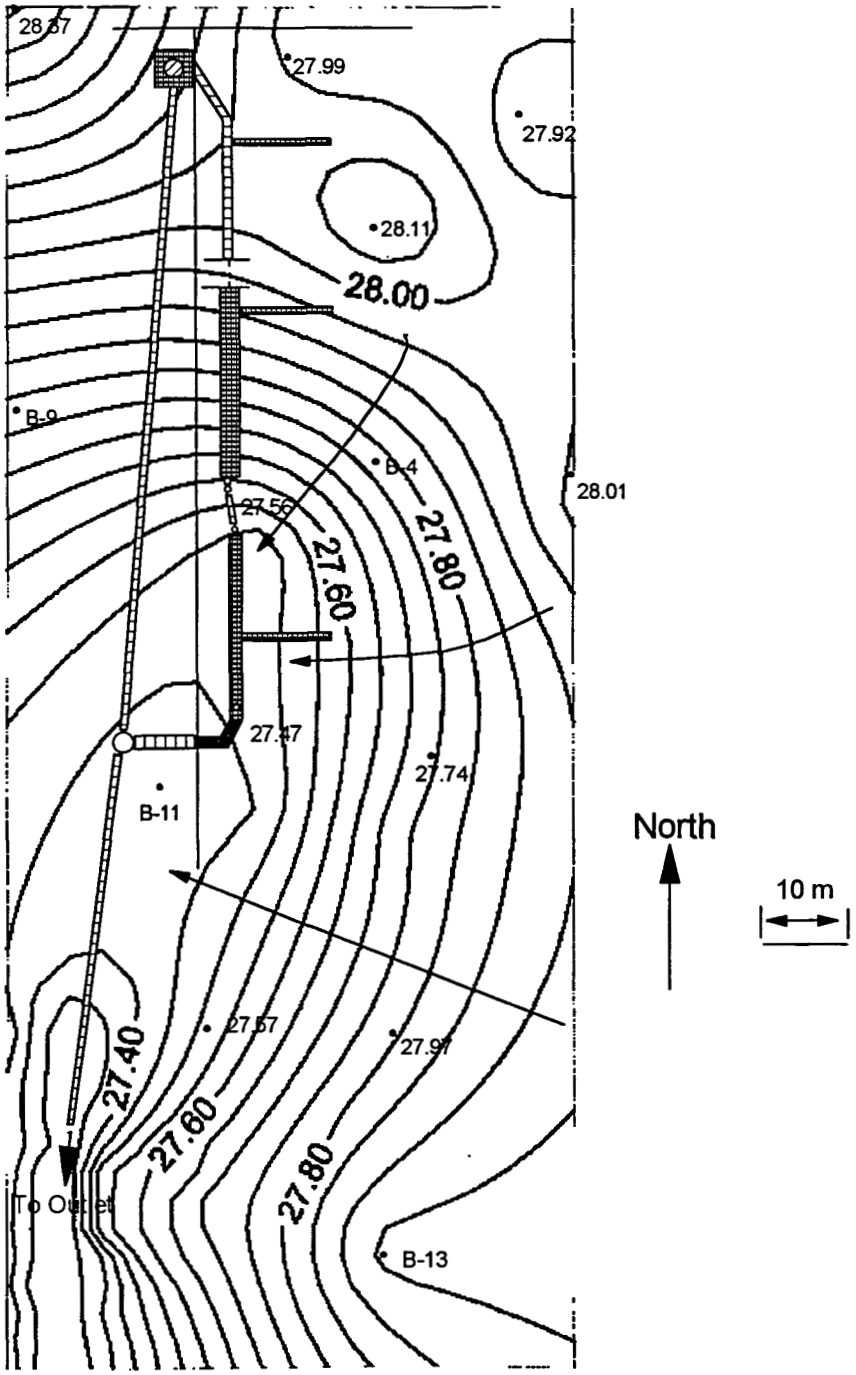

Figure 25. Contour map of the water table surface on 6/12/97. Contours generated using SURFER.

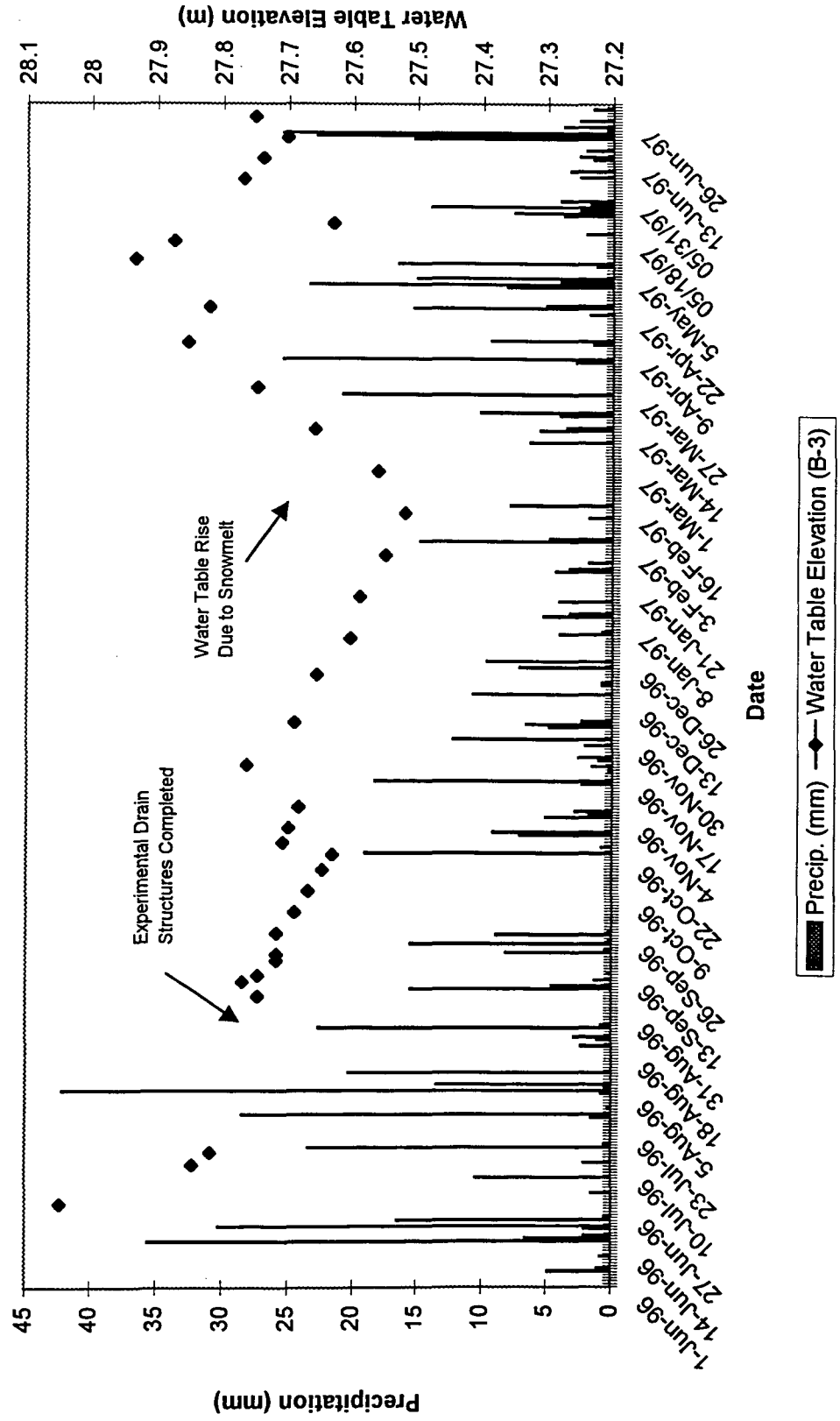

Figure 26. Precipitation data for field site and water table elevation in piezometer B-3. Precipitation is represented by vertical bars. Water table elevation is represented by data points.

occur over time due to creep. Figure 27 shows the elevations of the horizontal drain settlement plates. Gages placed on top of the shredded tires have the label "STG" and gages installed near the top of the backfill have the label "Soil".

The settlement gages were first surveyed before any backfill was placed and the shreds had undergone no vertical strain. The gages were then surveyed immediately after the backfill was placed and at various times thereafter. The largest settlement rates occurred during the first two days after construction and were due to backfill placement and the compactive effort of the excavator. The excavator was used for backfill compaction immediately upon placement and again on the following day. For this reason, the settlement of the tires appears to accelerate on day two after backfill placement. After day two, the settlement plates have settled at a fairly constant rate ranging from 0.02 to 0.03 mm/day. Table 5 shows the vertical stress on the shredded tire layer caused by the backfill. Table 6 shows the changes in elevation that the settlement plates underwent over time. Table 6 also shows the vertical strain of the tire shred layer on the survey dates. 0% vertical strain was represented as the height of the shredded tire layer before any compression or backfill placement had occurred.

4.4.3.1 STG 5

The settlement of STG5 can be seen on Figure 28. STG5 has settled at a fairly constant rate since its initial backfill. It is different from STG6 and STG7 in this respect because STG6 and STG7 showed high settlements on day 1 and day 2 and have since settled at fairly constant rates. The tire shreds below STG5 were not compacted as much by the excavator during placement. This is why the settlement gage did not show the same amount of settlement during the first two days after installation. Vertical strains of 33% to 42% in the tire shred layer at STG5 would be expected If the vertical stress (15.8 kN/m^2) is compared to lab compressibility data, but the tire shred layer has so far

only compressed to 29.4% vertical strain. STG5 might continue to settle at its current strain rate, but as it approaches 40% strain, it may settle at a slower rate.

4.4.3.2 STG6

The settlement of STG6 can be seen on Figure 29. The tire shreds beneath STG6 settled the most on days 1 and 2. This is due to the placement of backfill on day 1 and compaction by the excavator on days 1 and 2. The settlement has been fairly constant since day 2. Vertical strains of up to 42% in the tire shred layer at STG6 would be expected If the vertical stress (14.8 kN/m^2) is compared to lab compressibility data. STG6, with its vertical strain of 42.2% would not be expected to show much more vertical strain if field results mirror lab results.

4.4.3.3 STG7

The settlement of STG7 can be seen on Figure 30. The tire shreds beneath STG7 settled the most on days 1 and 2. This is due to the placement of backfill on day 1 and compaction by the excavator on days 1 and 2. The settlement has been fairly constant since day 2. It is not clear why STG7 showed a lessening of vertical strain on its last measurement. Vertical strains of 33% to 42% in the tire shred layer at STG7 would be expected If the vertical stress (15.8 kN/m^2) is compared to lab compressibility data, but the tire shred layer has so far only compressed to 29.1% vertical strain. STG7 might continue to settle at its current strain rate, but as it approaches 40% strain, it may settle at a slower rate.

4.4.3.4 Surface Settlement

Visual inspection of the ground above the horizontal drain verified that large settlements had occurred. Nine months after construction, surface settlement of approximately 0.25 m was evident over the horizontal drain (Figure 31). Settlement could have been minimized if more compaction of the shreds had taken place and if a

thinner tire shred layer with a thicker backfill layer had been used.

4.5 Flow Tests

An important performance issue was the ability of the shredded tire structures to transmit large volumes of water and to work effectively over a long period of time. Two tests were performed that were designed to demonstrate the horizontal drain effectiveness under high discharge. The first test was performed on October 26, 1997. The second test was performed on June 28, 1997,nearly eight months later, to determine whether the structures had less drainage capacity after being in place for eight months.

4.5.1 Test Procedure For First Flow Test

To test the flow capacity of the horizontal drain and stream crossing, a fire hose was used to discharge water into inlet A (shown on figure 21) between the truck tire culvert and the stream crossing structures. The first phase of the test was performed in order to gauge the amount of water that would flow through the structures. The second phase of the test was to determine the flow rate that resulted with a constant head maintained at the upstream end of the drainage structures.

Water flow tests were carried out with the use of a fire hose, which was connected to a metered hydrant. Water was discharged into inlet A. Using the water meter, the flow rate of water entering the drainage structures could be controlled and measured. The fire hose emptied into the open basin between the truck tire culvert and the shredded tire stream crossing. A piece of plywood was fitted tightly against the end of the culvert to prevent water from escaping from the basin into the culvert. Water levels in the basin were recorded on the plywood and later surveyed to determine elevations. Monitoring points were located 1 m downstream of the shredded tire stream

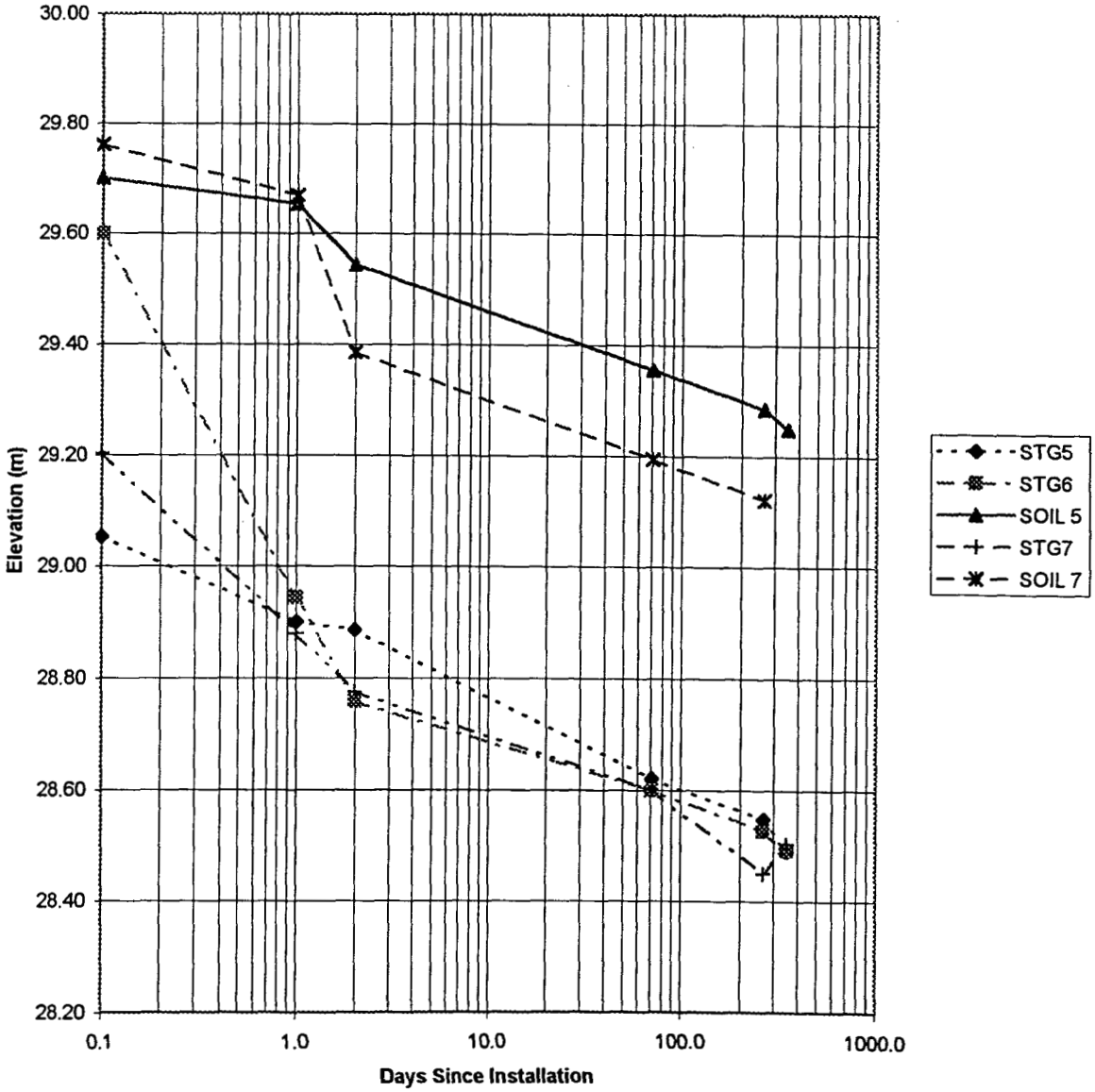

Figure 27. Elevation of horizontal drain settlement plates. Initial height at time = 0 is represented by time = 0.1 days.

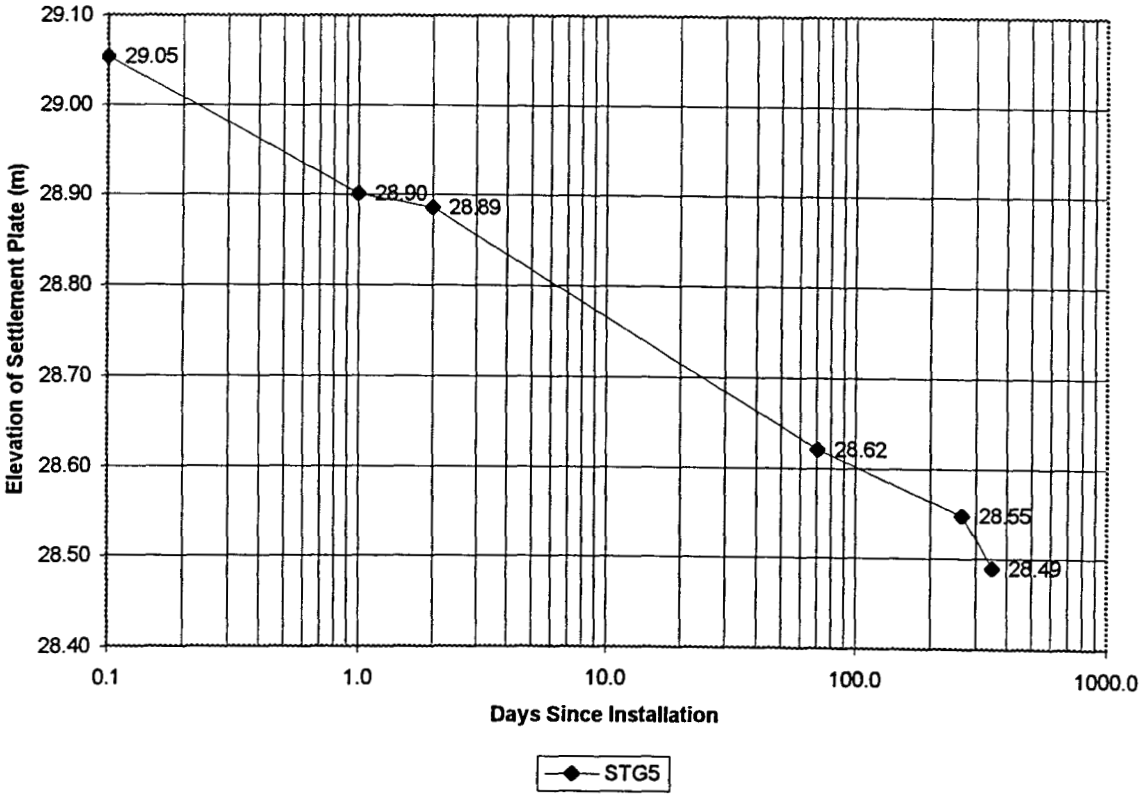

Figure 28. Elevation of shredded tire settlement gage STG5 over time.

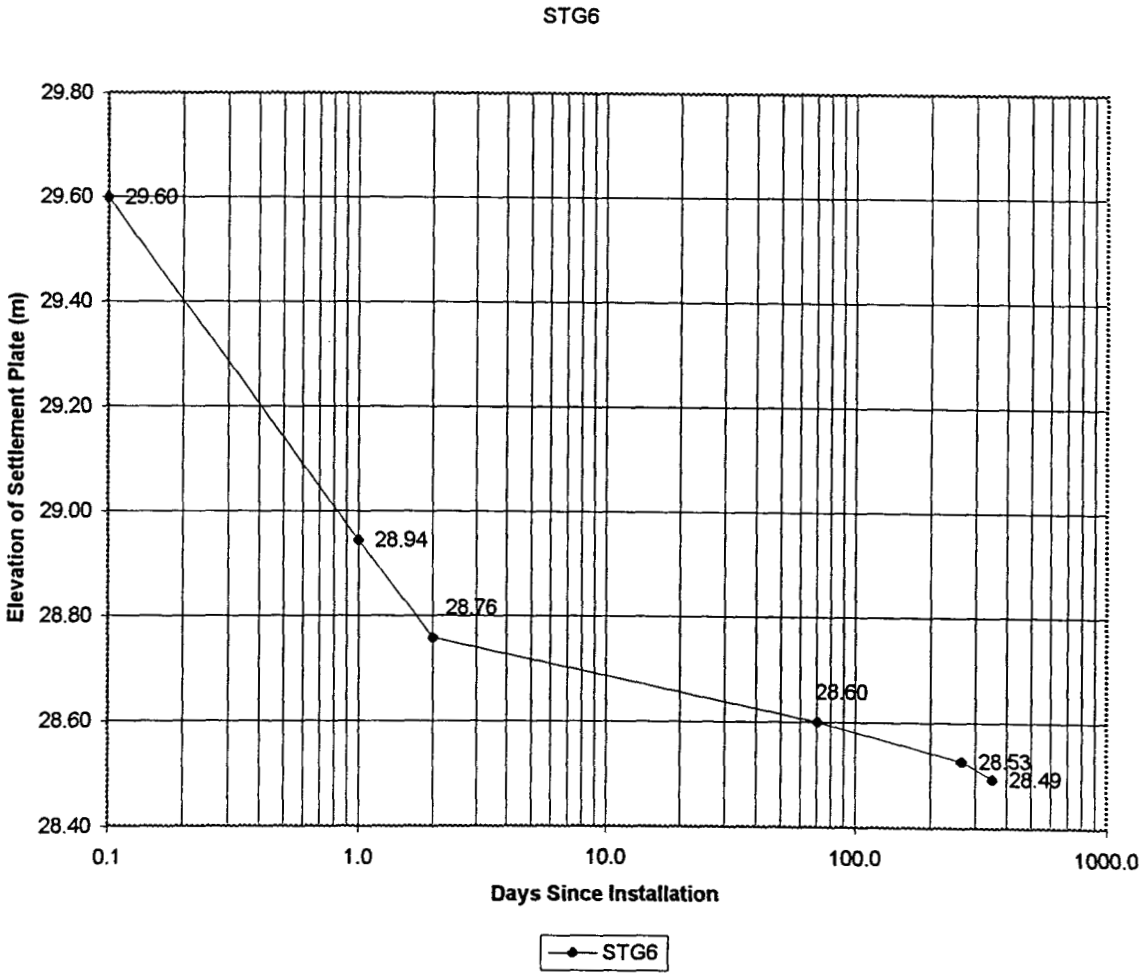

Figure 29. Elevation of shredded tire settlement gage STG6 over time.

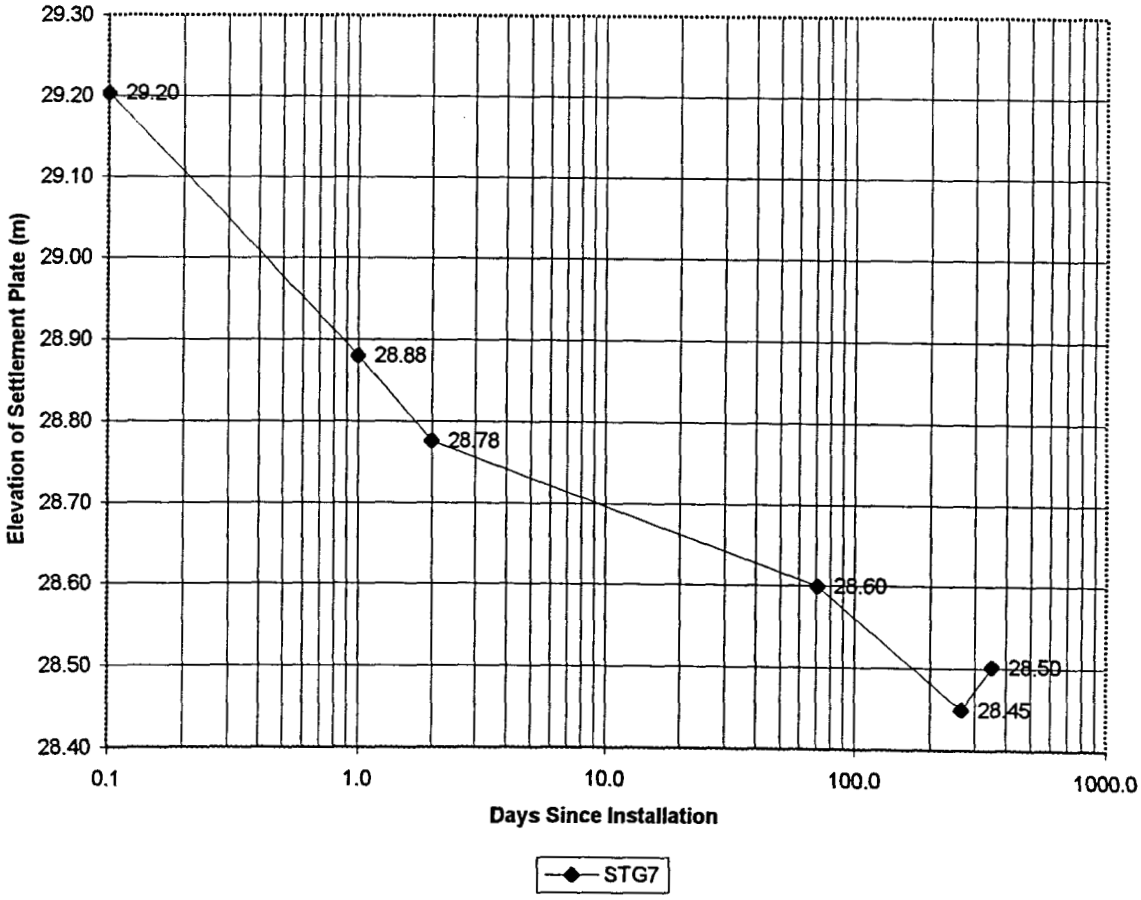

Figure 30. Elevation of shredded tire settlement gage STG7 over time.

Table 5. Soil loads (vertical stress) above shredded tire settlement gages assuming prism loading and γ_t = 17.3 kN/m^3.

Settlement Gage	Vertical Stress (kN/m^2)
STG5	15.8
STG6	14.8
STG7	15.8

Table 6. The thickness of the shredded tire layer beneath each shredded tire settlement gage, and the total vertical strain (%) of the shredded tire layer measured on the given dates.

Date	STG5		STG6		STG7		SOIL 5	SOIL 7
	Thickness (m)	% ε_v	Thickness (m)	% ε_v	Thickness (m)	% ε_v	Δ Elev. (m)	Δ Elev. (m)
8/28/96	1.92	0.0	2.62	0.0	2.41	0.0	0	0
08/29/96	1.76	7.9	1.97	25.0	2.09	13.4	-0.05	-0.09
8/30/96	1.75	8.7	1.78	32.1	1.98	17.7	-0.16	-0.37
11/7/96	1.48	22.6	1.62	38.1	1.81	25.0	-0.34	-0.57
5/21/97	1.41	26.4	1.55	40.9	1.66	31.2	-0.41	-0.64
8/14/97	1.35	29.4	1.52	42.2	1.71	29.1	-0.45	

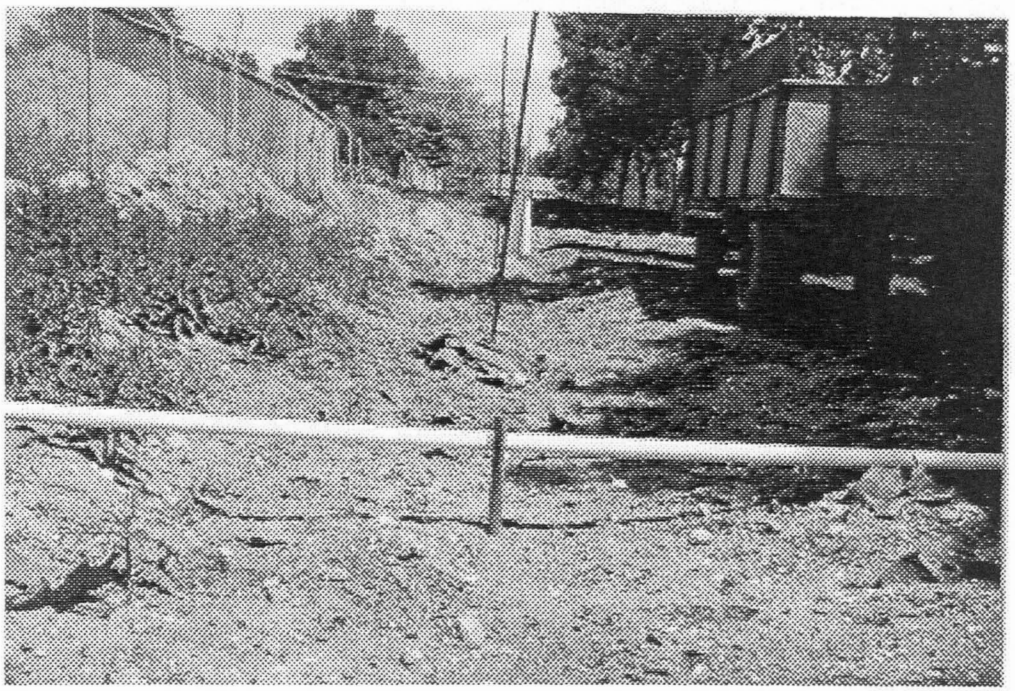

Figure 31. Photo of surface settlement. Horizontal pipe is laid across the surface depression caused by settlement. Vertical bar is 305 mm long and is set inside depression to show surface settlement.

crossing, at the beginning of the horizontal drain, and at the end of the horizontal drain (See figure 21). The first two monitoring points were 0.20 m diameter perforated PVC pipes, and the monitoring point at the end of the horizontal drain was a 0.10 m diameter slotted PVC pipe.

4.5.1.1 Test Phase I

During the first phase of the test, the maximum possible flow from the hydrant, 0.015 m^3/s (240 gpm), was discharged into the test structures for 21 minutes. The water level in the inlet continued to slowly rise until the water was shut off and then immediately began to lower. No water was added to inlet A for 52 minutes.

4.5.1.2 Test Phase II

The next phase of the test involved maintaining the water level in the inlet at a constant level while a constant flow of water was supplied to the basin. Water was added to the basin at a rate of 0.0058 m^3/s (92 gpm) for 134 minutes. After 134 minutes, the water was shut off and the water elevations in the drainage structures began to return to normal.

4.5.2 Test Procedure For Second Flow Test

The objective of the second flow test was similar to the second phase of the October 26, 1996 flow test. Water was added to the basin between the culvert and the steam crossing using a fire hose. The flow rate from the hydrant was 0.0058 m^3/s (92 gpm), which was the same flow rate that was used in the first flow test. Water was added to inlet A for a period of 185 minutes. Water levels in the monitoring points were measured while the water was flowing and after it had been shut off.

4.5.3 Results Of Flow Testing

Figure 32 shows the results of the first flow test. During the first phase of testing, the water level in inlet A continued to rise until the water was shut off, and then it

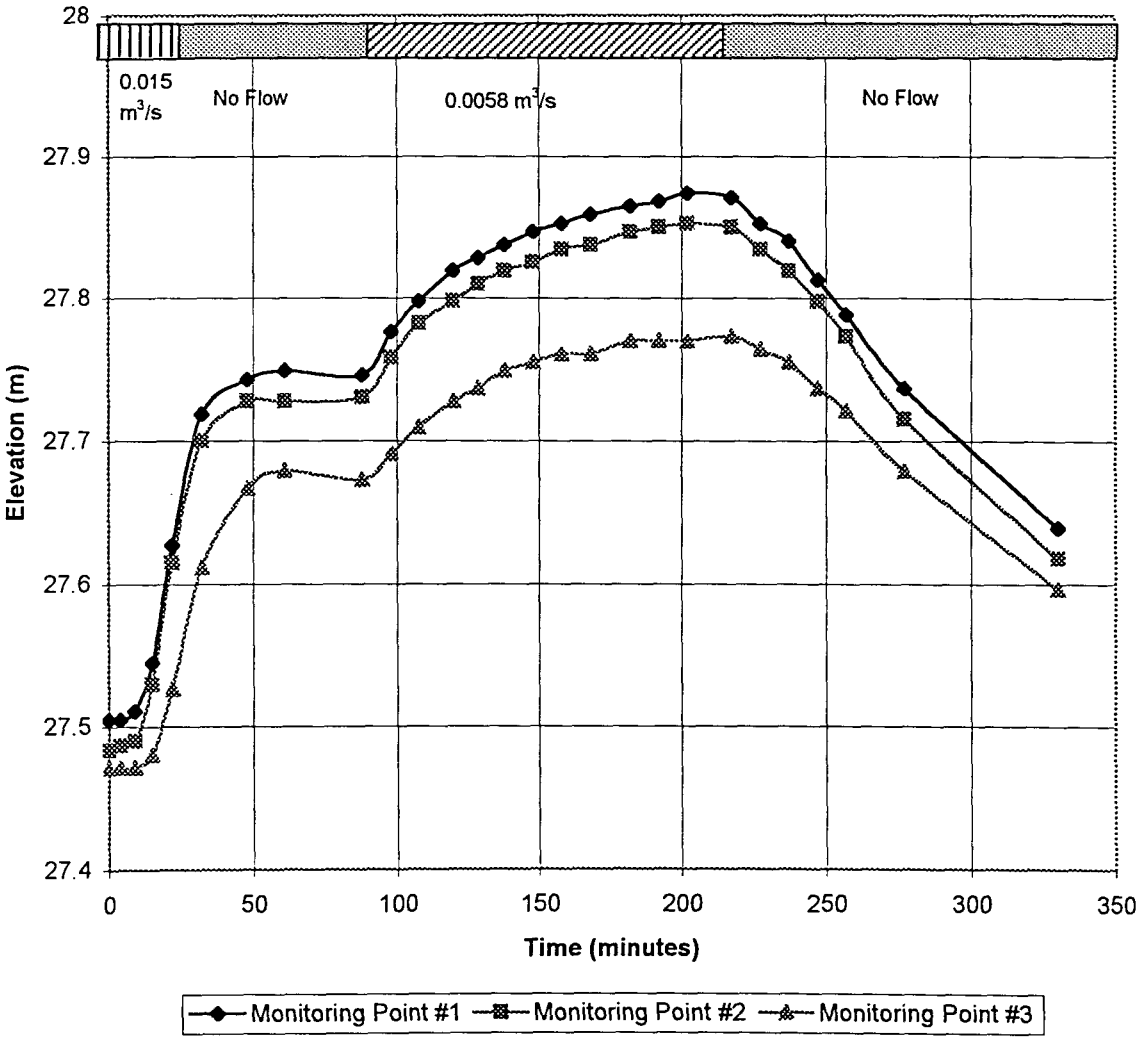

Figure 28. Water elevations at the monitoring points during the first flow test (October 26, 1996)

immediately began to lower. During the second phase of the test, the water level in inlet A was kept at a constant head by using a flow rate of 0.0058 m^3/s (92 gpm).

By using the same flow rate as the first flow test, the structures could be monitored to determine whether the shredded tire structures could still conduct water as effectively as they did eight months earlier. It was hypothesized that if soil had entered the shredded tire pore spaces then less water would be able to flow through the structures. Consequently, the same flow rate of 0.0058 m^3/s (92 gpm) would cause the water level in inlet A to rise higher than in the first flow test. The water level in the basin was monitored during the test, as well as the water elevations in the three monitoring points in the structures. The results of the test can be seen in Figure 33.
The results of the second flow test tended to confirm that very little change had occurred in the ability of the drainage structures to conduct water. The water level in the basin rose to approximately the same elevation of the first constant flow test where it remained steady. Also, water levels at the monitoring points dropped quickly after water flow was stopped, jus as had occurred during the first test.

During the second test, water elevations at the monitoring points were, on the average, about 0.2 m higher than during the first test. This can be seen by comparing Figures 32 and 33. There are at least two explanations for this small difference.

4.5.3.1 Effects of Soil Infiltration

One possible reason for the higher water levels in the second test was some soil migration into the tire shred voids. If soil had infiltrated into the shredded tire void spaces, water levels would be higher at the monitoring points. Assuming a relatively constant velocity of water passing through the horizontal drain, the same cross sectional area of pore space would be required to transmit the same flow as the first water flow test. If some tire shreds voids were plugged or were reduced in diameter, the original

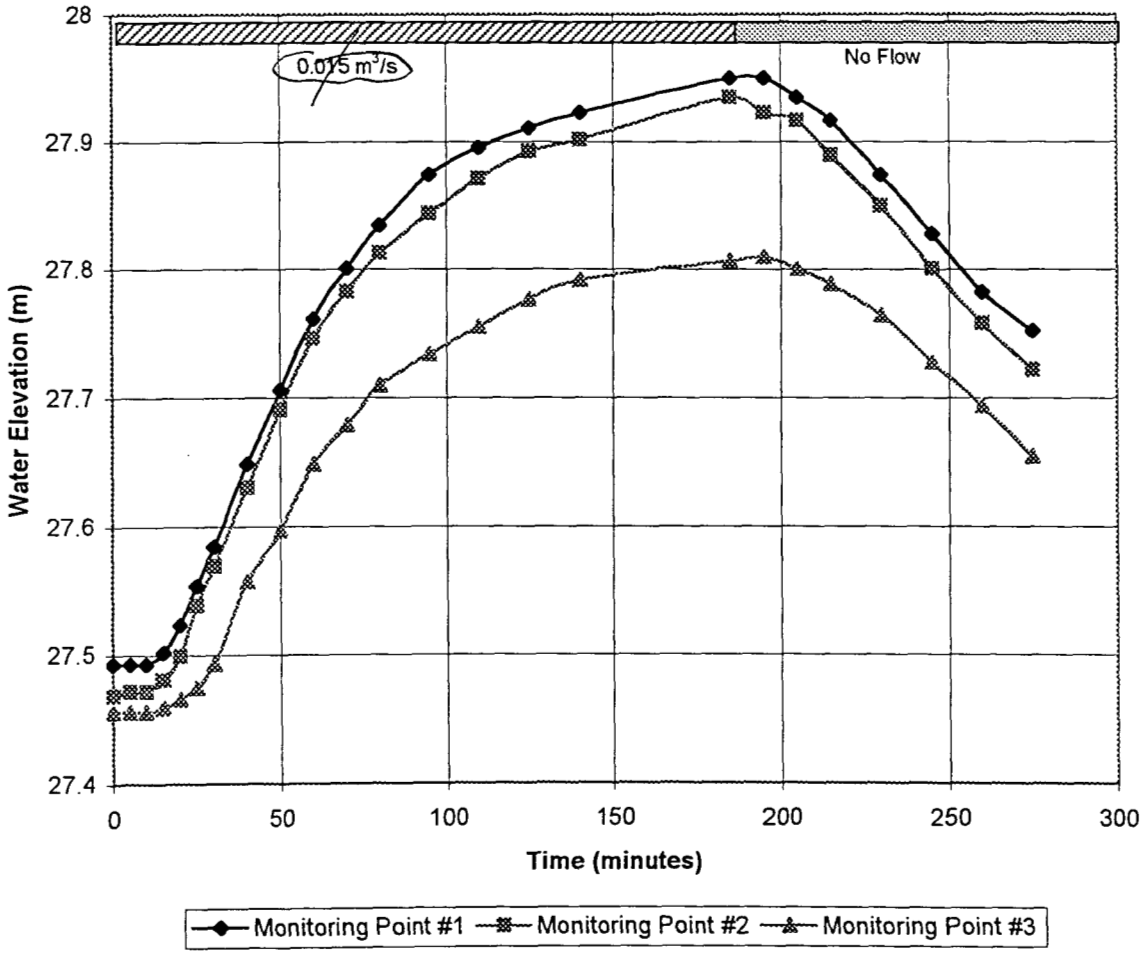

Figure 29. Water elevations at the monitoring points during the second flow test.

cross sectional area of flow would be reduced. The water level in the drain would be forced to rise in order to have water flow through the same pore area as during the first test. This would be observed as higher water elevations.

4.5.3.2 Effects of Settlement

Another possible reason for higher water levels during the second flow test was that settlement had occurred in the shredded tires, thereby reducing void space. Between the time of the first and second flow tests, an average of 0.1 m of settlement had occurred in the shredded tire drainage layer. This settlement would have had the effect of reducing the void space in the layer. The difference in hydraulic conductivity between the two tests due to settlement should not have been more than ~1cm/s. A combination of soil migration into the tire shreds and settlement of the layer probably led to reduced void space in the shredded tire layer. This reduction of void space led to higher water levels in the second flow test. The small difference in the tests indicatesthat although some changes in performance had occurred, the effectiveness of the horizontal drain had not been diminished.

4.5.3.3 Field Hydraulic Conductivity

The hydraulic conductivity of the horizontal drain tire shreds was estimated from the water level data after the water had been shut off. Unit weight and specific gravity from lab testing were assumed. For simplicity, the Darcy equation was used for the result. See Appendix E for the equations and calculations used to estimate field hydraulic conductivity. Hydraulic conductivity was estimated to be 10.7 cm/s. This value was very close to the hydraulic conductivity calculated during laboratory testing

4.6 Discussion Of Field Research Results

A horizontal drain structure was constructed of tire shreds. Water table elevations in the test site were monitored so that the effectiveness of the horizontal drain

in lowering the water table could be determined. A series of flow tests were conducted so as to determine the performance of the structure when subjected to high flow rates. Long term settlement was surveyed and the condition of the backfill above the drain was visually inspected.

The horizontal drain dramatically affected local water table elevations. Direction of groundwater flow was altered so that groundwater at the site drained into the shredded tire structures rather than towards the Des Moines River. Groundwater patterns were altered immediately upon completion of the drain structures and continued to differ from the pre-construction condition.

Flow tests showed that the shredded tire structures could conduct flow rates of at least 0.0058 m3/s (92 gpm) for several hours and flow rates of at least 0.015 m3/s (240 gpm) for at least 20 minutes. When a constant flow of 0.0058 m^3/s (92 gpm) was maintained into the structures, little difference was observed in the results of the second test compared to the first. This was an indication that soil migration into the shredded tire pore spaces was not significantly affecting the performance.

Settlement of the tire shred layer was significant and continued to occur over the long-term. More compaction of the tire shred layer prior to backfill placement would lead to less settlement, but if tire shreds were used in an area where surface settlement was acceptable, this would not be necessary. Differences in hydraulic conductivity due to varying vertical strain are not significant, usually less than 1.5 cm/s for a difference of 10% vertical strain.

Overall, the tire shred horizontal drained performed very well, satisfying all of the performance issues. The shredded tires are easy to place and construction of horizontal drains is straightforward. Lab and field data indicate that soil migration into the shredded tire void space does not degrade the performance of the structures. Use of shredded

tires has the additional benefit of using a product that otherwise would be an environmental liability.

APPENDIX A. ANALYSIS OF POSSIBLE ERRORS IN HYDRAULIC CONDUCTIVITY TESTING

Table A.1. This set of tables shows the value of hydraulic conductivity that was used to analize the laboratory results. Also shown are the high and low values of hydraulic cnoductivity that were calculated when errors for flow rate and correction factor were applied.

Flow (m3/s)	K (cm/s) for 0% Vertical Strain			K (cm/s) for 10.8% Vertical Strain		
	low	Test Value	high	low	Test Value	high
0.0001262	5.6	5.8	12.0	3.4	3.5	5.4
0.0001893	5.6	5.8	6.0	5.0	5.2	5.4
0.0002524	11.3	11.6	12.0	6.7	6.9	7.1
0.0003155	4.3	4.5	4.6	2.3	2.4	7.6
0.0003786	7.7	7.9	8.2	2.0	2.5	4.0
0.0004417	4.7	4.8	5.6	2.9	3.0	3.4
0.0005048	2.3	2.4	2.6	1.3	1.4	1.5
0.0005679	2.1	2.5	3.6	0.8	0.9	1.4

Flow (m3/s)	K (cm/s) for 21% Vertical Strain			K (cm/s) for 32% Vertical Strain		
	low	Test Value	high	low	Test Value	high
0.0001262	3.0	3.1	4.5	2.2	2.3	3.3
0.0001893	3.3	3.5	3.6	3.3	3.4	3.5
0.0002524	2.7	2.8	7.6	3.9	4.0	4.1
0.0003155	1.4	1.4	1.5	1.7	1.7	1.8
0.0003786	1.8	1.9	2.7	2.0	2.1	3.5
0.0004417	1.5	1.6	1.7	2.2	2.2	2.5
0.0005048	0.8	0.8	0.9	1.3	1.3	1.4
0.0005679	0.8	0.9	1.0			

Flow (m3/s)	K (cm/s) for 42% Vertical Strain			K (cm/s) for 53% Vertical Strain		
	low	Test Value	high	low	Test Value	high
0.0001262	1.3	1.3	1.7	1.8	1.8	2.8
0.0001893	2.2	2.2	2.3	4.0	4.1	4.2
0.0002524	2.0	2.1	5.5	1.2	1.2	2.2
0.0003155	1.2	1.3	2.0	0.9	1.0	1.0
0.0003786	1.0	1.2	1.7	1.0	1.2	1.9
0.0004417	1.1	1.2	1.3			

Table A.2. This table gives the hydraulic conductivity of the results used in interpretation of the laboratory testing results as well as the hydraulic conductivities that were calculated using the potential flowmeter error of ±3%.

Hydraulic Conductivity (cm/s) results used in interpretation of the laboratory testing data						
Flow (cm3/s)	K (0% Strain)	K (10.8%)	K (21%)	K (32%)	K (42%)	K (53%)
126.2	5.8	3.5	3.1	2.3	1.3	1.8
189.3	5.8	5.2	3.5	3.4	2.2	4.1
252.4	11.6	6.9	2.8	4.0	2.1	1.2
315.5	4.5	2.4	1.4	1.7	1.3	1.0
378.6	7.9	2.5	1.9	2.1	1.2	1.2
441.7	4.8	3.0	1.6	2.2	1.2	
504.8	2.4	1.4	0.8	1.3		
567.9	2.5	0.9	0.9			
631.0	3.4	1.4				
694.1						
Hydraulic Conductivity (cm/s) using flow rate read from flow meter +3%						
Flow (cm3/s)	K (0% Strain)	K (10.8%)	K (21%)	K (32%)	K (42%)	K (53%)
130.0	6.0	3.6	3.2	2.3	1.4	1.9
195.0	6.0	5.4	3.6	3.5	2.3	4.2
260.0	12.0	7.1	2.9	4.1	2.1	1.2
325.0	4.6	2.4	1.5	1.8	1.3	1.0
390.0	8.2	2.6	1.9	2.2	1.2	1.3
455.0	4.9	3.1	1.6	2.3	1.2	
519.9	2.5	1.4	0.9	1.3		
584.9	2.6	1.0	0.9			
649.9	3.5					
714.9						
Hydraulic Conductivity (cm/s) using flow rate read from flow meter -3%						
Flow (cm3/s)	K (0% Strain)	K (10.8%)	K (21%)	K (32%)	K (42%)	K (53%)
122.4	5.6	3.4	3.0	2.2	1.3	1.8
183.6	5.6	5.0	3.3	3.3	2.2	4.0
244.8	11.3	6.7	2.7	3.9	2.0	1.2
306.0	4.3	2.3	1.4	1.7	1.2	0.9
367.2	7.7	2.4	1.8	2.0	1.2	1.2
428.4	4.7	2.9	1.5	2.2	1.1	
489.7	2.3	1.3	0.8	1.3		
550.9	2.4	0.9	0.8			
612.1	3.3	1.4				
673.3	3.0					

Table A.3. This table shows the hydraulic conductivity that was calculated using the potential error in the flowmeter as well as the high values of the correction factors that was found during the three empty permeameter tests.

Hydraulic conductivity (cm/s) using high values of correction factor and +3% reading of flow meter					
K (0% Strain)	K (10.8%)	K (21%)	K (32%)	K (42%)	K (53%)
12.0	5.4	4.7	3.3	1.7	2.8
6.0	5.4	3.6	3.5	2.3	4.2
		7.6		5.5	2.2
4.6	2.4	1.5	1.8	1.3	1.0
	4.0	2.7	3.5	1.7	1.9
5.6	3.4	1.7	2.5	1.3	
2.6	1.5	0.9	1.4		
3.6	1.1	1.0			
6.7					
Hydraulic conductivity (cm/s) using high values of correction factor and -3% of flow meter reading					
K (0% Strain)	K (10.8%)	K (21%)	K (32%)	K (42%)	K (53%)
11.3	5.0	4.5	3.1	1.6	2.6
5.6	5.0	3.3	3.3	2.2	4.0
		7.1		5.2	2.1
4.3	2.3	1.4	1.7	1.2	0.9
	3.8	2.6	3.3	1.6	1.8
5.3	3.2	1.6	2.3	1.2	
2.4	1.4	0.8	1.3		
3.4	1.0	0.9			
6.3	1.7				
3.3					

Table A.4. This table shows the hydraulic conductivity that was calculated using the potential error in the flowmeter as well as the low values of the correction factors that was found during the three empty permeameter tests.

Hydraulic conductivity (cm/s) using low values of correction factor and +3% of flow meter reading					
K (0% Strain)	K (10.8%)	K (21%)	K (32%)	K (42%)	K (53%)
6.0	3.6	3.2	2.3	1.4	1.9
6.0	5.4	3.6	3.5	2.3	4.2
12.0	7.1	2.9	4.1	2.1	1.2
4.6	2.4	1.5	1.8	1.3	1.0
5.1	2.1	1.6	1.8	1.1	1.0
4.9	3.1	1.6	2.3	1.2	
2.5	1.4	0.9	1.3		
2.1	0.9	0.8			
2.7					
Hydraulic Conductivity (cm/s) using low values of correction factor and -3% of flow meter reading					
K (0% Strain)	K (10.8%)	K (21%)	K (32%)	K (42%)	K (53%)
5.6	3.4	3.0	2.2	1.3	1.8
5.6	5.0	3.3	3.3	2.2	4.0
11.3	6.7	2.7	3.9	2.0	1.2
4.3	2.3	1.4	1.7	1.2	0.9
4.8	2.0	1.5	1.7	1.0	1.0
4.7	2.9	1.5	2.2	1.1	
2.3	1.3	0.8	1.3		
2.0	0.8	0.8			
2.6	1.2				
2.8					

Table A.5. This table shows the percent error in the hydraulic conductivity from the value used for analysis to the hydraulic conductivity that was calculated using the potential error in the flowmeter as well as the low values of the correction factors that was found during the three empty permeameter tests.

Percent error in hydraulic conductivity using low values of correction factor and +3% of flow meter reading						
Flow (m3/s)	K (0% Strain)	K (10.8%)	K (21%)	K (32%)	K (42%)	K (53%)
0.000126	3.0	3.0	3.0	3.0	3.0	3.0
0.000189	3.0	3.0	3.0	3.0	3.0	3.0
0.000252	3.0	3.0	3.0	3.0	3.0	3.0
0.000316	3.0	3.0	3.0	3.0	3.0	3.0
0.000379	35.3	14.9	12.3	16.1	10.7	13.7
0.000442	3.0	3.0	3.0	3.0	3.0	
0.000505	3.0	3.0	3.0	3.0		
0.000568	16.8	6.3	6.6			
0.000631	20.4	100.0				
0.000694						
Percent error in hydraulic conductivity using low values of correction factor and –3% of the flow meter reading						
Flow (m3/s)	K (0% Strain)	K (10.8%)	K (21%)	K (32%)	K (42%)	K (53%)
0.0001262	3.0	3.0	3.0	3.0	3.0	3.0
0.0001893	3.0	3.0	3.0	3.0	3.0	3.0
0.0002524	3.0	3.0	3.0	3.0	3.0	3.0
0.0003155	3.0	3.0	3.0	3.0	3.0	3.0
0.0003786	39.0	19.8	17.4	21.0	15.9	18.8
0.0004417	3.0	3.0	3.0	3.0	3.0	
0.0005048	3.0	3.0	3.0	3.0		
0.0005679	21.7	11.7	12.1			
0.0006310	25.0	14.5				

Table A.6. This table shows the percent error in the hydraulic conductivity from the value used for analysis to the hydraulic conductivity that was calculated using the potential error in the flowmeter as well as the high values of the correction factors that was found during the three empty permeameter tests.

Percent error in hydraulic conductivity using high values of correction factor and +3% of flow meter reading						
Flow (m3/s)	K (0% Strain)	K (10.8%)	K (21%)	K (32%)	K (42%)	K (53%)
0.000126	106.0	54.5	54.5	44.2	28.7	54.5
0.000189	3.0	3.0	3.0	3.0	3.0	3.0
0.000252	100.0	100.0	167.8	100.0	167.8	85.4
0.000316	3.0	3.0	3.0	3.0	3.0	3.0
0.000379	100.0	59.7	46.2	67.7	39.3	53.4
0.000442	16.7	12.4	8.3	12.0	8.4	
0.000505	8.6	6.5	5.4	7.4		
0.000568	44.2	1 6.9	17.5			
0.000631	94.6	100.0				
Percent error in hydraulic conductivity using high values of correction factor and –3% of flowmeter reading.						
Flow (m3/s)	K (0% Strain)	K (10.8%)	K (21%)	K (32%)	K (42%)	K (53%)
0.0001262	94.0	45.5	45.5	35.8	21.2	45.5
0.0001893	3.0	3.0	3.0	3.0	3.0	3.0
0.0002524	100.0	100.0	152.2	100.0	152.2	74.6
0.0003155	3.0	3.0	3.0	3.0	3.0	3.0
0.0003786	100.0	50.4	37.6	58.0	31.1	44.4
0.0004417	9.9	5.8	2.0	5.4	2.1	
0.0005048	2.2	0.3	0.7	1.1		
0.0005679	35.8	10.1	10.7			
0.0006310	83.2	23.8				

APPENDIX B. DATA FROM SOIL SAMPLES TAKEN DURING BORING

CCE/DNR Waste Tire Project
Site Location: Dodger Enterprises, Fort Dodge, IA
Soils Classification Summary

Boring	Sample	Depth (ft)	Description	LL	PI	Classification
B-1	S-1	1-2	fat clay, Black	55	30	SC - Clayey sand contains organics, black
B-1	S-2	2.33-4.5	f-c clayey sand, tan	26	12	SC - F-C clayey sand, tan
B-1	S-3	4.5-5	f-c silty sand, light gray		non-plastic	SM - silty sand, light gray
B-1	S-4	5-6	sandy clay, light gray		non-plastic	SM - silty sand, light gray
B-1	S-5	6-6.5	sandy clay, light gray	25	13	SC - f-c clayey sand, light gray
B-2	S-1	0-1.5	fat clay, black	51	32	CH - sandy fat clay, black
B-2	S-2	1.5-3	sandy clay, brown-red	28	12	SC - f-c clayey sand, tan
B-2	S-3	3-4.33	f-c poorly graded sand w/gravel, tan		non-plastic	SP - f-c poorly graded sand w/silt & gravel, tan
B-2	S-4	4.33-5.5	f-c clayey sand, tan-red	24	11	SC - f-c clayey sand, tan-red
B-2	S-5	5.5-6.75	f-c clayey sand, tan-red	26	16	SC - f-c clayey sand, tan-red
B-3		0-3	fat clay, black			CH - fat clay, black
B-3		3-5	f-c clayey sand, light gray			SC - f-c clayey sand, light gray
B-3	S-1	5-9	f-c gravelly sand, gray		non-plast	SP-SM - poorly graded sand w/silt, gray
B-3	S-2	9-10	sandy clay w/gravel, gray-brown	30	18	SC - f-c clayey sand, gray-brown
B-3	S-3	10-15	sandy clay w/gravel, gray-tan	29	17	CL - sandy lean clay, gray-tan
B-4	S-1	0-0.75	fat clay, black	58	37	SC - clayey sand, black
B-4	S-2	0.75-3	f-c clayey sand, gray-tan			CL - sandy lean clay, gray-tan
B-4	S-3	3-6.5	f-c poorly graded sand w/silt, gray-tan		Non plastic	SP - poorly graded sand, gray-tan
B-4	S-4	6.5-10	sandy clay (till), gray-tan	28	16	SC - f-c clayey sand, gray-tan
B-4	S-5	10-15	sandy clay (till), gray-tan	26	15	SC - f-c clayey sand, gray-tan

Boring	Sample	Depth (ft)	Description	LL	PI	Classification
B-5	S-1	0-3	fat clay, black	53	29	CH - fat clay w/sand, black
B-5	S-2	3-4.5	f-c clayey sand, gray brown	38	21	SC - f-c clayey sand, gray-brown
B-5	S-3	4.5-5	f-c clayey sand contains limestone, gray-brown	32	16	SC - f-c clayey sand w/gravel, gray-brown
B-5	S-4	5-5.5	poorly graded sand w/silt, gray-brown	29	15	SC - f-c clayey sand w/silt, gray-brown
B-5	S-5	5.5-7.5	sandy clay w/silt (till), gray-brown	28	17	CL - sandy lean clay w/silt, gray-brown
B-5	S-6	7.5-10	sandy clay w/silt & gravel, gray-brown	30	18	CL - sandy lean clay, gray-brown
B-5	S-7	10-15	sandy clay w/silt & gravel, brown-gray	32	18	SC - f-c clayey sand w/silt, brown-gray
B-5	S-8	15-20	sandy clay w/silt & gravel, dark gray-tan	29	17	CL - sandy lean clay w/silt, dark gray-tan
B-5	S-9	20-25	silty clay w/gravel, dark gray	27	15	CL - sandy lean clay w/silt, dark gray
B-5	S-10	25-30	silty clay, dark gray	35	21	CL - sandy lean clay w/silt, dark gray
B-6	S-1	0-5	f-c silty sand, brown (fill)	37	20	SC - f-c clayey sand w/silt, brown
B-6	S-2	5-7.5	fat clay, black	56	30	CH - sandy fat clay, black
B-6	S-3	7.5-9	poorly graded sand w/silt & gravel, gray	25	13	SC - f-c clayey sand w/silt & gravel, gray
B-6	S-4	9-11	silty clay, gray	27	14	SC - f-c clayey sand w/silt, gray
B-6	S-5	11-15	silty clay, gray	25	14	SC - f-c clayey sand w/silt, gray
B-7	S-1	0-2	fat clay, black	69	52	CH - fat clay, black
B-7	S-2	2-3	f-c clayey sand, gray-tan	47	33	CL - sandy lean clay, gray-tan
B-7	S-3	3-6	f-c poorly graded silty sand, gray-tan	26	10	SC - f-c clayey sand w/silt & gravel, gray-tan
B-7	S-4	6-8	f-c clayey sand w/gravel, gray-tan	29	17	CL - sandy lean clay, gray-tan
B-7	S-5	8-10	silty clay w/gravel, dark gray	26	16	CL - sandy lean clay w/silt, dark gray
B-7	S-6	10-15	silty clay, dark gray	27	15	SC - f-c clayey sand w/silt, dark gray

Boring	Sample	Depth (ft)	Description	LL	PI	Classification
B-8	S-1	0-1	fat clay, black	59	43	CH - sandy fat clay, black
B-8	S-2	1-3	f-c clayey sand w/gravel, brown-orange			SC - f-c clayey sand w/gravel, brown-orange
B-8	S-3	3-5	f-c silty sand w/gravel, gray-tan		non-plastic	SM - f-c silty sand, gray-tan
B-8	S-4	5-10	f-c silty sand w/gravel, gray-tan	23	11	SC - f-c clayey sand w/silt, gray-tan
B-8	S-5	10-15	f-c silty sand w/gravel, gray-tan	28	16	CL - sandy clay, gray tan
B-9	S-1	0-3	f-c silty sand w/gravel, contains	34	19	SC - f-c clayey sand w/silt contains organics,
			organics, brown			brown
B-9	S-2	3-6	fat clay, black	48	30	SC - clayey sand w/gravel, black
B-9	S-3	6-11	poorly graded sand, tan-gray	28	12	SP-SC poorly graded sand w/clay, tan-gray
B-9		11-12	f-c silty clay, gray-tan (see S-5)			
B-9	S-4	12-12.5	poorly graded sand, tan-gray		non-plastic	SP-SM - poorly graded sand w/silt & gravel, tan-gray
B-9	S-5	12.5-15	f-c silty clay, gray tan	27	14	CL - sandy lean clay w/silt, gray-tan
B-10	S-1	0-1	f-c silty sand contains organics, brown	30	17	SC - f-c clayey sand w/silt contains organics, brown
B-10	S-2	1-3.5	fat clay, black	53	36	CH - sandy fat clay, black
B-10	S-3	3.5-4.5	silty clay, gray-tan	33	20	CL - sandy lean clay w/silt, gray-tan
B-10	S-4	4.5-7	silty sand, gray-tan		non-plastic	SP- SM - poorly graded sand w/silt, gray-tan
B-10	S-5	7-12	poorly graded sand w/gravel, gray-tan		non-plastic	SP-SM - poorly graded sand w/silt & gravel, gray-tan
B-10	S-6	12-15	silty clay, gray-tan	28	16	SC - sandy lean clay w/silt, gray-tan

Boring	Sample	Depth (ft)	Description	LL	PI	Classification
B-11	S-1	0-7	f-c clayey sand, black-brown	29	17	SC - f-c clayey sand, black brown
B-11	S-2	7-11	f-c gravelly sand, brown		non-plastic	SP - poorly graded sand w/gravel, brown
B-11	S-3	11-15.5	f-c clayey sand, gray-brown	26	15	SC - f-c clayey sand, gray-brown
B-11	S-4	15.5-19	sandy clay, gray-brown	27	15	CL - sandy lean clay, gray-brown
B-11	S-5	19-20	sandy clay, gray-brown	28	15	CL - sandy lean clay, gray-brown
B-11	S-6	20-27	sandy clay, gray-green	27	14	CL - sandy lean clay. gray-green
B-11	S-7	27-30	sandy clay, dark gray	27	15	CL - sandy lean clay, dark gray
B-12	S-1	0-5	fat clay, black	36	22	SC - f-c clayey sand w/gravel, black
B-12	S-2	5-6.5	f-c silty sand, gray	24	9	CL - sandy lean clay w/silt, gray
B-12	S-3	6.5-8	f-c clayey sand, gray		non-plastic	SP - poorly graded sand w/ gravel, gray
B-12	S-4	8-10	f-c gravelly sand, brown		non-plastic	SW - well graded sand w/gravel, brown
B-12	S-5	10-15	sandy clay w/silt, dark gray	27	16	CL - sandy lean clay, dark gray
B-13	S-1	0-2.5	sandy fat clay, black	47	31	CL - sandy lean clay, black
B-13	S-2	2.5-5	gravelly sand, brown-gray	26	11	SC - f-c clayey sand w/gravel, brown-gray
B-13	S-3	5-10	sandy clay, gray-tan	26	15	CL - sandy lean clay, gray-tan
B-13	S-4	10-15	sandy clay, gray	27	15	CL - sandy lean clay, gray

APPENDIX C. OUTLINE SUMMARY AND BIBLIOGRAPHY OF ENVIRONMENTAL ASPECTS OF THE USE OF TIRES AND TIRE PRODUCTS

Summary of Environmental Studies of Waste Tires

University of Maine , 1997, *Water Quality Effects of Tire Chip Fills Placed Above the Groundwater Table* (Humphrey, et.al., 1997)

- No evidence that tire chips increased the concentrations in of metals that have a primary drinking water standard
- No evidence that tire chips increased the concentrations of aluminum, zinc, chloride, or sulfate which have secondary (aesthetic) drinking water standards
- Under some conditions iron levels may exceed secondary drinking water standards
- Manganese may also sometimes exceed secondary standards, but it is naturally occurring in many areas
- Organics were below detection limits

University of Maine, 1996, *Water Quality Effects of Using Tire Chips Below the Groundwater Table* (Downs, et.al., 1996). 3 parts to study: 1) laboratory leaching tests, 2) laboratory simulation of subsurface conditions, and 3) small scale field trials

- Laboratory leaching tests: Used Toxicity Characteristics Leaching Procedure (TCLP) testing which is used to determine if a waste is a significant hazard to human health due to leaching of toxic compounds
  - Concentrations of TCLP regulated metals and organics did not exceed limits
  - Metals that were detected in the leachate but were below TCLP limits were: barium, cadmium, chromium, and lead
  - Organic compounds, both volatile and semi-volatile, were detected in the leachate, but none were above TCLP limits
- Laboratory simulation of ground conditions: used a batch reactor to simulate conditions
  - Chromium, copper, iron, zinc, and manganese leached from tires. Chromium did not exceed its primary drinking water standard. Iron and manganese exceeded the secondary drinking water standards. Zinc levels were below secondary drinking water standards
  - Several semi-volatile and volatile organic compounds were found in the leachate, but none above drinking water standards
- Small scale field study: trenches filled with tire chips were placed in sites with marine clay, glacial till, and fibrous peat. At each site, approx. 1.4 metric tons of shredded tires used. Trenches were approx. 0.6 m wide, 3 m long, and 1.8 m deep. Approx. 1.5 m of tire chips placed in each trench. Trenches had no outlet or inlet, so only groundwater and groundwater movement affected the results. Water samples were taken upgradient from the trench, downgradient from the trench, and from within the trench.
  - Iron concentrations up to two orders of magnitude higher than secondary drinking water standards (300μg/L) were found
  - Secondary drinking water standards for manganese (50 μg/L) were exceeded at the site
  - Zinc levels were increased, but they were well below the drinking water standard (5000 μg/L)
  - Volatile organic compounds detected include: 1,1-dichloroethane, cis-1,2-dicchloroethane, 1,1,1-trichloroethene, benzene, toluene, and napthalene. Except for cis-1,2-dichloroethane, volatile organics were measured below the primary drinking water standards on all occasions
  - cis-1,2-dichloroethane was measured above its primary drinking water standard (70 μg/L) at one sampling date at the till site sampled within the trench (85 μg/L)
  - No semi-volatile organic compounds with drinking water standards were detected
  - Recommended that tire chips only be used in locations where increased levels of iron and manganese can be accepted
  - Recommended that tire chips used in construction should be limited to application above the groundwater table

Laboratory Leaching Studies

1) Minnesota Pollution Control Agency Study (1990)
   - Recommended that the use of scrap tires be limited to the unsaturated zone
2) Wisconsin Department of Transportation Study (Edil et.al., 1992)
   - Concluded that scrap tires leached very small amounts of substances and have little or no effect on groundwater
3) Nelson, Mueller, and Hemphill, 1994, Identification of Tire Leachate and a Risk Assessment of Water Quality Effects Using Tire Reefs in Canals.
   - The authors conducted three tests using plugs cut from tires and whole tires.
   - Tire leachate was collected from two sets of plugs; one was used for toxicity testing, another was tested for organic contaminants.
   - Acute 24 hour toxicity tests were conducted using both Ceriodaphnia dubia and fathead minnows. The leachate was acutely toxic to C. dubia (24 hour LC_{50} 20.3%) but not to fathead minnows. Further tests indicated that the toxicity was caused by metals.
   - Chemistry tests of the leachate indicated that zinc was present in concentrations that could be toxic and that cadmium, lead, and copper were above background.
   - Laboratory analyses for organic compounds did not detect any analytical differences between tire leachate and the control water. All compounds tested for were below detection limits of 1.0 μm/L.
   - Tests with whole tires were analyzed for zinc and mercury. The amount of zinc declined over time. This shows that toxicants decreases with continuous leaching of water. Mercury was not detected in any samples.
   - The authors state that there may be some other situations such as landfills, disposal sites, or road beds where zinc leached from tires could result in water quality problems. If water is diluted or continually flushed, tire shreds should not pose a problem.

4) Park, Jae K., Kim, Jae Y., Edil, Tuncer B. (1996) Mitigation of Organic Compound Movement in Landfills by Shredded Tires
   - EPA's toxicity characteristics leaching procedure (TCLP) was used for various types of tires.
   - Carbon disulfide was detected ranging from no detection to 0.067 mg/L. Toluene was detected at the range from 0.007 to 0.19 mg/L. Phenol was detected at the range of no detection to 0.046 mg/L. Trace levels of barium, chromium, lead, and mercury were also detected. All results reported were below EPA's regulatory level.
   - Another series of leaching tests using the American Foundry Society procedure was conducted. Zinc and lead were detected at concentrations of 0.38 to 0.63 mg/L and no detection to 0.015 mg/L, respectfully. Iron and manganese concentrations ranged from no detection to 0.23 mg/L and 0.082 to 0.3 mg/L, respectfully.
   - EP toxicity tests for Barium, cadmium, chromium, lead, and mercury were all below detection limits.

Field Studies

1) Minnesota Pollution Control Agency Study (1990)
   - Water samples were taken from roadways built over wetlands using shredded tires and from surface tire stockpiles
   - Data indicated that scrap tires may impact groundwater quality
   - Indicated that barium, cadmium, chromium, and lead exceeded Recommended Allowable Limits (RALs) in groundwater
   - Samples at Pine county site exceeded the RALs for List 1 carcinogenic and List 2 non-carcinogenic PAHs
2) Wisconsin Department of Transportation Study (Edil et.al., 1992)
   - leachate generated by percolating water through tire chips used in construction of a roadway was monitored for a period of 2 years for a range of parameters (Edil and Bosscher, 1992). These studies indicated that the potential leaching of toxic pollutants from scrap tires is minimal.
   - Tires may have contributed organic compounds to groundwater but potential for pollution is

minimal

3) Tire Pond (Barris, 1987, as reported by Downs et. al., 1996)

- 32 acre pond ½ filled with 15 million tires
- most compounds tested were below detection limits
- Compounds detected but below regulatory limits include: ammonia-N, nitrate-N, nitrite-N, sulfate, nickel, zinc, trans-1,2-dichloroethylene, trichloroethylene, tetrachloroethylene, toluene, mixed xylenes, and benzene
- Iron was the only compound found which exceeded drinking water standards
- Data indicated that scrap tires may affect surface water and/or groundwater

References

Barris, D.C. (1987), "Report of Ground and Surface Water Analyses," by Environmental Consulting Laboratory, New Haven, CT, for Hampden Tire Salvage, Hampden, CT, from Downs et.al. 1996.

Downs, Lisa A., Humphrey, Dana N., Katz, Lynn E., Rock, Chet A., (1996), "Water Quality Effects of Using Tire Chips Below the Groundwater Table," A Study for the Maine Department of Transportation.

Edil, T.B., Bosscher, P.J. (1992), "Development of Engineering Criteria for Shredded Waste Tires in Highway Applications," Final Report to the Wisconsin Department of Transportation.

Humphrey, Dana N., Katz, L.E., and Blumenthal, M., (1997), "Water Quality Effects of Tire Chip Fills Placed Above the Groundwater Table," *Testing Soil Mixed With Waste or Recycled Materials, ASTM STP 1275*, Mark A. Wasemiller, Keith B. Hoddinott, Eds., American Society for Testing and Materials.

Minnesota Pollution Control Agency (1990), "Environmental Study of the Use of Shredded Waste Tires For Roadway Sub-grade Support," by Twin City Testing Corp., St. Paul, MN, for Andy Ronchak, Waste Tire Management Unit, Site Response Section, Groundwater and Solid Waste Division, Minnesota Pollution Control Agency, St. Paul, MN.

Nelson, S. M., Mueller, G., and Hemphill, D. C. (1994) Identification of Tire Leachate and a Risk Assessment of Water Quality Effects Using Tire Reefs in Canals. *Bulletin of Environmental Contamination and Toxicology*. 52: 574-581.

Park, Jae K., Kim, Jae Y., Edil, Tuncer B. (1996) Mitigation of Organic Compound Movement in Landfills by Shredded Tires. *Water Environment Research*. Vol. 68, Number 1, 4-10.

APPENDIX D. CROSS SECTION OF EXPERIMENTAL TRUCK TIRE CULVERT, STREAM CROSSING, AND HORIZONTAL DRAIN. DRAWING BY SHIPING YANG

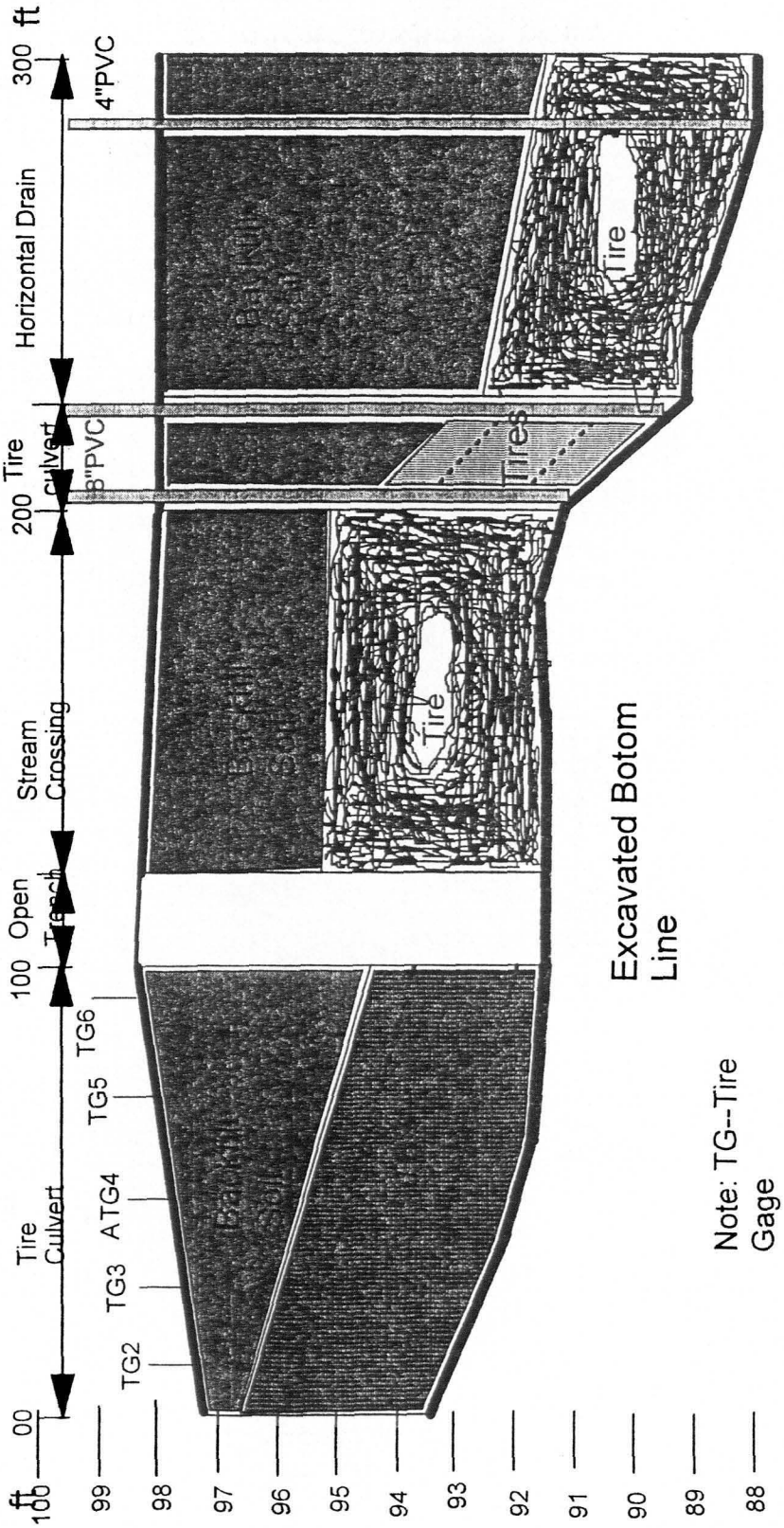

APPENDIX E. EQUATIONS AND CALCULATIONS USED TO ESTIMATE HYDRAULIC CONDUCTIVITY OF THE SHREDDED TIRES IN THE FIELD

The hydraulic conductivity of the shredded tires in the field drain was estimated using data from the second flow test. The Darcy equation was used to arrive at the hydraulic conductivity estimate. Laminar flow through the tire shreds was assumed. Even though a constant flow was put into the shredded tire drainage structures, it was evident that an equal amount of flow was not exiting the drain. The best evidence of this was that the water elevations in the drain continued to rise through the entire test. Some of the water that entered the drain was being stored in the drain instead of exiting through the outlet. Instead of using the input flow of the test, a flowrate was estimated from data taken after the water flow into the drain was turned off. The amount of water that drained from the horizontal drain in a given time period could be calculated using the water elevations in the standpipes and the volume of pore space that was drained.

The following water elevation data was taken from the second flow test (see figure 33):

Time (minutes)	Depth to Water in Monitoring Point 2	Depth to Water in Monitoring Point 3
230	2.74 m	2.97 m
245	2.79 m	3.00 m
Water Level Drop →	**0.0488 m**	**0.0366 m**

The average water level drop along the horizontal drain was 0.0427 m.

Length of the horizontal drain = 27.43 m
Width of the horizontal drain = 1.37 m

∴ The total volume of tire shreds drained during the fifteen minute period = 0.0427m x 27.43 m x 1.37 m = 1.61 m^3

The tire shreds in the drain are mostly compressed to around 30% - 35% vertical strain. The density of the tire shred layer at this strain is around 500 kg/m^3 or Unit weight of 4.91 kN/m^3

The weight of the tire shreds that were drained = unit weight x volume

$$4.91\ kN/m^3 \times 1.61\ m^3 = 7.9\ kN$$

The specific gravity of the individual tire shreds on the average is 1.15.

$$G = 1.15 = \gamma_{tires} / \gamma_w = \gamma_{tires} / 9.81\ kN/m^3$$

$$\gamma_{tires} = 11.28\ kN/m^3$$

The weight of the tires divided by the unit weight of the tires gives the volume of tire the tire shreds.

$$7.9\ kN / \gamma_{tires} = 0.7\ m^3 = V_{tires}$$

The void ratio of the tire shreds at this vertical strain is 1.3

$$e = V_{voids} / V_{solids} = 1.3$$

$$V_{voids} = V_{total} - V_{tires} = 1.61\ m^3 - 0.7m^3 = 0.91\ m^3$$

The quantity of flow is equal to the volume of voids that was drained (V_{voids})

The flow rate is equal to the quantity of flow divided by the time (15 min or 900 s)

$$Q = \text{Quantity of flow / time} = 0.91\ m^3 / 900\ s = 0.001\ m^3/s = 1000\ cm^3/s$$

The gradient is the change in water elevation between monitoring points (0.7 m) divided by the distance between the monitoring points (90 m)

$$i = 0.7 / 90 = 0.008$$

The area of flow is equal to the average height of water (0.85 m) in the drain multiplied by the width of the drain (1.37 m)

$$A = 0.85\ m \times 1.37\ m = 1.17\ m^2 = 11705\ cm^2$$

$$K = Q/iA = (1000\ cm^3/s) / (0.008)(11705\ cm^2) = 10.7\ cm/s$$

WORKS CITED

Ahmed, I. and Lovell, C.W., "Use of Rubber Tires in Highway Construction," *Utilization of Waste Materials in Highway Construction*, Proc. Of sessions sponsored by Materials Div. Of Am. Soc. of Civil Engs. H.I. Inyang and K.L. Bergeson (Eds.). 1992, pp. 166-179.

Chen, Lawrence, and Humphrey, "Use of Tire Chips/Soil Mixtures to Limit Frost Heave and Pavement Damage of Paved Roads," A Study for the New England Transportation Consortium, Department of Civil Engineering, University of Maine, Orono, ME, 1997.

Edil, T.B. and Bosscher, P.J., "Engineering Properties of Tire Chips and Soil Mixtures," *Geotechnical Testing Journal,* GTJODJ, Vol. 17, No. 4, December 1994, pp. 453-464.

Fetter, C.W., *Applied Hydrogeology, 3rd Edition*, Macmillian College Publishing Company, Inc., New York, 1994, pp. 86, 98.

Fung, Ping Kan, "Loess Soil as Highway Material," MS Thesis, Iowa State University, Ames, Iowa, 1945, page 41.

Hall, T.J., "Reuse of Shredded Waste Tire Material for Leachate Collection Systems at Municipal Solid Waste Landfills," for Iowa Department of Natural Resources Waste Management and Authority Division, by Shrive-Hattery Engineers and Architects, Inc., 1990.

Humphrey, D.N., Sandford, T.C., Cribbs, M.M., Gharegrat, H., and Manion, W.P., "Tire Chips as Lightweight Backfill for Retaining Walls - Phase I," A Study for the New England Transportation Consortium, Department of Civil Engineering, University of Maine, Orono, ME, 1992.

Humphrey, D.N., Sandford, T.C., Cribbs, M.M., Gharegrat, H., and Manion, W.P., "Shear Strength and Compressibility of Tire Chips for Use as Retaining Wall Backfill," *Transportation Research Record No. 1422*, Transportation Research Board, 1993.

Humphrey, D.N., "Civil Engineering Applications of Chipped Tires," Nebraska DEQ Seminar, Omaha, Nebraska, Nov. 15, 1995.

Kersten, Ernie, Dodger Enterprises, Fort Dodge, Iowa. Personal Correspondence, October 6, 1997.

Manion, W.P. and Humphrey, D.N., "Use of Tire Chips as Lightweight and Conventional Embankment Fill, Phase I - Laboratory," *Technical Paper 91-1*, Technical Services Division, Maine Department of Transportation, Augusta, ME, 1992.

Ng, Kam Weng, "Field tests and analyses of high density polyethylene pipes for highway applications," MS Thesis, Iowa State University, Ames, Iowa, 1997

Roe, Harry Burgess, and Ayres, Quincy Claude, *Engineering for Agricultural Drainage*, McGraw-Hill Book Company, 1954, pp. 249-251.

Shackelford, C.D. and Javad, F., "Large Scale Laboratory Permeability Testing of a Compacted Clay Soil," *Geotechnical Testing Journal*, GTJODJ, Vol. 14, No. 2, June 1991, pp. 171-179.

Townsend, F. C., Shiau, Jih-Min, and Pietrus, T. J., "Piping Susceptibility and Filter Criteria for Sands," *Engineering Aspects of Soil Erosion, Dispersive Clays and Loess, Proceedings of a Symposium sponsored by the Soil Properties Committee of the American Society of Civil Engineers in conjunction with the ASCE* Convention in Atlantic City, New Jersey, Ed. C. W. Lovell, April 29, 1987, 46-66.

Tsai, Chin-Ta, "Constant head pumping tests in oxidized glacial till," M.S. Thesis, Iowa State University, Ames, Iowa, 1991.